

CHAPTER 3

Building Blocks for SiC Devices: Ohmic Contacts, Schottky Contacts, and p-n Junctions

V. Saxena and A. J. Steckl

DEPARTMENT OF ELECTRICAL AND COMPUTER ENGINEERING AND COMPUTER SCIENCE
UNIVERSITY OF CINCINNATI
CINCINNATI, OH

I. INTRODUCTION	77
II. ELECTRICAL PROPERTIES OF METAL-SiC SYSTEMS	81
1. <i>The Schottky-Mott and Bardeen Limits for Barrier Height</i>	81
2. <i>Metal Contacts for High-Power Applications</i>	84
III. SURFACE PREPARATION TECHNIQUES	86
IV. METAL CONTACTS TO 6H-SiC	87
1. <i>Ohmic Contacts to 6H-SiC</i>	87
2. <i>Schottky Contacts to 6H-SiC</i>	96
3. <i>High-Voltage Schottky Diodes on 6H-SiC</i>	109
4. <i>Edge Termination in 6H-SiC Schottky Diodes</i>	113
5. <i>Excess Leakage Current in SiC Schottky Diodes</i>	114
V. METAL CONTACTS TO 4H-SiC	118
1. <i>Ohmic Contacts to 4H-SiC</i>	118
2. <i>Schottky Contacts and High Voltage Schottky Diodes on 4H-SiC</i>	118
VI. METAL CONTACTS TO 3C-SiC	125
1. <i>Ohmic Contacts to 3C-SiC</i>	125
2. <i>Schottky Contacts and Diodes on 3C-SiC</i>	126
VII. SiC p-n JUNCTIONS DIODE RECTIFIERS	131
1. <i>3C-SiC p-n Junctions</i>	133
2. <i>6H-SiC p-n Junctions</i>	138
3. <i>4H-SiC p-n Junctions</i>	147
VIII. SUMMARY AND CONCLUSIONS	149
References	151

I. Introduction

In this chapter we provide a review of the essential building blocks necessary for operating SiC structures as electronic devices: ohmic contacts, Schottky contacts, and p-n junctions. Many of the advantages of SiC devices

77

are due to its wide forbidden energy bandgap, enabling, for example, operation at high voltage or current and/or high temperature. However, this wide bandgap also creates difficulties in the fabrication of well-controlled metal-SiC contact properties. At the same time, operation under the extreme conditions of which SiC is capable introduces additional requirements on the physical and electronic properties of the metal contacts.

As discussed in detail in Chapter 1, SiC takes the form of many polytypes. Only one polytype takes the cubic form. This is the so-called β -SiC, with a three bilayer (Si/C) stacking period (or 3C). The noncubic polytypes, referred to as α -SiC, take on hexagonal, rhombohedral, and other structures. The most heavily investigated forms of SiC for electronic applications are the 3C, 4H, and 6H polytypes, of which only the hexagonal types are commercially available at this time. Some of the materials properties relevant to contact formation on each SiC polytype are summarized in Table I. They include the energy bandgap, electric field at which dielectric breakdown occurs; the saturated electron drift velocity; the carrier mobility; the electron work function; and affinity. While the breakdown field and saturated drift velocity appear to be close in value for all three polytypes, the mobility varies significantly. The cubic polytype has the highest reported electron mobility but unfortunately has not been grown in bulk crystal sizes larger than a few millimeters. Nelson *et al.* [Nelson 66] have reported a Hall electron mobility at 300 K ranging from ~ 700 to ~ 1000 cm²/V-sec for n-type 3C-SiC with carrier concentrations of $\sim 10^{16}$ to 10^{17} /cm³. These crystals were grown from a Si melt solution in a graphite crucible. Aivazova *et al.* [Aivazova 77] have measured a Hall electron mobility of 1020 cm²/V-sec in a very lightly doped sample (with a carrier concentration of 7×10^{15} /cm³ and a total impurity concentration of 2×10^{15} /cm³). These crystals were grown by decomposition from trichlorosilane [Gorin 65] and have been shown [Steckl 96] to exhibit excellent structural and optical properties. 3C-SiC material can also be obtained by growth on α -SiC substrates or on Si. Kelner *et al.* [Kelner 89] have reported very good electron mobilities for n-type ($\sim 3 \times 10^{16}$ /cm³) 3C films grown on p-type Acheson 6H-SiC crystals: room-temperature Hall effect and field effect mobilities of 470 and 565 cm²/V-sec, respectively.

The commercial hexagonal SiC substrates are typically cut perpendicular (or offset a few degrees) to the c-axis of the crystal. In these cases, one needs to be concerned with the carrier mobility either perpendicular to the c-axis (i.e., carrier motion in the basal plane of the lattice) or parallel to it, depending on the device structure and operation. In the α -SiC polytypes, the carrier transport properties exhibit an anisotropic behavior with regard to crystallographic orientation in each polytype. Schadt *et al.* [Schadt 94] have reported the electron mobility anisotropy present in heavily N-doped 4H-

TABLE I
MATERIALS PROPERTIES OF THE THREE MAIN SiC POLYTYPEs RELEVANT TO OHMIC AND RECTIFYING CONTACTS

Materials Properties at 300 K	4H-SiC ~3.24 ^e - excitonic	6H-SiC ~2.86 ^b - optical	3C-SiC ~2.2 ^a - optical
Energy bandgap (eV)	—	—	1.5 ^d , 3.0 ^e
Breakdown electric field (MV/cm) at 10 ¹⁷ /cm ³ doping	—	—	—
⊥ c-axis	3.0 ^e	3.2 ^d	—
∥ c-axis	—	—	—
Saturated electron drift velocity (× 10 ⁷ cm/s)	2.0 ^f	2.0 ^f	~2.0 ^g ; 2.5 ^h
⊥ c-axis	—	—	—
∥ c-axis	—	—	—
Electron (Hall) mobility (cm ² /V-sec) in n-type SiC (~10 ¹⁶ /cm ³)	790 ⁱ	370 ⁱ	980 ⁱ
⊥ c-axis	950 ⁱ	75 ⁱ	—
∥ c-axis	—	—	—
Hole (Hall) mobility (cm ² /V-sec) in p-type SiC (~10 ¹⁶ /cm ³)	115 ⁱ	90 ⁱ	40 ^f
⊥ c-axis	—	—	—
∥ c-axis	—	—	—
Work function (eV)	—	4.7 ^k for n-SiC 4.85 ^k for p-SiC	5.2 ^k
Electron affinity (eV)	—	3.3 ^k	4.0 ^k

^aChoyke *et al.* (64)

^bPhilip and Taft (60)

^cPalmour *et al.* (94)

^dNeudeck *et al.* (94a)

^eBhatnagar and Baliga (93); calculated based on 6H-SiC value

^fCree Research, 97 Product Data Sheets

^gKelner *et al.* (89)

^hFerry (75)

ⁱSchaffer *et al.* (94)

^jNelson *et al.* (66)

^kPorter and Davis (95a)

6H-, and 15-RSiC bulk crystals grown by the modified Lely method. Schaffer *et al.* [Schaffer 94] have investigated this effect using epitaxial SiC layers with total (donors plus acceptors) impurity levels varying from ~10¹⁵/cm³ to 10²⁰/cm³. The room-temperature mobilities reported by Schaffer *et al.* [Schaffer 94] for lightly doped (~10¹⁶/cm³) 4H- and 6H-SiC epitaxial layers are shown in Table I. In the case of 6H-SiC, the electron

mobility in the direction of the c-axis is much lower than the mobility in the basal plane. This leads to a significant electron mobility anisotropy ratio for 6H-SiC:

$$A_e(6H) = \frac{\mu_{\perp}}{\mu_{\parallel}} \approx 4.9.$$

The electron mobility anisotropy of epitaxial layers doped to levels of 10¹⁷ and 10¹⁸/cm³ [Schaffer 94] is essentially identical at room temperature and changes only slightly (from 4.7 to 5.1) over a wide temperature range (300–600 K). A similar anisotropy ratio of 4.8 is reported by Schadt *et al.* [Schadt 94] for bulk crystals with a total impurity level of ~6 × 10¹⁵/cm³.

The basal plane electron mobility in 4H-SiC, which is the condition routinely measured using wafers cut perpendicular to the c-axis, is reported by Schaffer *et al.* [Schaffer 94] to be approximately twice the basal plane mobility of 6H-SiC, for total impurity concentrations up to ~10¹⁷/cm³. Furthermore, in 4H-SiC, the electron mobility parallel to the c-axis is reported by Schaffer *et al.* to be actually slightly higher than the mobility in the basal plane, leading to an anisotropy ratio smaller than unity:

$$A_e(4H) = \frac{\mu_{\perp}}{\mu_{\parallel}} \approx 0.83.$$

Very similar values were also reported by Schadt *et al.* [Schadt 94]. The significantly larger electron mobility in 4H-SiC, along with the reduced anisotropy, indicate that this polytype should be superior to 6H-SiC in many applications. This is particularly true for power devices, where the current flow is frequently perpendicular to the substrate plane. However, one must also bear in mind that the larger energy bandgap of 4H SiC can also lead to larger Schottky barriers and more resistive contacts.

The work function and electron affinity of the SiC polytype chosen are important in determining the nature of the metal-SiC contact (ohmic vs. rectifying). The resulting "internal" characteristics (barrier height, resistivity) are also a function of additional basic materials properties such as mobility, carrier concentration, and so on. These in turn affect the important "external" characteristics, including forward DC bias current and associated voltage drop, reverse bias DC stand-off voltage and leakage current, DC and AC rectifying efficiency, and high-temperature operating capability.

In Section II, we discuss the basic properties and measurement issues of metal contacts to SiC. Surface preparation prior to metallization is briefly considered in Section III. The properties of ohmic and Schottky contacts to 6H-SiC, 4H-SiC, and 3C-SiC are reviewed in Sections IV, V, and VI,

respectively. The properties and characteristics of SiC p-n junction diodes are reviewed in Section VII. Finally, in Section VIII, a brief summary and conclusions are given.

II. Electrical Properties of Metal-SiC Systems

Metal-semiconductor contacts are indispensable for operation of all electronic circuits. High-quality ohmic contacts are necessary to transfer signals to and from the semiconductor and the external circuitry. Stable rectifying (Schottky) contacts may also be required, either by themselves, to perform switching or to provide rectification, or for the efficient operation of other devices utilizing them. In this section, the theory behind both types of contacts is briefly discussed. The parameters determining the quality of these contacts are discussed next, followed by the techniques commonly utilized to measure these parameters.

1. THE SCHOTTKY-MOTT AND BARDEEN LIMITS FOR BARRIER HEIGHT

In the Schottky model for an ideal intimate metal-semiconductor contact, the respective work functions ϕ_M and ϕ_S of the metal and semiconductor determine the ohmic or rectifying nature of the contact. Figures 1 and 2 show the energy-level diagrams of the metal contacts to n-type and p-type semiconductors, respectively [van der Ziel 68]. As seen from Fig. 1b, metal contact to an n-type semiconductor with $\phi_M > \phi_S$ results in a rectifying contact with a barrier to the flow of electrons in either direction. The barrier to the movement of electrons from the n-type semiconductor into the metal is $\phi_M - \phi_S$. The barrier to the reverse flow of electrons from the metal to the semiconductor is $(\phi_M - \chi_S)$, where χ_S is the electron affinity of the semiconductor. Under forward bias conditions (n-type semiconductor-negative with respect to the metal), the forward barrier reduces to $q(V_D - V_F)$, where V_D is the built-in potential and V_F is the applied voltage. However, the barrier to reverse flow, which is not affected by the applied bias, is defined to be the barrier height for the metal-semiconductor pair

$$\phi_{Bn} = \phi_M - \chi_S \quad (1a)$$

For a metal to n-type semiconductor contact with $\phi_M < \phi_S$, it is seen from Fig. 1d that virtually no barrier exists in the conduction band and that the nature of the contact is ohmic.

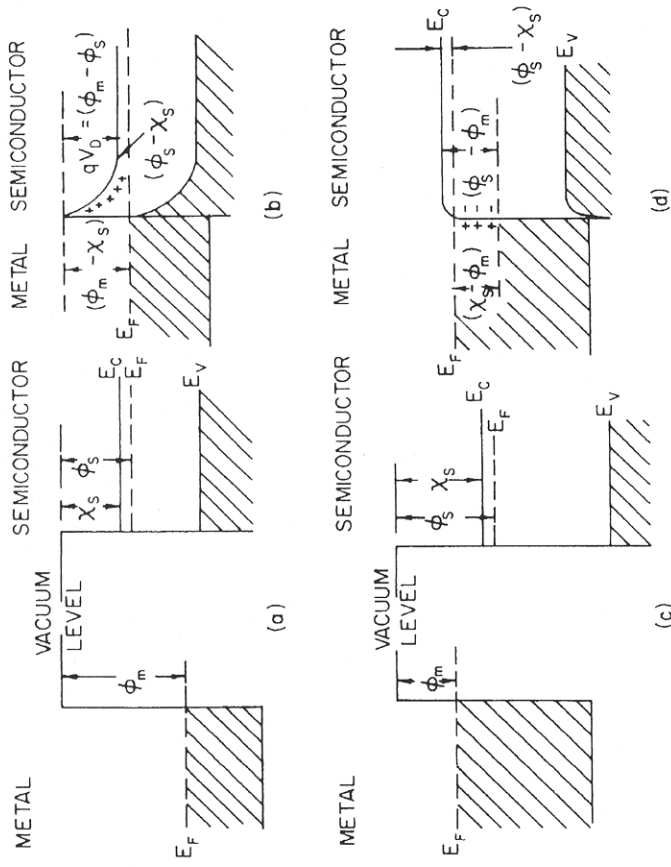


Fig. 1. Energy-level diagram of a metal contact to an n-type semiconductor [van der Ziel 68].

In Fig. 2, the corresponding band diagrams for a metal contact to a p-type semiconductor are shown. For $\phi_M < \phi_S$, the contact is rectifying because a barrier $(\phi_S - \phi_M)$ exists to the flow of holes from semiconductor to metal. This barrier decreases under forward bias condition (p-type semiconductor-positive with respect to the metal). The barrier to reverse flow, however, remain unaffected and is defined as the barrier height

$$\phi_{Bp} = E_G - (\phi_M - \chi_S) \quad (1b)$$

For a metal to p-type semiconductor contact with $\phi_M > \phi_S$, there is virtually no barrier for current flow from either side, and the contact is ohmic.

The barrier height $\phi_B (= \phi_{Bn}$ or $\phi_{Bp})$ for a metal-semiconductor pair is also known as the Schottky-Mott limit [Mott 38] and is independent of the applied bias and doping level of the semiconductor. If the contact is rectifying, ϕ_B is positive and is called the Schottky barrier height (SBH). In the case of an ohmic contact, the barrier has a small negative value and is referred to as the dipole surface charge barrier (DSCB). As seen from Eq.

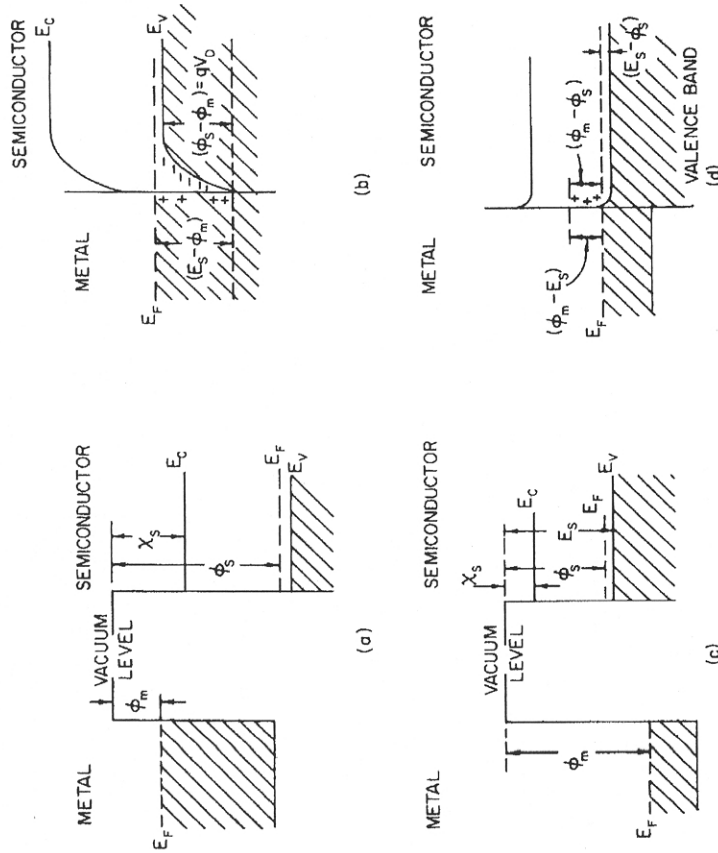


FIG. 2. Energy-level diagram of a metal contact to a p-type semiconductor [van der Ziel 68].

(1), this theory predicts that for any given semiconductor, the sum of the barrier heights in n-type and p-type materials for the same metal should be equal to the bandgap of the semiconductor.

Schottky-Mott theory for ideal metal-semiconductor therefore predicts that the SBH should be linearly dependent on the metal work function ϕ_M . Frequently, actual Schottky contacts fabricated on various semiconductors exhibit a much weaker dependence than that predicted by Eq. (1). Indeed, under certain conditions for many semiconductors, the SBH is independent of the choice of metal. A possible explanation suggested by Bardeen [Bardeen 47] is the presence of a continuous distribution of surface states at the interface between the semiconductor and the thin interfacial oxide layer. These surface states are characterized by a neutral level, φ_0 , measured from the top of the valence band. For a large density of surface states, φ_0 approaches the surface Fermi level (E_F), and the barrier height becomes

$$\varphi_{Bn} = E_G - \varphi_0 \quad \text{for n-type} \quad (2a)$$

and

$$\varphi_{Bp} = \varphi_0 \quad \text{for p-type.} \quad (2b)$$

This is the so-called Bardeen limit. In this situation, the barrier height is said to be "pinned" by the high density of surface states. In most practical metal-SiC Schottky contacts, the SBH takes on a value between the limits given by Eqs. 1 and 2.

2. METAL CONTACTS FOR HIGH-POWER APPLICATIONS

Many important applications for SiC devices place a requirement of high blocking voltages and/or high current-handling capability. In this section, we discuss the important parameters that characterize the metal-SiC contacts in light of these requirements for high-power applications.

a. Specific Contact Resistivity and Ohmic Contacts

The intrinsic electrical property of an ohmic contact is characterized by a parameter termed *specific contact resistivity*, which is given as

$$\rho_C = R_C A_E \quad (\Omega\text{-cm}^2), \quad (3)$$

where R_C is the contact resistance and A_E is the effective contact area of the device. The frequency and noise characteristics, and the power capability of a device are significantly affected by the quality of the ohmic contact. A condition for good ohmic contact is $R_C \ll R_{ON}$, where R_{ON} is the total on-resistance of the device. Satisfying this condition results in negligible voltage drop across the contact, which is necessary for high device efficiency. A lower value of R_C is particularly important in high-power devices because the power dissipated across R_C can cause substantial heating of the devices.

The specific contact resistivity of ohmic contacts can be measured by using a variety of different techniques. The size of the contacts and the resistivity of the metal may affect the accuracy of the measurements [Marlow 82]. Some techniques of measuring the contact resistivity include the linear transmission line method (TLM) [Shockley 64; Berger 72], the circular TLM method [Chen 95], the Kelvin technique [Proctor 82, 83], and the Cox and Strack method [Cox 67]. The experimental details for these and several other techniques have also been reviewed by Schroder [Schroder 90].

b. Schottky Barrier Height and Schottky Contacts

For power devices based on Schottky contacts, the most important parameter is the SBH. Optimization of SBH plays a key role in the determination of the on-state voltage drop and the leakage current in such devices. A larger barrier height of the metal-SiC junction leads to a higher on-state voltage drop, but also results in a much smaller leakage current density. For high-temperature device operation, it is safer to choose metals that result in a higher barrier height to SiC because the leakage current increases exponentially with temperature.

Rhoderick and Williams [Rhoderick 88] have reviewed the different techniques for measuring the SBH. The current-voltage characteristics [Norde 79; Cheung 86] are extensively utilized to obtain the SBH. The SBH can also be obtained from capacitance-voltage measurements [Goodman 63], photoelectric measurements [Anderson 75], and photoelectron emission spectroscopy [Rhoderick 88].

c. On-Resistance and Power Losses in Power Rectifiers

For efficient operation of high-power devices, it is also essential to minimize their overall power losses. The current-handling capability of power rectifiers is often limited by their on-resistance. The theoretical on-resistance for these (Schottky and p-n junction) rectifiers can be written as follows:

$$R_{\text{on}} = R_c + R_{\text{on}}(\text{epi}) + R_{\text{on}}(\text{sub}) \quad (4a)$$

$$= R_c + \rho_{\text{epi}} W_{\text{epi}} + \rho_{\text{sub}} W_{\text{sub}}, \quad (4b)$$

where R_c is (are) the contact resistance (s), $R_{\text{on}}(\text{epi})$ and $R_{\text{on}}(\text{sub})$ are the resistances per unit area of the epilayer and substrates, ρ_{epi} and ρ_{sub} are the epilayer and substrate resistivities, and W_{epi} and W_{sub} are the thickness of the epilayer and substrate, respectively. For p-n rectifiers, R_c would include contacts to both p- and n-type layers, and $R_{\text{on}}(\text{epi})$ would include the resistance from all the epilayers.

The average power loss dissipated per unit area of the diode during the on-state and off-state for 50% duty cycle is given by [Itoh 96a]

$$P_L = \frac{1}{2}(J_F V_F + J_R V_R), \quad (5)$$

where V_F and J_F are the forward voltage drop and the corresponding

forward current density, while V_R and J_R are the reverse blocking voltage and corresponding leakage current density. Since V_F depends on R_{ON} and φ_B , and J_R depends on φ_B , the decrease in R_{ON} and the optimization of φ_B leads to the reduction of P_L .

III. Surface Preparation Techniques

The properties of an ohmic contact can strongly depend on the surface cleaning procedure used prior to forming the contact. The electrical characteristics of Schottky barrier diodes are also very sensitive to surface preparation techniques. Presence of contamination or oxide at the metal-semiconductor interface can reduce metal adhesion, affect barrier heights, increase the specific contact resistance, and create electrically active defects that may alter the conduction of carriers through the contact. Thus, it is of utmost importance to provide a reproducibly clean semiconductor surface prior to performing the metallization to form the contact. This involves removing surface contamination and any interfacial oxide layer. From a purely materials standpoint, it may be possible to obtain a very clean and oxide-free SiC surface by doing a wet chemical cleaning followed by a heat treatment. Studies utilizing procedures involving such combination of chemical cleaning processes and subsequent thermal processing have been reviewed by Porter and Davis [Porter 95a]. However, most studies on the electrical behavior of metal contacts to SiC have reported using only the wet chemical cleaning procedure prior to doing metallization. These procedures may involve the use of solvents such as trichloroethylene, trichloroethane, acetone, methanol, and propanol to degrease the SiC wafer. Buffered hydrofluoric acid ($\text{HF} + \text{NH}_4\text{F} + \text{H}_2\text{O}$) is widely used for oxide removal. Varying mixtures of acids and bases such as HF , H_2SO_4 , HCl , NH_4OH , H_2O_2 , HNO_3 , and KOH are commonly utilized for surface cleaning.

Some specific procedures utilized for cleaning SiC surfaces prior to forming metal contacts are discussed next. The standard RCA clean procedure has routinely been used by several researchers, sometimes with certain modifications. A Huang clean procedure (10-min dip in $\text{NH}_4\text{OH}:\text{H}_2\text{O}_2:\text{H}_2\text{O}::1:1:5$ followed by a 10-min dip in $\text{HCl}:\text{H}_2\text{O}_2:\text{H}_2\text{O}::1:1:5$ solution at 70°C) has been used by the NCSU group [Ragunathan 95] before depositing the Schottky contact. Researchers at Kyoto clean the as-grown epitaxial layers in organic solvents, heated K_2CO_3 , aqua regia, and HF , and then rinse in deionized water. Yoshida and co-workers at the Electrochemical Laboratory [Yoshida 85] cleaned the epilayer surface in four steps: etching in 5% HF for 5 min, followed by a 10-min hot bath in 20% K_2CO_3 , a 5-min dip in HCl , and a 5-min etch in 5% HF once again prior to doing

Schottky metallization. Waldrop and co-workers at Rockwell [Waldrop 90, 92, 93] cleaned the wafers serially in solutions of detergent, 5:1:1 $\text{NH}_4\text{OH}:\text{H}_2\text{O}_2:\text{H}_2\text{O}$, 5:1:1 $\text{HCl}:\text{H}_2\text{O}_2:\text{H}_2\text{O}$, and then followed the four-step procedure used by Yoshida *et al.* [Yoshida 85]. At Cincinnati, initially an RCA cleaning is performed on the SiC wafers. The successive steps for this procedure are solvent removal, organic cleaning, oxide removal, ionic cleaning, and nitrogen dry. The solvents used for cleaning are warm TCE, acetone, and methanol. Organic cleaning is performed in 5:1:1 $\text{NH}_4\text{OH}:\text{H}_2\text{O}_2:\text{H}_2\text{O}$ for 5 min, and the ionic cleaning in 5:1:1 $\text{HCl}:\text{H}_2\text{O}_2:\text{H}_2\text{O}$ for 5 min. BHF is used for oxide removal, and DI water for the rinsing performed between all the previously mentioned steps. An oxide layer is then grown thermally on the epilayer, and it serves as a sacrificial layer for regions where the contacts are formed. Prior to Schottky metal deposition, this sacrificial oxide layer is etched away using BHF from the regions where contacts are to be formed. At regions outside the Schottky contact, the oxide on the epilayer serves as a passivation layer.

IV. Metal Contacts to 6H-SiC

1. OHMIC CONTACTS TO 6H-SiC

Ohmic contacts to both n- and p-type 6H-SiC for various metallization schemes studied are summarized in Table II. Early schemes for forming ohmic contacts on either n- or p-type SiC were reported by Hall, who utilized the alloying of SiC with tungsten at a temperature of about 1900°C [Hall 58]. High-temperature heating with other metal alloys, such as Si-Al or Si-B for p-type and Si-P for n-type, also resulted [Hall 58] in good ohmic characteristics of the contacts.

The first deposited ohmic contacts on 6H-SiC [Palmour 91] were fabricated using Ni and subsequent high-temperature annealing. Glass *et al.* [Glass 91, 92] obtained as-deposited ohmic contacts on fairly highly doped ($1.6 \times 10^{18} \text{ cm}^{-3}$) SiC by ion-assisted reactive evaporation in ultra high vacuum of TiN, with the substrates held at 350°C. In this case, the ohmic contact is due to the formation of a thin ($>10 \text{ \AA}$) layer of amorphous silicon nitride (a-Si-N), resulting in the metal-insulator-semiconductor (MIS) structure shown in Fig. 3. The a-Si-N layer appears to free the Fermi level at the SiC surface and promotes ohmic behavior. The contact resistance was found to be $4 \times 10^{-2} \Omega\text{-cm}^2$.

Petit and Zeller [Petit 92] performed studies of ohmic contacts using metals (Ni and Ni/Mo) and silicides (MoSi_2 , TaSi_2 , TiSi_2). As expected, the silicide films were stable and showed little reaction on either the Si-

TABLE II
OHMIC CONTACTS TO 6H-SiC

Metallization	SiC Type	Annealing Conditions	SiC Carrier Conc. (cm^{-3})	ρ_c at RT ($\Omega\text{-cm}^2$)	Method of ρ_c Measurement	Ref.
Al	p	700°C, 10 min	1.8×10^{18}	1.7×10^{-3}	TLM	[Crofton 92]
Al-Si	p	1700°C	NR	NR	—	[Hall 58]
Al-Si	p	900–1000°C	NR	NR	—	[Shier 70]
Al-Ti	p	950°C, 5 min	NR	NR	—	[Nakata 89]
Al-Ti	p	1000°C, 5 min	5×10^{15}	2.9×10^{-2}	Circular TLM	[Crofton 93]
Cf	n	Melting ($\geq 2130^\circ\text{C}$)	NR	NR	—	[Addamiano 70]
Cu-Ti	p	$> 880^\circ\text{C}$	NR	NR	—	[Hall 58]
Mo	n	as-deposited	$> 1 \times 10^{19}$	$\sim 1 \times 10^{-4}$	TLM, 4 pt. probe	[Petit 94]
Mo	p	as-deposited	$> 1 \times 10^{19}$	2×10^{-4}	TLM, 4 pt. probe	[Petit 94]
Ni	n	1000°C, 20 s	4.5×10^{17}	1.7×10^{-4}	TLM	[Kehner 91]
Ni	n	950°C, 5 min	4.7×10^{18}	mid 10^{-2}	4 pt. probe	[Crofton 92]
Ni	n	950°C, 2 min	7.9×10^{18}	$< 5 \times 10^{-6}$	TLM	[Crofton 94]
Ni	n	1050°C, 5 min	9.8×10^{17}	10^{-3} – 10^{-4}	TLM	[Porter 95a]
Ni	n	1000°C, 5 min	4.5×10^{20}	1×10^{-6}	Contact area	[Uemoto 95]
Ni-C	n	950°C, 5 min	4.7×10^{18}	1.8×10^{-3}	Circular TLM	[Crofton 92]
Ni/3C-SiC	n	1000°C, 30 s	1.2×10^{18}	1.7×10^{-5}	Cox and Strack	[Dmitrev 94]
(C-face)				6×10^{-5}		

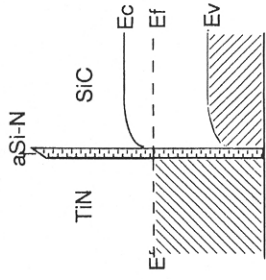


FIG. 3. Schematic representation of band diagram expected for MIS structure [Glass 92].

or C-face. Ni was unstable on both the faces and reacted to yield free carbon at the interface. The Ni/Mo bilayers films were rectifying, with SBH of 1.8 eV on the C-face and 0.9 eV on the Si-face. High-temperature anneal made these contacts ohmic, with specific contact resistance values between $(7-20) \times 10^{-4} \Omega\text{-cm}^2$. Later investigations [Petit 94] on refractory metals found that Mo, Ta, Ti, and Zr contacts were ohmic as-deposited on highly doped ($>10^{19} \text{cm}^{-3}$) 6H-SiC. These contacts resulted in contact resistivity in the $10^{-4} \Omega\text{-cm}^2$ range. Mo contacts resulted in the lowest as-deposited ρ_c for n-type SiC, and Ti contacts had the lowest ρ_c for p-type SiC.

Anikin *et al.* [Anikin 92] investigated W/Au-based ohmic contacts on n-type and W/Au/Al-based ohmic contacts on p-type 6H-SiC. For W/Au contacts to n-type SiC, ρ_c varied from $1 \times 10^{-2} \Omega\text{-cm}^2$ to $5 \times 10^{-4} \Omega\text{-cm}^2$ for the C-face, and from $1 \times 10^{-4} \Omega\text{-cm}^2$ to $5 \times 10^{-3} \Omega\text{-cm}^2$ for the Si-face. For W/Au/Al contacts to p-type SiC, ρ_c varied from $(2-5) \times 10^{-4} \Omega\text{-cm}^2$.

Crofton *et al.* [Crofton 92] found that TiW, Ni, and NiCr form ohmic contacts on n-type SiC and that Al and AlSi form ohmic contacts on p-type 6H-SiC after high-temperature annealing. For contacts to n-type SiC, TiW resulted in the lowest contact resistivity of $7.8 \times 10^{-4} \Omega\text{-cm}^2$. For contacts to p-type, Al metallization resulted in a contact resistivity of $1.7 \times 10^{-3} \Omega\text{-cm}^2$. The authors hypothesized that for TiW contacts annealing is necessary only to remove the interfacial oxide layer. In contrast to the Ni and NiCr contacts, where the ohmic nature is due to a reaction between Ni and SiC at the metal-semiconductor interface, using TiW it should be possible to form as-deposited or nonalloyed contacts with ohmic characteristics. The ohmic nature in Al and AlSi contacts is due to a heavy doping of the p-type SiC under the contact that occurs upon high-temperature annealing. The same group [Crofton 93] reported the specific contact resistance as a function of p-type doping of the epitaxial 6H-SiC for Al-Ti contacts. As shown in Fig. 4, ρ_c varied from 2.9×10^{-2} to $1.5 \times 10^{-5} \Omega\text{-cm}^2$ for doping concentrations ranging from 5.5×10^{15} to $2 \times 10^{19} \text{cm}^{-3}$. A good theoretic-

Material	Structure	Measurement	Temperature	Time	Carrier Type	Contact Resistivity (ρ_c)	Reference
Pt	W/Au	TLM	450-850°C	20 min	p	$>1 \times 10^{18}$	[Glass 94]
Si-B	W/Au	TLM	1700-2000°C		p	NR	[Hall 58]
Ta	W/Au	TLM	as-deposited		n	$>1 \times 10^{19}$	[Petit 94]
Ta	W/Au	4 pt. probe	as-deposited		p	$>1 \times 10^{19}$	[Petit 94]
Ti	W/Au	4 pt. probe	as-deposited		n	$>1 \times 10^{19}$	[Petit 94]
Ti	W/Au	Circular TLM	as-deposited		n	4.5×10^{17} - $<2 \times 10^{-5}$	[Alok 93]
Ti	W/Au	TLM	as-deposited		p	$>1 \times 10^{19}$	[Petit 94]
Ti/Al	W/Au	4 pt. probe	1000°C	5 min	p	NR	[Umoto 95]
Ti/Al/3C-SiC	W/Au	TLM	950°C	2 min	p	$2-3 \times 10^{-5}$	[Dmitriev 94]
TiN	W/Au	TLM	600°C	30 min	n	$\sim 1 \times 10^{18}$	[Glass 91, 92]
TiW	W/Au	Circular TLM	O_2 plasma + 600°C		n	4.7×10^{18}	[Crofton 92]
TiW	W/Au	5 min	750°C	5 min	n	$7-8 \times 10^{18}$	[Crofton 93]
W	W/Au	1200-1600°C		n		3×10^{18} - 1×10^{19}	[Anikin 92]
W	W/Au	1900°C		p		NR	[Hall 58]
W/Au/W/W/Al	W/Au	1900°C, 120 s		p		NR	[Anikin 92]
W/P/Al	W/Au	800-850°C, 10 min		p		8×10^{18}	[Porter 95a]
W/Ti/Ni	W/Au	1050°C, 5 min		n		9.8×10^{17}	[Porter 95a]

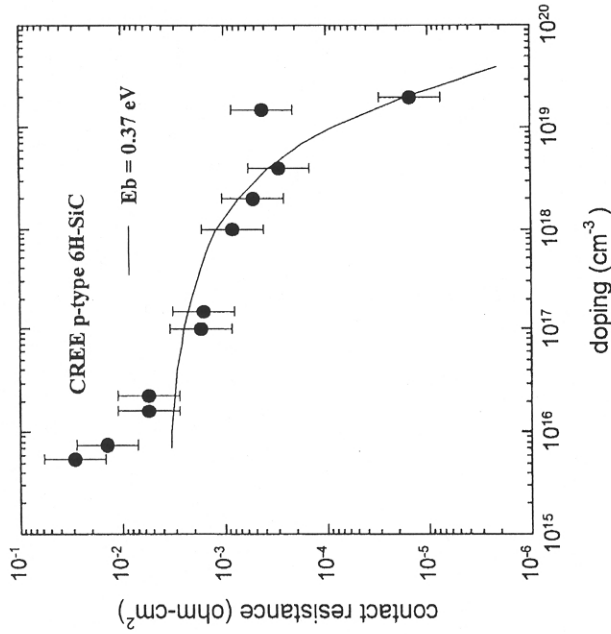


FIG. 4. Specific contact resistance versus doping for Al-Ti ohmic contacts on p-type 6H-SiC [Crofton 93].

cal fit to the contact resistance data was obtained by assuming the barrier height for the contact to equal 0.37 eV. This low value of ϕ_B has been attributed to the image force lowering of the Schottky barrier. In another study, Crofton *et al.* [Crofton 95] reported Ni/6H-SiC ohmic contacts capable of operating with low contact resistance at high temperatures. ρ_c less than $5 \times 10^{-6} \Omega\text{-cm}^2$ was obtained at room temperature, and it decreased with increasing temperature up to 500°C.

The dependence of the specific contact resistance on doping of n-type 6H-SiC was also studied. Crofton *et al.* [Crofton 95] reported that a good Ni/6H-SiC ohmic contact is possible on moderately to heavily doped SiC (i.e., for material with carrier concentration higher than the mid- 10^{17} range). As shown in Fig. 5, the specific contact resistance decreases from $2 \times 10^{-4} \Omega\text{-cm}^2$ for a doping concentration of $3.2 \times 10^{17} \text{cm}^{-3}$ to $5 \times 10^{-6} \Omega\text{-cm}^2$ for $7.8 \times 10^{18} \text{cm}^{-3}$. The specific contact resistance for this doping range was found to further decrease to the lower $10^{-6} \Omega\text{-cm}^2$ range after the contacts were annealed at 1200°C. For doping concentrations below 10^{17}cm^{-3} , annealing temperatures in excess of 1400°C were necessary. Reliable measurements could not be made after subjecting the contacts to such high

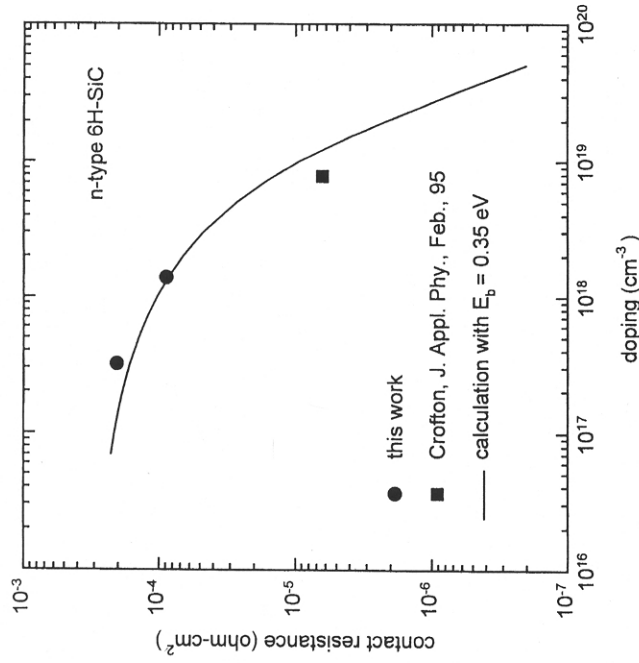


FIG. 5. Specific contact resistance as a function of doping for annealed Ni on n-type 6H-SiC [Crofton 94].

temperature, possibly due to graphitization occurring at the unprotected SiC surface, which in turn resulted in excessive leakage.

Dmitriev and co-workers [Dmitriev 94] reported low resistivity ($1.7 - 3 \times 10^{-5} \Omega\text{-cm}^2$) ohmic contacts to n and p-type 6H-SiC by depositing the metal on a thin 3C-SiC layer grown by CVD on 6H-SiC. Ni was used for forming n-type contacts, and Al/Ti for the p-type contacts. This procedure for forming ohmic contacts requires single crystal heteroepitaxy of 3C-SiC films on 6H-SiC.

Uemoto [Uemoto 95] reported the dependence of specific contact resistance of Ni contacts on the doping level of n-type 6H-SiC. As shown in Fig. 6, ρ_c values as low as $10^{-6} \Omega\text{-cm}^2$ were obtained at a doping level of $(2-5) \times 10^{20} \text{cm}^{-3}$, when the contacts were annealed at 1000°C for 5 min. He also reported that it is possible to form ohmic contacts to n-SiC by using Ti/Al, which formed good ohmic contacts to p-SiC. Therefore, the same metallization scheme could now be used to form good contacts to both n- and p-type regions in a single device.

Goesmann and Schmid-Fetzer [Goesmann 95] showed that as-deposited

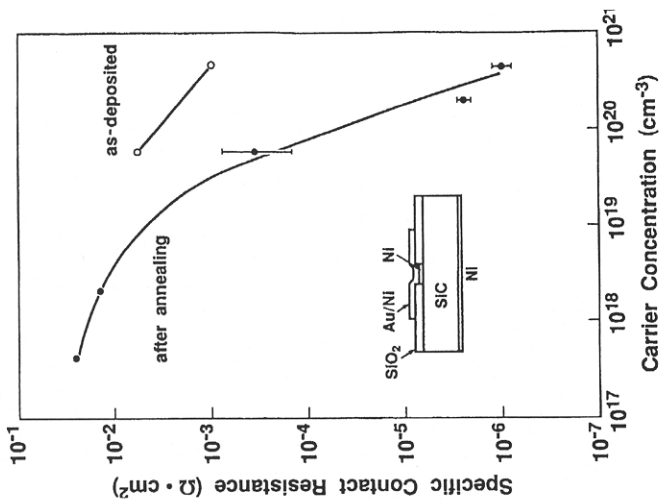


FIG. 6. Specific contact resistance before and after annealing of Ni contacts on 6H-SiC as a function of carrier concentration [Uemoto 95].

Ti/6H-SiC Schottky contacts became ohmic after a 5-min anneal at 900°C. TiC ohmic contacts to n-type 6H-SiC with a doping concentration of $4 \times 10^{19} \text{ cm}^{-3}$ were reported by Chaddha *et al.* [Chaddha 95]. The resulting contact resistivity, sheet resistance (R_s), contact resistance (R_c), and transfer length (L_T) were calculated from total resistance (R_T) versus contact spacing (d) measurements on TLM structures. The average values of these parameters were found to be $R_c = 1.3 \times 10^{-5} \Omega\text{-cm}^2$, $R_s = 14.4 \Omega/\text{square}$, $R_T = 1.6 \Omega$, for a spacing of $d = 9.5 \mu\text{m}$.

Hallin *et al.* [Hallin 96] compared Ni and Ni-Al metallizations for ohmic contacts on n-type SiC. As-deposited Ni contacts were found to be rectifying, whereas the Ni/Al contacts had an ohmic behavior with contact resistivity of $4.4 \times 10^{-4} \Omega\text{-cm}^2$. The specific contact resistivity for the Ni and Ni-Al contacts after a 5-min anneal at 1000°C were 2.1×10^{-4} and $1.2 \times 10^{-4} \Omega\text{-cm}^2$, respectively. Annealing for longer duration resulted in an increase in the contact resistivity, which according to the authors is due to the formation of a relatively large content of graphite in the subsurface

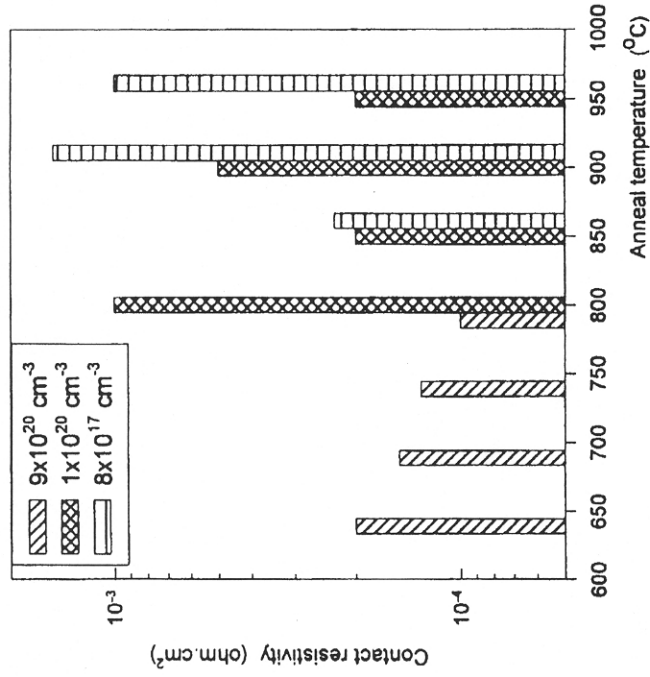


FIG. 7. Contact resistivity of Al/Ti/Al ohmic contacts as a function of anneal temperature on wafers with different carrier concentration in the active region [Nordell 96].

region. Other interesting conclusions drawn from the XPS studies by this group include that: (1) Al forms Al_2O_3 by reducing the residual SiO_2 when it comes in contact with SiC; (2) Ni or Al may have a catalytic effect in dissociating SiC into Si and C at higher temperatures ($>400^\circ\text{C}$); (3) in Ni/SiC contacts, C remains mainly in the graphite state; on the other hand, in Ni/Al/SiC contacts, C reacts with Al to form Al_4C_3 , which is a stable compound; and (4) ohmic contact is formed at high temperatures through the formation of Al and/or Ni silicide at the interface.

Nordell *et al.* [Nordell 96] reported that the contact resistivity of Al/Ti/Al contacts on 6H-SiC samples is dependent on the doping concentration of the samples and on the postmetallization annealing conditions for the contact. Figure 7 indicates the values of contact resistivity as a function of anneal temperature on SiC wafers with different active doping concentrations. It is seen that for highly doped samples ($\sim 9 \times 10^{20} \text{ cm}^{-3}$), the contact resistivity decreases to values below $10^{-4} \Omega\text{-cm}^2$ as the anneal temperature is increased from 650 to 800°C. However, much higher anneal temperatures are required for forming comparable ohmic contacts to

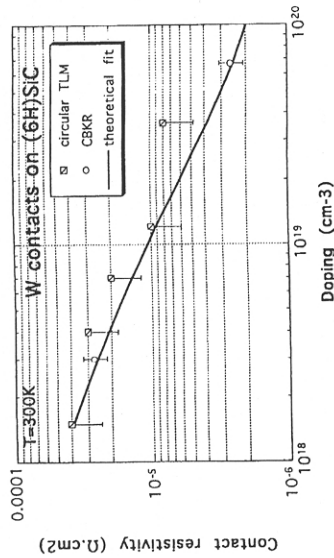


FIG. 8. Specific contact resistance as a function of doping concentration of n-type 6H-SiC [Baud 96].

samples with lower doping levels. These higher temperatures produce a resistive film over the metal surface, thus making measurements difficult. Hence, good ohmic contacts could not be realized for samples with doping levels $< 1 \times 10^{20} \text{ cm}^{-3}$.

The presence of Ni_2Si and of carbon-containing regions near the interface of Ni/6H-SiC contacts was also reported by Rastegaeva [Rastegaeva 96]. After annealing these contacts at 1000°C for 2 min, the specific contact resistivity was measured as $(8-9) \times 10^{-5} \Omega\text{-cm}^2$.

Teraji *et al.* [Teraji 96] reported ohmic behavior in as-deposited Ti and Al contacts on n-type 6H-SiC. To prevent Fermi-level pinning, they removed the surface layer (which is likely to have imperfections) by thermal oxidation followed by HF etching of the oxide. The dangling bonds left behind were passivated by dipping in pH-modified BHF or in boiling water (BW) for 10 min. ρ_c values in the range of 6×10^{-3} to $1.5 \times 10^{-2} \Omega\text{-cm}^2$ were obtained on samples with doping concentrations of $2 \times 10^{17} \text{ cm}^{-3}$. A similar procedure was utilized to produce Ti ohmic contacts on 6H-SiC requiring no annealing or excessive doping of the contacting layer Teraji *et al.* [Teraji 97]. These contacts were realized by sacrificial oxidation followed by HF and BW dip prior to Ti deposition. The resulting contact resistivity was found to be $(6 \pm 1) \times 10^{-3} \Omega\text{-cm}^2$.

Baud *et al.* [Baud 96] measured ρ_c of W contacts on n-type 6H-SiC using the circular TLM pattern and a cross bridge Kelvin resistor (CBKR). As shown in Fig. 8, the contact resistivity obtained by the two methods for different doping levels provides a good linear fit of decreasing ρ_c as the doping increases.

The high work function combined with the wide bandgap of SiC makes it difficult to form ohmic contacts with low contact resistivity, especially for lightly doped substrates or epilayers. Al forms a good ohmic contact to

p-SiC only after diffusing into SiC during annealing. This creates a highly doped surface and reduces the width of the barrier through which carriers can then tunnel. Unfortunately, the resulting contact resistivity is not low enough. Furthermore, Al oxidizes rapidly, thereby degrading the contact. The high contact resistivity for Al/p-SiC contacts could be due to several factors

1. Interfacial oxide layer
2. Oxidation of the contact metal surface
3. Depletion of carriers in the SiC surface below the contact due to the formation of SiO_2 upon annealing; this depletion would result in a higher contact resistivity because current transport across the contact occurs by carrier tunneling and is thus dependent on the carrier concentration in SiC at the surface.

Porter and Davis [Porter 96] deposited metal contacts by electron-beam evaporation in UHV. Ni and Au contacts were rectifying and resulted in high SBHs ($\sim 1.3 \text{ eV}$). As-deposited Ni/Ni-Al/6H-SiC contacts were also rectifying. After annealing at 1000°C for 80 s, the Ni/Ni-Al contacts showed ohmic behavior with somewhat large contact resistivity ranging from 1.9×10^{-2} to $3.1 \times 10^{-2} \Omega\text{-cm}^2$.

Spieß *et al.* [Spieß 96] reported Al-Ti ohmic contacts to p-type 6H-SiC, with room-temperature values of ρ_c varying between 5×10^{-4} and $5 \times 10^{-3} \Omega\text{-cm}^2$. These contacts were deposited on two types of samples. The first type of samples as unimplanted but had different epitaxial doping levels. The second type of samples was implanted with different doses of Al at 50 keV, and subsequently annealed at 1650°C for 30 min. Table III shows the summary of their results. For contacts on unimplanted samples, the lowest ρ_c achieved was $1.2 \times 10^{-2} \Omega\text{-cm}^2$ after annealing at 1050°C . The implanted contacts with an implant dose of $1 \times 10^{15} \text{ cm}^{-2}$ show the best specific contact resistance of $5.6 \times 10^{-4} \Omega\text{-cm}^2$ after annealing at 550°C .

2. SCHOTTKY CONTACTS TO 6H-SiC

Schottky diodes based on both n- and p-type 6H-SiC reported to date are summarized in Table IV. The first rectifying junctions on 6H-SiC were prepared by fusing small pellets of Si-Al and Si-B alloys to SiC single crystals at 1700°C and $> 2000^\circ\text{C}$, respectively [Hall 58]. These rectifiers showed a sharp breakdown at voltages around $\sim 50 \text{ V}$, and several of them had reverse currents less than 1 mA before breakdown occurred. Typically these junctions had a reverse current of 1 mA at a reverse bias of 14 V, and a forward drop of 4.5 V at a forward current of 0.5 A.

The first barrier height studies on Schottky contacts to 6H-SiC were reported by Mead and Spitzer [Mead 64] and by Mead [Mead 66] using Al and Au on n-type SiC. These studies concluded that the SBH (determined using differential capacitance-voltage techniques) is almost independent of the work function of the metals utilized for the contact, and has a value of 1.95-2.0 V. This was strong evidence for Fermi-level pinning due to the presence of surface states. Similar conclusions were also drawn by Hagen [Hagen 68] from studies on the SBHs of Au, Ag, and Al on both p- and n-type samples of cleaved and etched 6H- and 15R-SiC polytypes. The ideality factor determined from the I-V characteristics of these diodes was found to be between 1.5 and 2.0.

TABLE III
SPECIFIC CONTACT RESISTANCE FOR THE NONIMPLANTED AND IMPLANTED Al/Ti CONTACTS ON P-TYPE 6H-SiC [Spieß 96]

Nonimplanted Samples			
N_A [cm ⁻³]	Annealing Temperature [K]	ρ [Ω -cm ²]	Effective N_A [cm ⁻³] (calculated)
1.2×10^{15}	500-1320	Not ohmic	9.5×10^{14}
2.6×10^{17}	500-1320	Not ohmic	2.9×10^{16}
1.4×10^{18}	Unannealed	Not ohmic	7×10^{16}
	500	7.1×10^{-1}	
	620	5.4×10^{-1}	
	820	1.9×10^{-1}	
	1320	8.2×10^{-2}	
Implanted Samples			
Implant Dose [Al ⁺ /cm ²]	Annealing Temperature [K]	ρ [Ω -cm ²]	Effective N_A [cm ⁻³] (Calculated)
3.3×10^{13}	Unannealed	4.5×10^{-1}	1.5×10^{17}
	500	7.9×10^{-2}	
	770	2.5×10^{-2}	
1.0×10^{14}	Unannealed	1.7×10^{-1}	2.1×10^{17}
	500	3.1×10^{-2}	
	770	1.8×10^{-2}	
3.3×10^{14}	Unannealed	3.3×10^{-2}	4.8×10^{17}
	500	3.6×10^{-2}	
	770	2.0×10^{-2}	
1.0×10^{15}	Unannealed	9.7×10^{-3}	8.7×10^{17}
	500	5.6×10^{-3}	
	770	5.6×10^{-4}	

TABLE IV
SCHOTTKY CONTACTS TO 6H-SiC

SBH ϕ_b (eV)	Method of ϕ_b Measurement	Comments	Ref.
1.45	C-V, PR	Samples cleaved in vacuum	[Hagen 68]
1.10-1.21 (C-face), 0.83-0.97 (Si-face)	I-V, C-V, XPS	Interface layer suspected	[Waldrop 92]
1.15	PR		[Hagen 68]
2	C-V		[Mead and Spitzer 64]
1.45	C-V, PR		[Hagen 68]
1.7	C-V	Anneal: 900°C, 3 min	[Yasuda 87]
0.84-0.96 (C-face)	I-V, C-V, XPS		[Waldrop 92]
0.26-0.30 (Si-face)	I-V, C-V, XPS	Anneal: 600°C, 30 sec	[Waldrop 93]
0.82-1.21 (Si-face)	I-V, C-V, XPS		[Waldrop 93]
0.678 (I-V)	I-V, C-V	Oxide-like interface layer suspected	[Zhang 96]
1.36, 1.45	PR, C-V		[Hagen 68]
1.71	I-V	AlTi backside ohmic contact	[Hagen 68]
1.95	C-V		[Mead and Spitzer 64]
1.45	C-V, PR		[Hagen 68]
1.40	I-V, C-V, PR		[Wu 74]
1.4-1.63	I-V	Vacuum deposition: 500°C	[Anikin 91]
2	C-V	Properties improved with etching damage layer	[Dmitryev 92]
1.14-1.19 (C-face)	I-V, C-V, XPS		[Waldrop 92]
1.37-1.40 (Si-face)	I-V		[Urusidani 94]
0.693 (I-V)	I-V, C-V	Oxide-like interface layer	[Zhang 96]
1.54 (C-V)	PR, C-V		[Hagen 68]
1.07, 1.37	I-V		[Porter 94]
1.27	I-V		[Lundberg 94]
0.79	I-V, C-V		[Lundberg 93]
1.06-1.15	I-V, C-V, XPS		[Porter 95b]
1.05 (C-V)	C-V, I-V		[Lundberg 94]
0.96 (I-V)		Anneal: 500-900°C	

Wu and Campbell [Wu 74] performed a study of the I-V characteristics of Au/6H-SiC Schottky barrier diodes. They found the ideality factor to be 1.07 ± 0.02 for voltages between 0.35 and 0.85 V. The forward I-V characteristics were found to agree quantitatively with the theory based on thermionic emission with the barrier height modified by image-force lowering. The barrier height for contacts on n-type samples was deduced from photoresponse, differential capacitance-voltage, and forward I-V characteristics, and was found to be 1.40 ± 0.05 V.

Yasuda *et al.* [Yasuda 87] studied the annealing effects on Al/n-type 6H-SiC Schottky contacts deposited on both the Si- and the C-face. Their study showed significant improvement in the electrical characteristics of the diodes when they were annealed at 900°C. The ideality factor decreased from a wide range of 3.2 to 10.0 to the fairly narrow range of 2.0 to 2.3 as the diodes were annealed at 660 to 900°C. The built-in voltage (V_{BI}) for diodes on the Si-face was found to be stable at 1.7 V and did not change as the anneal temperature was increased from 660 to 900°C. However, V_{BI} for diodes on the C-face decreased from 3.5 to 1.7 V as the temperature was increased progressively in this range. The capacitance characteristics of the diodes on the C-face also showed dependence on the anneal temperature, which is believed to be due to the possible formation of Al_2O_3 or SiO_2 at the Al/SiC interface.

Anikin *et al.* [Anikin 91] reported Au/6H-SiC diodes capable of operating at temperatures up to 300°C. A forward current density exceeding 300 A/cm² was observed at a forward drop of ~4 V. The barrier height of Au on n-type 6H-SiC was found to be 1.4 to 1.63 V at room temperature, and an abrupt breakdown was observed under reverse bias at 100 to 170 V. The capacitance was found to be independent of frequency in the 1 to 100-kHz range.

Schottky barriers for Pd, Au, Ag, Tb, Er, Mn, Al, and Mg to n-type SiC were investigated by Waldrop *et al.* [Waldrop 92]. They reported on the interface chemistry and also presented values of SBH for these metals on both Si- and C-faces of 6H-SiC obtained by different methods, including I-V and C-V characteristics, and x-ray photoemission spectroscopy (XPS). Figure 9 shows a plot of these values of SBH for both Si- and C-face versus the respective metal work function value. ϕ_{Bn} for different metals is seen to take a wide range of values, extending from 0.3 eV for Mg (Si-face) to 1.6 eV for Pd (C-face), thus providing strong evidence against Fermi-level pinning. In later studies, Waldrop and Grant [Waldrop 93] reported the crystal-face dependence of barrier height and interface chemistry for Ni, Ti, and Al on n-type 6H-SiC. As the contacts were annealed at higher temperatures (400°C), it was observed that Al had a limited reactivity and no crystal-face dependence, whereas Ni and Ti were found to be significantly more reactive

[Lundberg 94]	Anneal: 500-900°C	I-V, C-V	1.41 (I-V)	p	CoSi ₂
[Zhang 96]	Oxide-like interface layer suspected	I-V, C-V	1.9 (C-V) 0.681 (I-V)	n	Cr
[van Elsborgen 96]	Fermi-level pinning	MIGS	0.57 ± 0.05	n	Cs
[van Elsborgen 96]	Fermi-level pinning	MIGS	2.28 ± 0.1	n	Cs
[Porter 93]	Anneal: 700°C, 20-60 min	I-V, C-V	0.97	n	Hf
[Porter 93]		I-V, C-V	1.01-0.86	n	Hf
[Waldrop 92]		I-V, C-V, XPS	0.33 (C-face)	n	Mg
[Waldrop 92]	Anneal: 400°C	I-V, C-V, XPS	0.30-0.34 (Si-face)	n	Mn
[Waldrop 92]		I-V, C-V, XPS	0.79-0.81	n	Mn
[Waldrop 93]		I-V, C-V, XPS	1.59-1.76 (C-face)	n	Ni
[Waldrop 92]	Anneal: 600°C	I-V, C-V, XPS	1.24-1.29 (Si-face)	n	Ni
[Waldrop 93]		I-V, C-V, XPS	1.51-1.66 (C-face)	n	Ni
[Waldrop 93]		I-V, C-V, XPS	1.23-1.25 (Si-face)	n	Ni
[Waldrop 93]		I-V, C-V, XPS	1.16-1.41 (Si-face)	n	Ni
[Lang 96]	Sacrificial oxidation, Ni	I-V	1.17	n	Ni
[Lang 96]	backside ohmic contact	I-V, C-V	0.696 (I-V)	n	Ni
[Zhang 96]	Oxide-like interface layer suspected	I-V	1.02 (C-V)	p	Ni
[Lang 96]	AlTi backside ohmic contact	I-V	0.96	p	Ni
[Porter 96]	Unannealed	I-V, C-V, XPS	1.37	p	NiAl
[Porter 96]		I-V	1.36	p	NiAl
[Waldrop 92]		I-V, C-V, XPS	1.58-1.62 (C-face)	n	Pd
[Waldrop 92]		I-V, C-V	1.11-1.26 (Si-face)	n	Pd
[Bhatnagar 92]	Films deposited at 140°C	I-V, C-V	1.04-1.10	n	Pt
[Porter 93, 95d]	Anneal: 450-750°C, 20 min	I-V, XPS	1.06-1.33	n	Pt
[Porter 93, 95d]		I-V	1.15-1.26	n	Pt
[Shahish 96]	Au-TaSiN overlayer	I-V	0.71 (before anneal)	n	TaSi ₂
[Shahish 96]		I-V	0.62 (after anneal)	n	TaSi ₂
[Spellman 92, Porter 93, 95a]	Unannealed	I-V, C-V, XPS	0.84-0.88	n	Ti
[Spellman 92, Porter 93, 95c]	Anneal: 700°C, 40-60 min	I-V, C-V	0.86-1.04	n	Ti
[Waldrop 93]		I-V, C-V, XPS	1.00-1.09 (C-face)	n	Ti
[Waldrop 93]	Anneal: 400°C	I-V, C-V, XPS	0.73-0.75 (Si-face)	n	Ti
[Waldrop 93]		I-V, C-V, XPS	0.98-1.05 (C-face)	n	Ti
[Lang 96]	AlTi backside ohmic contact	I-V	0.51	p	Ti
[Lundberg 96a, 96b]	Anneal: 800°C, 2 hrs	I-V	0.79-0.87	p	Ti
[Lundberg 96a, 96b]		I-V	1.57-1.8	p	Ti

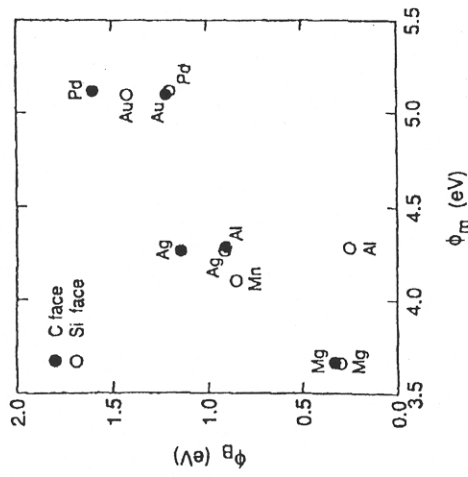


Fig. 9. Plot of the SBH of various metal contacts to n-type 6H-SiC as a function of ϕ_m [Waldrop 92].

to the C-face than the Si-face. Figure 10 shows the representative I-V data for the Ti and Ni contacts that were characterized by XPS studies. The solid curve is for unannealed contacts, whereas the dashed curves are for contacts annealed at 400°C for 30 s. SBHs of Pd, Ni, Au, Ag, Mg, Ti, and Al to p-type 6H-SiC were also reported by Waldrop [Waldrop 94]. Figure 11 summarizes these results in a form similar to that of Fig. 9. Values of ϕ_{Bp} are shown to be in the range of 1.17 to 2.56 eV and are dependent on the metal work function and the crystal face. A comparison with the previously reported values of ϕ_{Bn} for similar metals showed that, as predicted by theory, the sum of ϕ_{Bp} and ϕ_{Bn} is close to the value of the bandgap for 6H-SiC.

Dmitriev *et al.* [Dmitriev 92] reported that the SBH of Au/6H-SiC contacts is sensitive to damage on the surface due to substrate polishing or to high-temperature annealing during final stages of epitaxial growth. These damaged regions can evidently be removed by etching a thin layer off the top surface. As seen in Fig. 12, this damage layer is 1 to 2 μm thick for epitaxial films grown by the sublimation technique at high temperature ($\sim 2000^\circ\text{C}$) and $\sim 5 \mu\text{m}$ thick for substrates grown by the Lely technique. ϕ_B was consistently determined to be 2 eV when the surface was etched beyond this damage layer. The I-V characteristics also showed an improvement when the damaged layer was etched off.

Spellman *et al.* [Spellman 91, 92], Porter *et al.* [Porter 93, 94], and Porter and Davis [95c] reported the effect of annealing conditions on the electrical characteristics of Ti/6H-SiC Schottky diodes. The SBH of unannealed

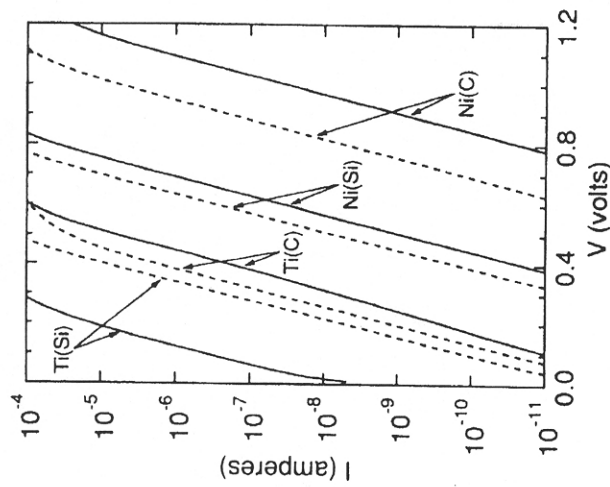


Fig. 10. Forward current-voltage characteristics of Ni and Ti Schottky diodes on Si-face and C-face 6H-SiC. Solid curves are for unannealed contact and dashed curves are for contact annealed at 400°C for 30 s. [Waldrop 93].

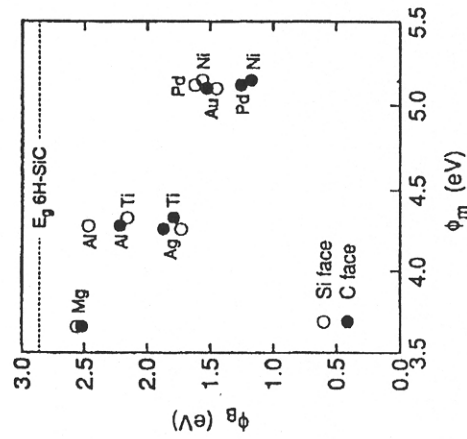


Fig. 11. SBH versus ϕ_m for different metals on p-type 6H-SiC [Waldrop 94].

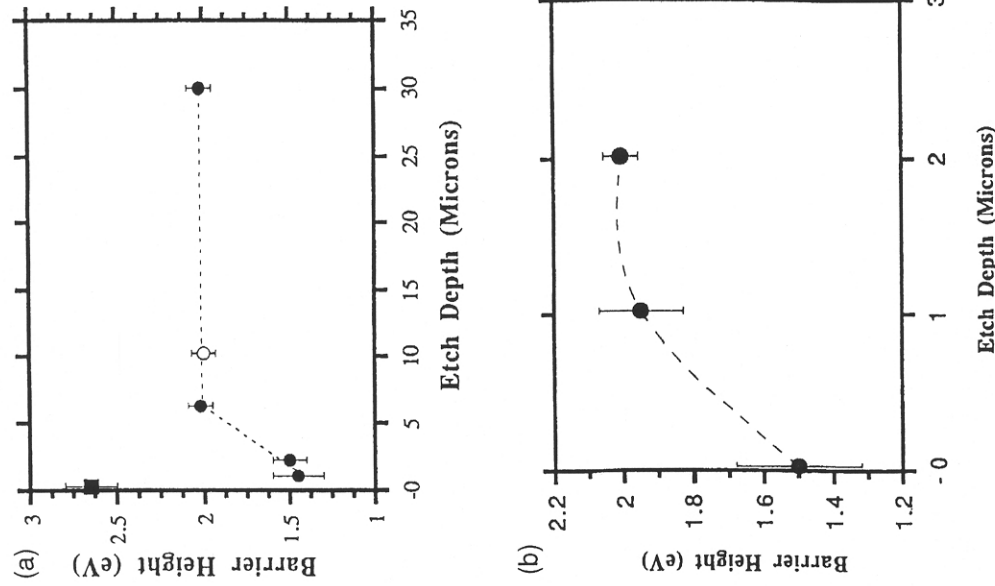
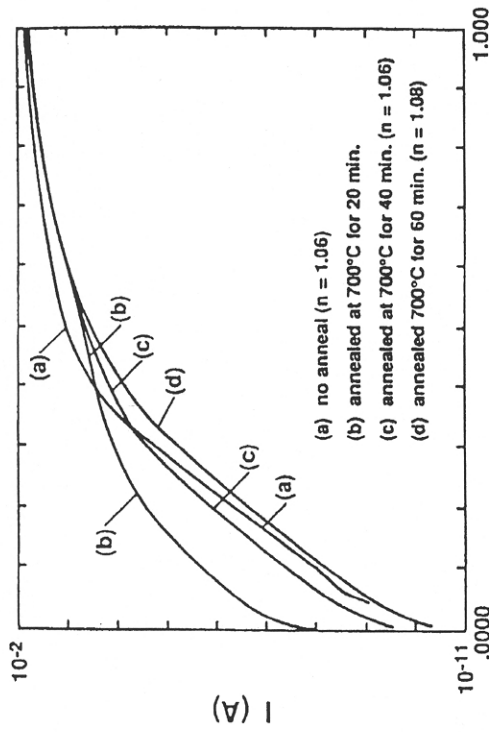


FIG. 12. Variation of SBH on the etch depth of: (a) 6H-SiC substrate; (b) 6H-SiC epitaxial film [Dmitriev 92].

contacts was found to be $\phi_{Bn} = 0.79 \pm 0.1$ eV. Low ideality factors ($1.02 - 1.09$) and reverse leakage currents (9×10^{-8} A/cm² at -10 V) were reported for these epitaxially grown rectifying contacts. Figure 13 shows the effect of annealing conditions on the forward current-voltage characteristics of these diodes. A degradation of the characteristics is evidenced from the more restricted linear regime after a 20-min anneal in UHV at 700°C .



V. (V)

FIG. 13. Effect of annealing conditions on forward current-voltage characteristics of Ti/6H-SiC Schottky diodes [Spellman 92].

However, the characteristics are seen to improve again after each subsequent 20-min anneal. The SBH of these contacts determined from differential capacitance-voltage measurements was found to increase from 0.88 eV for as-deposited contacts to 1.04 eV after a 60-min anneal at 700°C .

Porter *et al.* [93, 94] and Porter and Davis [95b, 95c] the interfacial chemistry, microstructure, and the effect of high-temperature annealing on the electrical behavior of Pt, Co, and Hf contacts on n-type 6H-SiC. The metals were deposited in UHV by electron beam evaporation and formed Schottky contacts in the as-deposited state. The SBH for the unannealed Pt and Co contacts as determined from XPS analysis was found to be 1.33 ± 0.1 and 1.06 ± 0.1 eV, respectively. The SBH for the unannealed Hf contact was reported to be 0.97 eV. Ideality factors below 1.1 and leakage currents in the 10^{-8} A/cm² range at a reverse voltage of 10 V were reported for Schottky diodes formed using these metals. As shown in Fig. 14, Pt contacts remained rectifying even after annealing at 700 to 750°C , and their SBH was found to increase with anneal temperature. Hf contacts also maintained rectifying behavior upon high-temperature annealing at 700°C . The Hf-SiC SBH first increased after a 20-min anneal at 700°C but then successively decreased after the 40-min and 60-min anneals. Co contacts became ohmic after heating to 1000°C , but their resistivity increased when the anneal time was increased from 2 to 3 min.

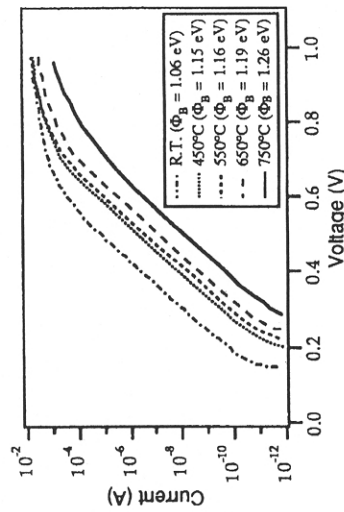


Figure 4. Log I vs. V of Pt/SiC (contact area = 2.0×10^{-3} A/cm 2).

FIG. 14. Effect of annealing on forward characteristics of Pt/6H-SiC diodes [Porter 93].

Cobalt disilicide Schottky contacts on both n- and p-type 6H-SiC were investigated by Lundberg and Östling [94] and Lundberg [95]. The contacts showed good rectifying characteristics after annealing at 700°C, and the SBH was found to be 1.05 ± 0.05 and 1.90 ± 0.05 eV to n- and p-type SiC, respectively. Lundberg *et al.* [96a and Lundberg and Östling 96b] also studied tungsten contacts deposited by chemical vapor deposition (CVD) on n- and p-type 6H-SiC. With n-type SiC these contacts had a low room-temperature barrier height of 0.87 eV and ideality factors close to unity. Figure 15a shows the I-V characteristics of these diodes as a function of temperature. It can be seen that there is only a slight change in the value of the SBH and ideality factor when the temperature was increased up to 160°C. Upon annealing these contacts at 800°C for 2 hr, ϕ_{Bn} at room temperature decreased to 0.79 eV. For contacts to p-type SiC, the room-temperature barrier height decreased from 1.8 to 1.57 eV, and the ideality factor decreased from 1.51 to 1.2 when the contacts were annealed under similar conditions. Figure 15b shows the variation of I-V characteristics of these contacts as a function of temperature. It can be seen that for these diodes, the current grows nearly exponentially over more than six decades. The SBH increases and the ideality factor becomes closer to unity as the temperature is increased to 200°C.

The effect of post deposition annealing of Al Schottky contacts to n-type 6H-SiC has also been studied by Reddy *et al.* [Reddy 96]. Figure 16 shows the systematic improvement in the forward current-voltage characteristics when these contacts are annealed at different temperatures. Low-temperature electrical behavior of these Schottky barriers was also studied, and it

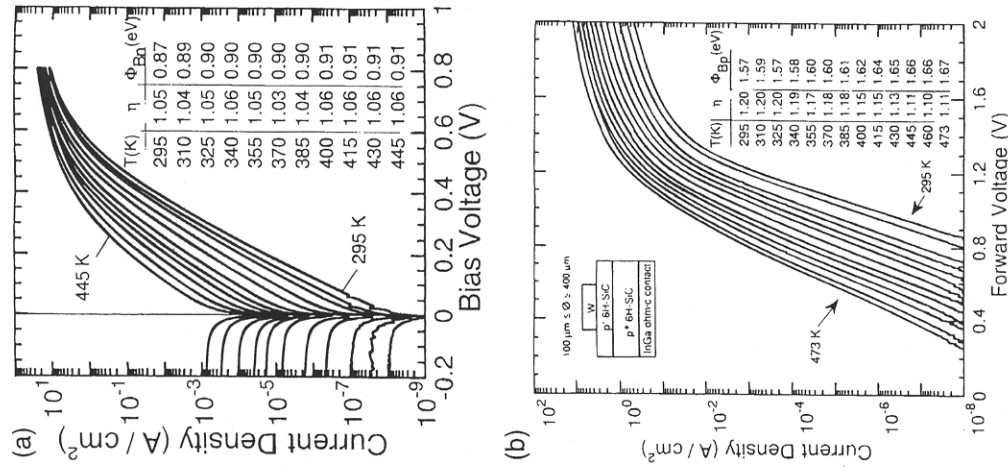


FIG. 15. Forward current-voltage characteristics as a function of temperature for: (a) n-type W/6H-SiC contacts; (b) p-type W/6H-SiC contacts [Lundberg 96b].

was observed that the ideality factor increased, while the SBH decreased significantly as the temperature was reduced to 77 K.

Andreev *et al.* [Andreev 95] found that the barrier height of Au, Mo, Cr, and Al on n-type 6H-SiC was in the range of 1.22 to 1.40 eV and was virtually independent of the metal work function. This was attributed to the large surface state density resulting from their surface preparation techniques. They also reported that ϕ_{Bn} decreases with increasing doping concentration of the epilayer.

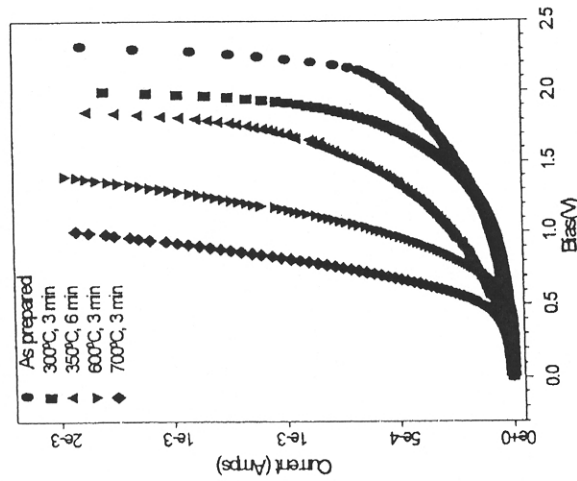


FIG. 16. Improvement of I-V characteristics of Al/6H-SiC diodes as a function of anneal temperature [Reddy 96].

Smith *et al.* [Smith 95] observed that the barrier height of metal Schottky contacts to 6H-SiC changes dramatically with temperature. This change is 10 to 20 times the change in the bandgap over the same temperature range. The change in the diffusion potential for contacts to n-type SiC, and the SBH for contacts to p-type SiC, are shown in Figs 17a and 17b, respectively. It is seen that for n-type material, the diffusion potential, and hence ϕ_{Bn} , decreases with temperature, whereas for p-type material, ϕ_{Bp} increases with temperature. For the same metal, the rate of change in barrier heights to n- and p-type material with temperature is not the same, and therefore their sum deviates from the bandgap of SiC at any given temperature. Fröjdh and Petersson [Fröjdh 1996] argued that for the barrier height extracted from the CV measurements to be reliable, no frequency dependence should exist at the measurement frequencies, and the slope of the $1/C^2$ vs voltage curve should not be temperature dependent. They stated that the existence of this frequency and temperature dependence indicates the presence of deep levels in the SiC samples studied. However, in their reply to the argument of Fröjdh and Peterson, Smith *et al.* [Smith 1996] reported the deep level transient spectroscopy (DLTS) spectrum which showed the absence of deep levels in their samples. They concluded that the argument of Fröjdh and Peterson is valid only at relatively lower temperatures (up to 320 K), and

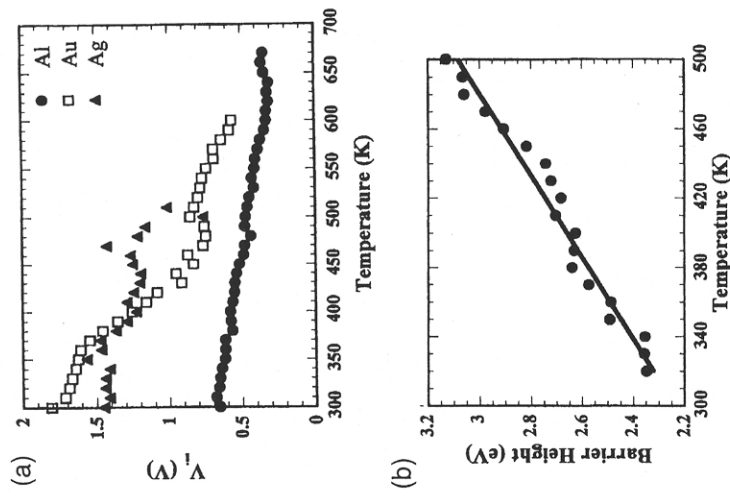


FIG. 17. Contacts to 6H-SiC: (a) n-type diffusion potential versus temperature for Al, Au, and Ag contacts; (b) p-type SBH versus temperature for Al contacts [Smith 95].

that at higher temperatures (300–673 K), this temperature dependence of the barrier height does exist.

Cs/6H-SiC Schottky contacts were studied by van Elsbergen *et al.* [van Elsbergen 96]. The surface preparation technique followed by them resulted in Fermi-level pinning at 1.2 eV above the valence-band maximum, irrespective of doping. The barrier height of the contact was found to be 0.57 ± 0.05 eV with n-type and 2.28 ± 0.1 eV with p-type doped samples.

The effect of postdeposition annealing conditions on the SBH and ideality factors for Au-Ta_{0.2}Si_{0.4}N_{0.4}TaSi₂/6H-SiC and Re/6H-SiC Schottky diodes on n-type SiC have been reported by Shalish *et al.* [Shalish 96]. The SBH and the ideality factor of contacts with Au overlayers decrease from 0.71 eV and 1.55 for the as-deposited case to 0.62 eV and 1.18 when annealed at 600°C for 30 min. ϕ_{Bn} and η for Re contacts changed from 0.71 eV and 1.6 to 1.04 eV and 1.16 after annealing at 700°C and to 0.76 eV and 1.36 after annealing at 900°C.

3. HIGH-VOLTAGE SCHOTTKY DIODES ON 6H-SiC

SiC-based Schottky diodes that are capable of operating at high (>100 V) reverse voltages are summarized in Table V. A predictive model of SiC power Schottky diode has been reported by Kneifel et al. [Kneifel 1996]. The great majority of Schottky diodes to date have been fabricated on n-type SiC. The first high-voltage Schottky barrier rectifiers were reported by the North Carolina group [Bhatnagar 92]. As shown in Figs. 18a and 18b, these Pt/6H-SiC diodes had a blocking voltage in excess of

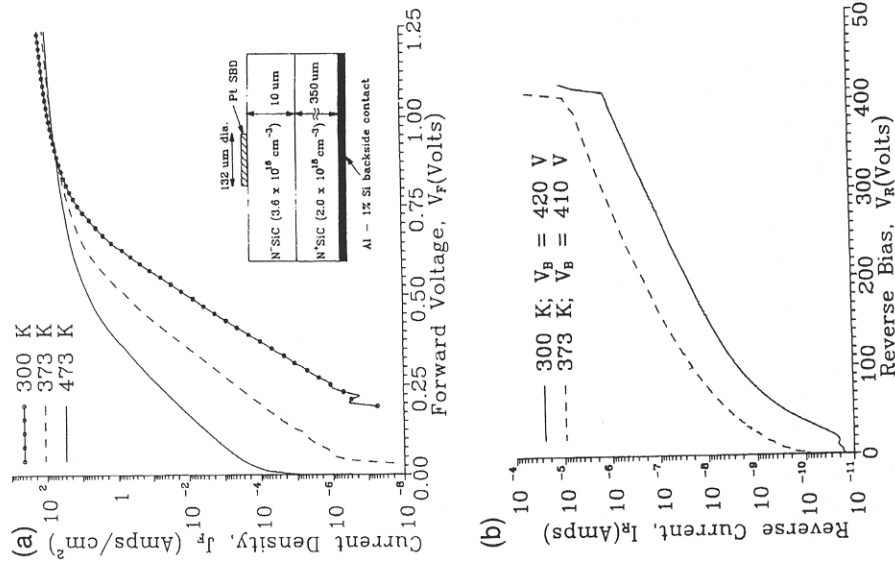


Fig. 18. Current-voltage characteristics of Pt/6H-SiC diode: (a) forward bias; (b) reverse bias [Bhatnagar 92].

TABLE V
HIGH VOLTAGE (>100 V) SCHOTTKY BARRIER DIODES ON 4H- AND 6H-SiC

Scheme: M_1/M_2	Doping Conc. of Drift Layer (n-type) (cm^{-3})	Thickness of Drift Layer (μm)	Diode Ideality Factor	Forward Current Density at X Volts (A/cm^2)
M_1 : Schottky Metal				
M_2 : Ohmic Metal				
Au/Ni/4H	5×10^{15}	10	1.08	100 at 1.67
Ni/Ni/4H	5×10^{15}	10	1.01	100 at 1.50
Ti/Ni/4H	5×10^{15}	10	1.03	100 at 1.12
Ti-Al (1:1)/Ti-Al (1:1)/4H	1×10^{16}	10	1.2	100 at 1.06
Ti/Ni/4H	$7-20 \times 10^{15}$	10	1.03	100 at 1.3
edge termination: B ⁺ impl.				(200 at 2.5)
Ti-Al (1:3)/Ni/6H	9×10^{15}	2.4	1.07	~1 at 1
Ti-Al/Ni/6H with guard ring	1.3×10^{16}	4.7	NR	NR
Ni/Ni/6H	1.3×10^{16}	10	1.08-1.12	55 at 2
Ti-Al/Ti-Al/6H	2×10^{16}	10	NR	NR
edge termination: Ar ⁺ impl.				
Au/Ni/6H	5.8×10^{15}	9.6	1.1-1.3	42 at 2
Ni/Ni/6H	7.2×10^{15}	10	1.19	63.37 at 2
Ni/Ni/4H	6.1×10^{15}	10	1.29	100 at 1.86
Pt/Ni/4H	6.1×10^{15}	NR	1.11	100 at 1.76
Au/NR/6H	$5-10 \times 10^{16}$	NR	1.05-1.07	333 at 4
Pt/Al-Si/6H	4×10^{16}	10	1.1	100 at 1.1
4H	7.5×10^{15}	10	—	100 at 1.1
edge termination: Ar ⁺ impl.				
Ni/4H	3.5×10^{15}	13	—	100 at 2
edge termination: B ⁺ impl.				
Ti/4H	3.5×10^{15}	13	—	70 at 1
edge termination: B ⁺ impl.				

400 V and a low forward drop of ~1.1 V at an on-state current density of 100 A/cm². The reverse current density was $\sim 7.3 \times 10^{-3}$ A/cm² at a reverse bias of 400 V. This translates into an $I_{\text{ON}}/I_{\text{OFF}}$ ratio of $\sim 1.4 \times 10^4$. The breakdown voltage obtained for these diodes was only 40 to 70% of the ideal parallel plane breakdown voltage. This was explained to be due to the formation of a surface depletion layer on SiC caused by the presence of a high density of defect states at the interface. The fabrication of these diodes was a significant achievement, and it convinced researchers of the potential success of Schottky contact-based devices on SiC in the coming years.

Subsequently, high-voltage Au/6H-SiC Schottky diodes were reported by the Kyoto group [Urushidani 94, Kimoto 93]. As seen in Fig. 19, these diodes had breakdown voltages exceeding 1100 V and were shown to be capable of operating at temperatures up to 400°C. The ideality factor and the SBH were determined [Kimoto 93] as 1.2 and 1.4 eV, respectively, and a forward current density of 42 A/cm² was obtained at a voltage drop of 2 V. Figure 20 shows the temperature dependence of the specific on-resistance for these SiC Schottky diodes (experimental data) and for a Si Schottky rectifier with the same blocking voltage (theoretical data). The R_{on} for a Si

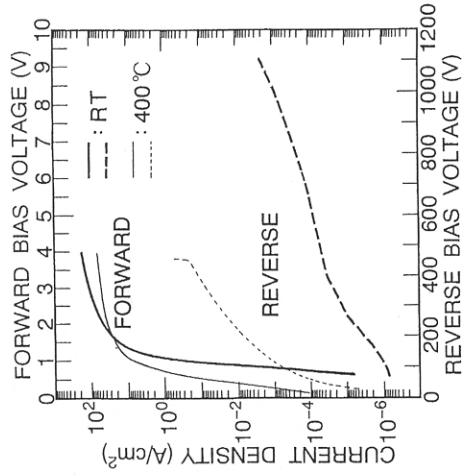


FIG. 19. Current-voltage characteristics of 1100-V 6H-SiC SBD at room temperature and 400°C [Kimoto 95].

Breakdown Voltage (V)	Theoretical Breakdown Voltage	% Theoretical Breakdown Voltage	Reverse Leakage Current Density (A/cm²) at X Volts	Specific On-Resistance Ω-cm²	Ref.
790	31.2		2.9×10^{-4} at 700	1.4×10^{-3}	[Itoh 95a, 95c]
~790	31.2		$\sim 2.9 \times 10^{-4}$ at 700	$\sim 2 \times 10^{-3}$	[Itoh 95a, 95c]
~790	31.2		$\sim 2.9 \times 10^{-4}$ at 700	$\sim 2 \times 10^{-3}$	[Itoh 95a, 95c]
1000	48.4		6×10^{-5} at 100	2.1×10^{-3}	[Raghunathan 95]
1100-1750	46.9-74.6		$\sim 1 \times 10^{-4}$ at 500	$1-3 \times 10^{-3}$	[Itoh 96]
250	34.7		$\sim 3 \times 10^{-5}$ at 200	NR	[Ueno 95, 96]
550	44.5		~ 0.1 at 500	NR	[Ueno 95, 96]
1100	55.4		1.4×10^{-3} at 900	NR	[Su 96]
~1000	75.2		~ 0.1 at 600	NR	[Alok 94]
>1100	42.8		2.1×10^{-3} at 1100	8.5×10^{-3}	[Kimoto 93]
800-1000	31.6-40.0		4.8×10^{-3} at 800	3.5×10^{-2}	[Saxena 96]
1000	41.2		3.6×10^{-4} at 600	8×10^{-3}	[Saxena 98]
1000	41.2		1.14×10^{-6}	8.39×10^{-3}	[Saxena 98]
100-170	—		$\sim 3.3 \times 10^{-6}$ at 150	$6-9 \times 10^{-3}$	[Anikin 91]
400	58.5		2.19×10^{-5} at 100	3×10^{-3}	[Bhatnagar 92]
1400	—		0.8 at 1000	1.5×10^{-3}	[Weitzel 96]
1720	—		10^{-4} at 1000	5.6×10^{-3}	[Cooper 98]
1500	—		0.1 at 1000	—	[Cooper 98]

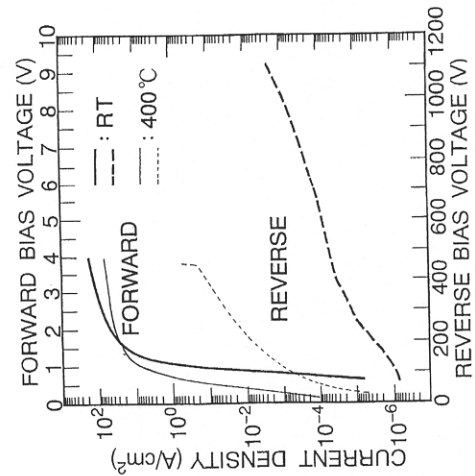


FIG. 20. Temperature dependence of specific on-resistance for SiC (experimental results) and Si (theoretical results) [Kimoto 93].

device is calculated to be ~20 times larger than the value measured for the SiC device. In addition, R_{on} for SiC is somewhat less sensitive to temperature as compared to that for Si.

High-voltage Schottky diodes utilizing Ni for both ohmic and Schottky contacts were reported by the Cincinnati group [Su 95, 96; Saxena 96, 98]. These Ni/6H-SiC SBDs showed a high breakdown voltage (>1000 V) at both 25 and 300°C. The diodes utilized grown oxide for surface passivation and device isolation. Figure 21a shows the cross-sectional view of the Ni/6H-SiC diode structure. As seen in Fig. 21b, these diodes had breakdown voltages exceeding 1100 V and operated at elevated temperatures up to 300°C. The current mechanisms for these diodes in the temperature range of 100 to 573 K have also been reported [Saxena 96]. Under forward bias, the diodes showed exponential behavior over a large voltage range at all temperatures. Figure 21c shows the forward voltage drop (V_F) as a function of temperature for different current densities. At low current-density levels (0.1-10.0 A/cm²), V_F was found to decrease with increasing temperature, from 1.5 to 2.0 V at 100 K to 0.6 to 1.3 V at 300°C. At higher current-density levels (50-80 A/cm²), V_F exhibits a minimum at 200 to 250 K, after which it increases slightly, with temperature reaching values of 2.5 to 3.5 V at 300°C. The rectifier efficiency of these diodes was essentially independent of temperature, with near ideal values (37-39%) up to 600 kHz. The AC power dissipation was also fairly constant over the entire high-temperature range for current values up to 0.1 A, but showed a monotonic increase with temperature for higher current levels.

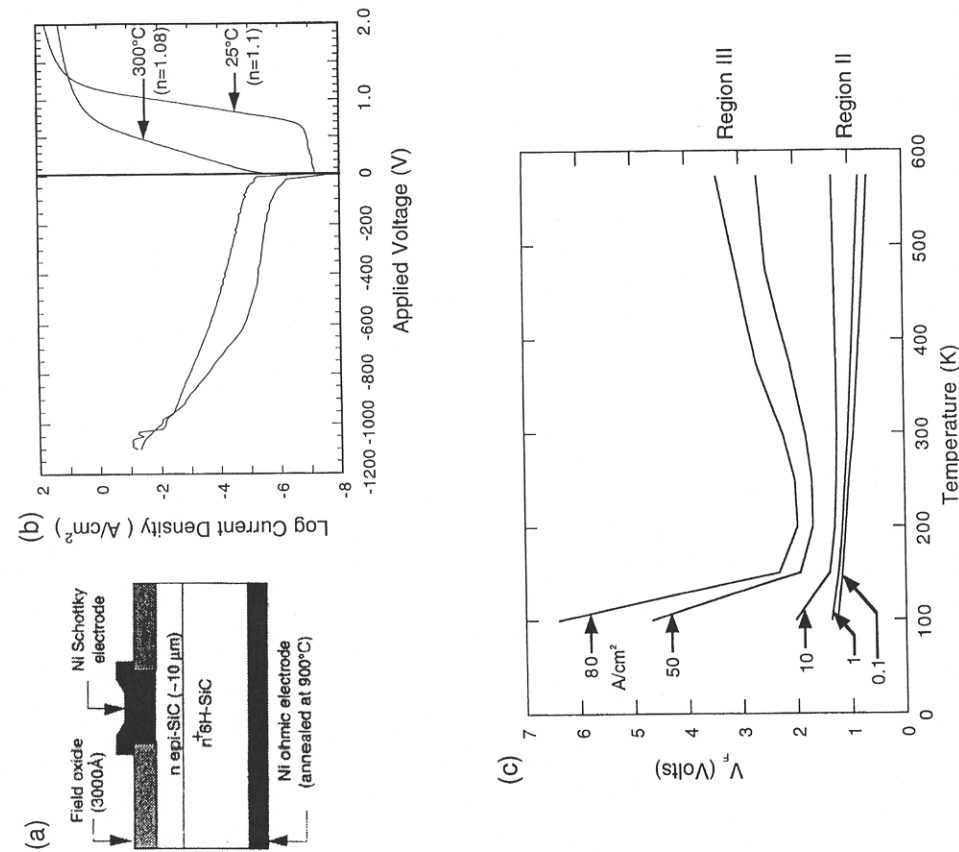


FIG. 21. Ni/6H-SiC Schottky diode with field plate structure: (a) cross-sectional view; (b) I-V characteristics of Ni/6H-SiC SBD at 25 and 300°C; (c) forward voltage drop as a function of temperature for different levels of J_F [Saxena 96]. Region I: current dominated by thermionic emission. Region II: current limited by series resistance.

4. EDGE TERMINATION IN 6H-SiC SCHOTTKY DIODES

For high-voltage Schottky diodes, edge termination plays an important role in determining the breakdown voltage. The experimentally obtained values of breakdown voltages for Schottky diodes without edge termination are usually considerably less than the theoretically calculated values for a parallel plane structure. This is due to the electric field crowding at the diode

edges. For high-voltage SiC SBDs, several techniques have been shown to reduce field crowding at the edges, thus resulting in higher breakdown voltages. The simplest of these is the SiO₂ field plate structure, in which the metal overlaps the oxide so that the maximum electric field (E_{max}) is at the SiO₂-metal interface. In this case, the breakdown voltage should ideally not be affected by electric field crowding. However, since the field plate length in SiC is shorter than in Si because of the smaller space charge region (due to higher E_{max}), a more precise alignment is necessary between the Schottky metal pattern and the contact-hole pattern [Bhatnagar 93a]. Thus, other techniques for edge termination have been investigated. These include: (1) the use of floating metal field rings (FMRs) and resistive Schottky barrier field plates (RESPs) as reported by Bhatnagar and Baliga [Bhatnagar 93b]; (2) the use of implantation of neutral species at the periphery of the diode to form an amorphous layer, reported by Alok *et al.* [Alok 94]; and (3) the guard ring termination, reported by Ueno *et al.* [95, 96].

In their study performed on SiC Schottky barrier diodes with a theoretical breakdown voltage of 1125 V, Bhatnagar *et al.* [96] calculated the breakdown voltage for the unterminated diode and the diode with FMR termination to be 225 and 600 V, respectively. The experimentally determined breakdown voltages for these two diodes were 220 and 400 V, respectively.

Alok *et al.* [94] reported a further improvement in blocking voltages of diodes, with edge termination achieved by Ar implantation. As shown in Fig. 22, nearly ideal breakdown voltage was obtained when a dose of $10^{15}/\text{cm}^2$ was utilized to implant the periphery of Ti/6H-SiC diodes.

Figure 23a shows the cross-sectional view of the Al-Ti/6H-SiC Schottky barrier diode with the guard ring termination reported by Ueno *et al.* [95, 96]. Al-Ti forms a Schottky contact with the n-type drift region, and an ohmic contact with p-type guard rings. Hence, the guard ring is electrically at the same potential as the Schottky contact. E_{max} therefore appears at the edge of the guard ring and not at the Schottky contact. The breakdown voltage is thus not affected by electrical field crowding. Figure 23b shows the improvement in the reverse characteristics of the Schottky diodes with the guard ring structure. These diodes show a breakdown voltage in excess of 550 V, which is about 70% of the ideal breakdown voltage for the epilayer.

5. EXCESS LEAKAGE CURRENT IN SiC SCHOTTKY DIODES

Experimental tests on SiC Schottky diodes have shown that they generate larger leakage currents than theoretically predicted. Figure 24 shows the reverse leakage current observed in Ti and Pt/6H-SiC Schottky barrier

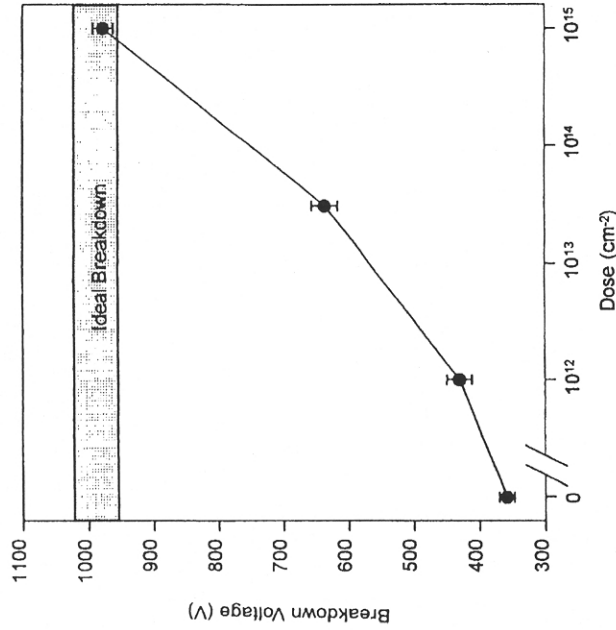


FIG. 22. Breakdown voltage as a function of implant dose on the edge of SBDs [Alok 94].

diodes, and the calculated theoretical values [Bhatnagar 96]. The theoretical values have been calculated assuming thermionic emission and by using the barrier height extracted from C-V measurements [Bhatnagar 92, Urushidani 94]. It can be seen that the observed leakage current is about two orders of magnitude larger than the theoretical value. An attempt has been made to explain the excess leakage currents using a model based on localized defects in the epitaxial layer at the metal-SiC interface. These defects lower the barrier height of the contact at the defect site [Bhatnagar 96]. Analytical and numerical analysis have been performed to study the effect of these barrier height inhomogeneities on the I-V of 6H-SiC SBDs, and good agreement has been achieved with the measured characteristics.

A related explanation for the high reverse currents in SiC Schottky diodes has been offered along similar lines by Schroder *et al.* [Schroder 96]. This explanation is based on the formation of a very thin inhomogeneous interfacial layer between metal and semiconductor. The SBH therefore becomes voltage-dependent. The formation of this layer is postulated to cause the voltage dependence of the reverse current in SiC Schottky contacts, due to pinch-off effects of low barrier regions that surround high barrier regions on the inhomogeneous interfacial layer.

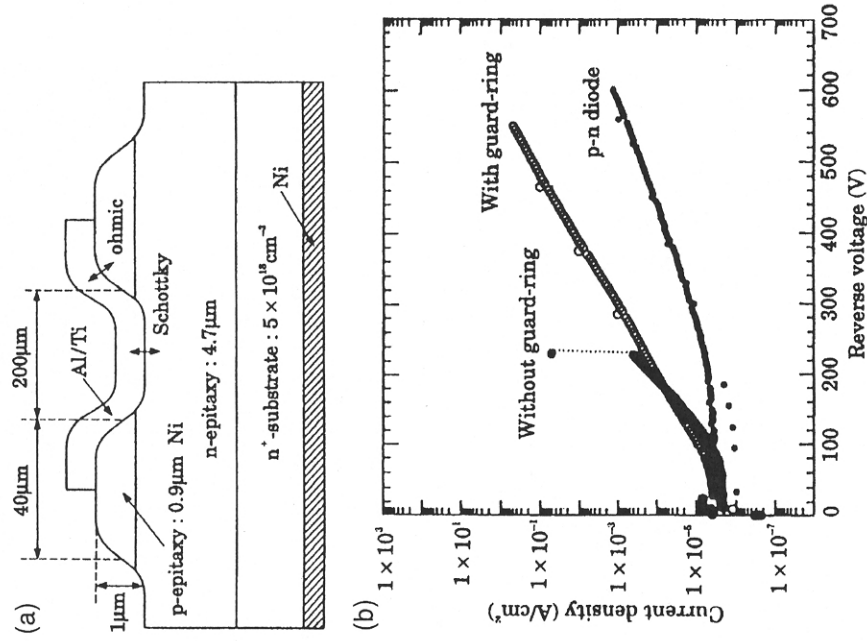


FIG. 23. Al-Ti Schottky barrier diode with guard ring: (a) cross-sectional view; (b) reverse current-voltage characteristics of SBDs with and without guard ring, and the p-n junction [Ueno 95].

Yet another possible cause for larger reverse currents in SiC Schottky diodes could be quantum mechanical tunneling through the Schottky barrier. Crofton and Sriram [Crofton 96b] reported calculations of the reverse current density, which were performed for 6H-SiC using a WKB evaluation of the tunneling probability through a reverse biased Schottky barrier. The image force lowering of the SBH was taken into account in these calculations. Figure 25 shows the comparison of the calculated and experimental reverse leakage currents for Pt-SiC Schottky diodes on n-type

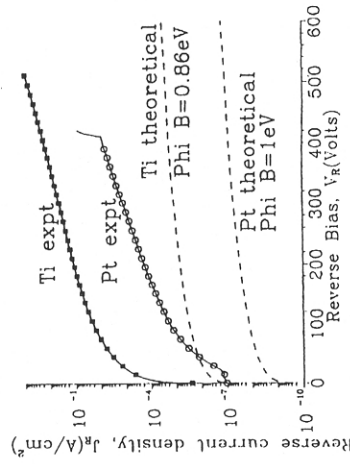


FIG. 24. Experimental and theoretical reverse leakage currents at 300 K for Ti/6H-SiC and Pt/6H-SiC Schottky diodes [Bhatnagar 96].

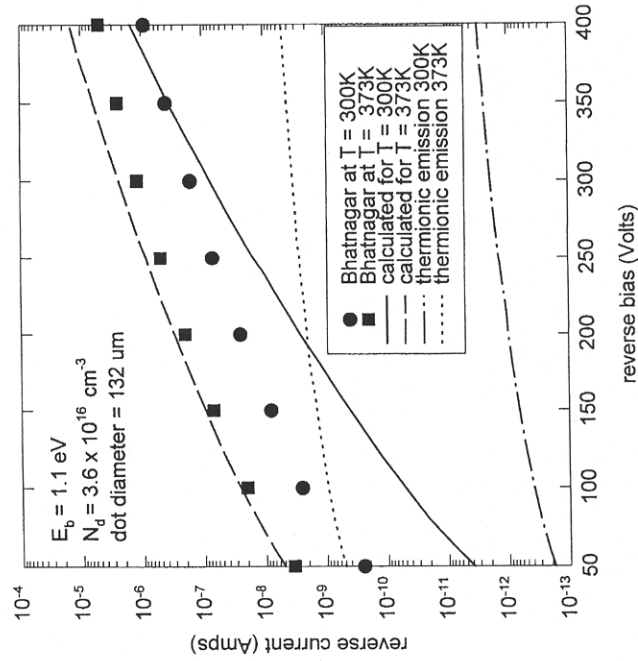


FIG. 25. Comparison of calculated and experimental reverse leakage currents for Pt/6H-SiC Schottky diodes [Crofton 96b].

6H-SiC. It can be seen from this figure that the calculated values of the reverse currents based on the quantum mechanical tunneling theory show better agreement with the previously reported experimental values.

V. Metal Contacts to 4H-SiC

1. OHMIC CONTACTS TO 4H-SiC

Relatively few studies have been performed on ohmic contacts to the 4H polytype of SiC. These studies are summarized in Table VI. Arnodo *et al.* [Arnodo 96] studied ohmic contacts using Ni and Mo. Ni contacts were annealed in the temperature range of 950 to 1000°C, whereas higher temperatures in the 1000 to 1600°C range were utilized for Mo contacts. At doping levels no greater than $5 \times 10^{18} \text{ cm}^{-3}$, both metals offered similar contact resistance (R_c), with best R_c values in the low $10^{-5} \Omega\text{-cm}^2$ range. At higher doping levels, however, R_c for Ni ohmic contacts continues to decrease to values in the low $10^{-6} \Omega\text{-cm}^2$ range, whereas for Mo contacts, no improvement is observed.

Low-resistivity alloyed Al/Ni/Al contacts on 4H-SiC with an R_c value of $1.8 \times 10^{-5} \Omega\text{-cm}^2$ have been reported by Hallin *et al.* [Hallin 97]. This is lower than that obtained for single-layer Ni contacts. Their studies indicate that the first layer of Al prevents void formation at the interface and reduces the interface oxide layer. The Al is also believed to react with the excess carbon left behind due to silicide formation as a result of strong Ni-Si chemical affinity.

2. SCHOTTKY CONTACTS AND HIGH-VOLTAGE SCHOTTKY DIODES ON 4H-SiC

Table VII gives a summary of the studies performed on Schottky barriers for different metals to 4H-SiC. The first high-voltage Schottky barrier diodes on the 4H-SiC polytype were reported by Itoh *et al.* [Itoh 95a, 95c]. Au, Ni, and Ti were employed for forming the Schottky contact. The SBH for these metals was determined by I-V and C-V analysis to be 1.73 to 1.8, 1.6 to 1.7, and 1.1 to 1.15 eV, respectively. Figure 26 shows the SBH for these metals as a function of the respective metal work functions. It can be seen that for metal-4H-SiC structures, the pinning of the Fermi level at the surface does not occur, and the barrier height depends on the metal work function with

TABLE VII
SCHOTTKY CONTACTS TO 4H-SiC

Metallization	Carrier conc. of active region (cm ⁻³)	SiC Type	SBH ϕ_B (eV)	Method of ϕ_B Measurement	Ref.
Au	5×10^{15}	n	1.73-1.8	I-V, C-V	[Itoh 95b]
Ni	5×10^{15}	n	1.6-1.7	I-V, C-V	[Itoh 95b]
Ni	6×10^{15}	n	1.67	I-V	[Saxena 98]
Pt	6×10^{15}	n	1.31	I-V	[Saxena 98]
Ti	5×10^{15}	n	1.1-1.15	I-V, C-V	[Itoh 95b]
Ti	1×10^{16}	n	0.99	I-V	[Ragunathan 95]

TABLE VI
OHMIC CONTACTS TO 4H-SiC

Metallization	Annealing Condition	SiC Carrier Conc. (cm ⁻³)	SiC Type	ρ_c at RT ($\Omega\text{-cm}^2$)	Method of ρ_c Measurement	Ref.
Ni	1000-1200°C, 1 min	3.2×10^{17} and 1.4×10^{18}	n	1.3×10^{-5} to 3.6×10^{-6}	TLM	[Crofton 96a]
Ni	950-1000°C	2×10^{18} to 2×10^{19}	n	4×10^{-4} to 4×10^{-6}	TLM	[Arnold 96]
Mo	950-1000°C	2×10^{18} to 2×10^{19}	n	4×10^{-4} to $\sim 10^{-5}$	TLM	[Arnold 96]
Ni, Ni ₂ W, Ni ₃ Ti ₂ W, Ni/Cr/W	1000-1050°C, 5-10 min	10^{17} - 10^{18}	n	10^{-3} - 10^{-6}	TLM	[Liu 96]
Ct/W, Ct/Mo/W	1000-1050°C, 5-10 min	10^{17} - 10^{18}	n	10^{-2} - 10^{-4}	TLM	[Liu 96]
Al/Ni/Al	1000°C, 5 min	1×10^{19}	n	1.8×10^{-5}	XPS	[Hallin 97]

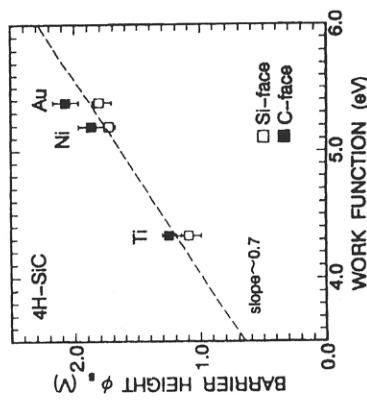


FIG. 26. Barrier height as a function of metal work function for 4H-SiC [Itoh 96b].

a slope of ~ 0.7 . The room-temperature breakdown voltage for these diodes was reported to be 800 V. A current density of 100 A/cm^2 was obtained at a forward drop of 1.67 V. The functional device yield was $\sim 70\%$. Interestingly, the ideal breakdown voltage calculated using the breakdown field and the thickness of the drift region for this device structure should be $\sim 2000 \text{ V}$. The variation of R_{on} as a function of breakdown voltage for Si, 6H-, and 4H-SiC SBDs is plotted in Fig. 27 [Kimoto 93]. The specific on-resistance for these Au/4H-SiC diodes is $1.4 \times 10^{-3} \Omega\text{-cm}^2$, which is two orders of magnitude lower than silicon SBDs with comparable breakdown voltage, and less than one fifth of that observed for similar Schottky diodes on 6H-SiC [Kimoto 93], as discussed before. More recently, the same group [Itoh 96] improved the breakdown of Ti/4H-SiC Schottky diodes by using

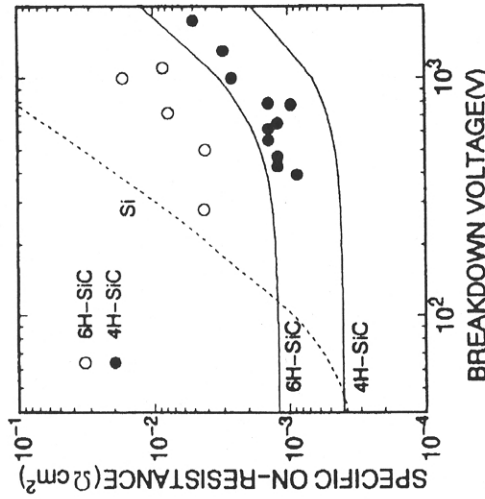


FIG. 27. Dependence of specific on-resistance on the breakdown voltage in Si, 6H-, and 4H-SiC rectifiers [Itoh 95c].

a highly resistive layer at the periphery of the contact for edge termination. The layer was formed by B^+ implantation, followed by a heat treatment to reduce damage to the implanted areas. These diodes showed a higher breakdown voltage of 1100 V compared to 760 V for diodes that did not have any edge termination. Figure 28 shows the current-voltage characteristics of diodes with and without edge termination. Though there is no significant difference in the forward bias characteristics, the leakage current under reverse bias is reduced for diodes with edge termination, thereby allowing higher breakdown voltage exceeding 1100 V.

Raghunathan *et al.* [Raghunathan 95] also reported high breakdown (1000 V) Ti/4H-SiC SBDs with a forward drop of only 1.06 V at a forward current density of 100 A/cm². The SBH for Ti was determined to be 0.99 V by I-V analysis. The specific on-resistance was found to be $2 \times 10^{-3} \Omega\text{-cm}^2$.

Weitzel *et al.* [Weitzel 1996] reported 1400 V 4H-SiC Schottky diodes with an on-resistance of $1.5 \text{ m}\Omega\text{-cm}^2$. These diodes were fabricated on $10 \mu\text{m}$ thick epitaxial layers with a doping level of $7.5 \times 10^{15} \text{ cm}^{-3}$ and utilized Ar implant damage termination. The diodes had a high forward current density of 732 A/cm² at 2 V, but exhibited higher leakage currents ($\sim 0.8 \text{ A/cm}^2$ at -1000 V).

Recently, Saxena and Steckl [Saxena 97, 98] reported SBDs on 4H-SiC using Ni and Pt for Schottky contacts. The current-voltage characteristics

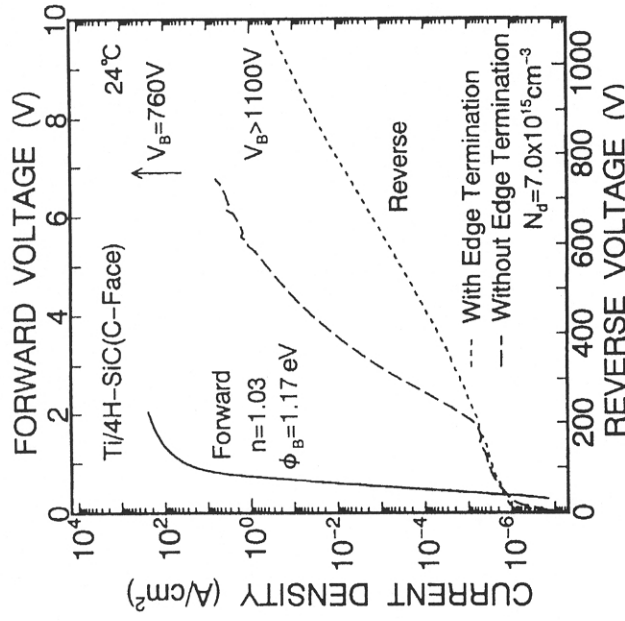


FIG. 28. I-V characteristics of Ti/4H-SiC Schottky rectifiers with and without edge termination [Itoh 96].

of typical Pt/4H SiC and Ni/4H SiC SBDs at room temperature are shown in Fig. 29. A forward current density (J_F) of 100 A/cm² was achieved at a forward voltage drop of 1.76 and 1.86 V, respectively. The ideality factors for the Pt and Ni diodes were calculated from the forward J-V plots as 1.11 and 1.29, respectively. The Schottky barrier height (ϕ_B) and the specific on-resistance (R_{on}) for the Ni/4H-SiC diodes were found to be 1.31 eV and $8 \text{ m}\Omega\text{-cm}^2$, respectively. The saturation current density was found to be $4.7 \times 10^{-15} \text{ A/cm}^2$. Both Ni and Pt diodes were able to withstand reverse voltages in excess of 1000 V. Some diodes had a breakdown voltage as high as 1200 V. Under reverse bias of 600 V, leakage current densities of 1.14×10^{-6} and $3.6 \times 10^{-4} \text{ A/cm}^2$ were measured for the Pt and Ni diodes. The current "on-off" ratio (corresponding to J_F at 2 V divided by J_R at -600 V) was measured at 25°C to be 1.623×10^8 and 2.85×10^6 for the Pt and Ni diodes. Figure 30 shows the forward drop for Ni/4H-SiC diodes versus temperature for current densities 1, 10, and 80 A/cm². It can be seen that the forward voltage drop increases with temperature when the diode is operating at higher current densities, such as

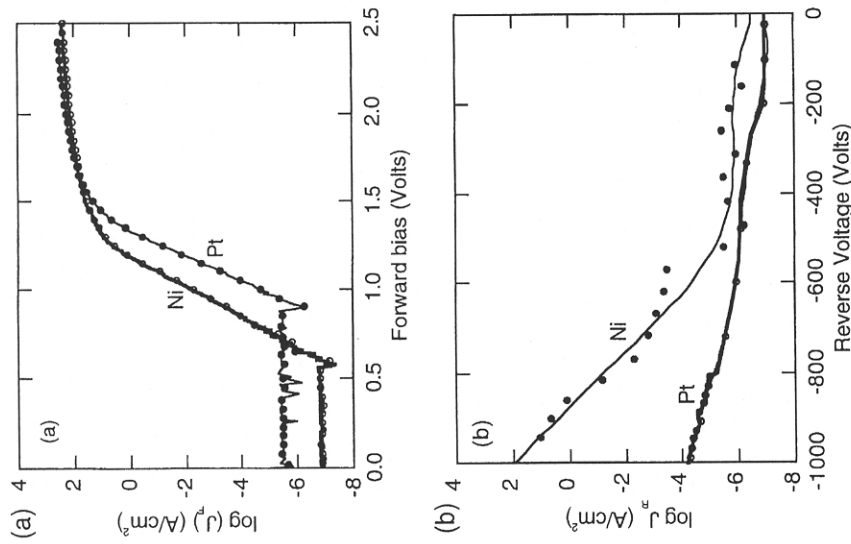


FIG. 29. Current-voltage characteristics of Pt/4H-SiC and Ni/4H-SiC SBD at 25°C: (a) forward bias; (b) reverse bias [Saxena 98].

80 A/cm². This allows for parallel operation [Shenoy 94] of several such diodes for power-switching applications, without current filamentation. The current on-off ratio for the Ni/4H-SiC diodes does not show a significant reduction with temperature up to more than 300°C, where this ratio is still in excess of 10⁶.

Schottky diodes with B-implanted edge termination were reported by Cooper [Cooper 98] on 13 μm 4H-SiC epitaxial layers with doping concentration $3.5 \times 10^{15} \text{ cm}^{-3}$. The Ni/4H-SiC diodes had a high blocking voltage of 1720 V, and a specific on-resistance of 5.6 mΩ-cm². The barrier heights for Ti and Ni on 4H-SiC were determined to be 0.8 and 1.3 eV, respectively.

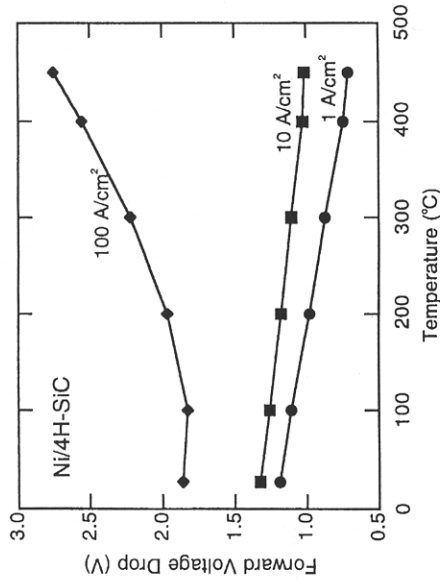


FIG. 30. Forward voltage drop versus temperature for different current densities in Ni SBDs on 4H-SiC [Saxena 98].

Kimoto *et al.* [Kimoto 97, Wahab 98] at Linköping have also recently reported high-voltage (2.2–3.0 kV) Schottky rectifiers fabricated on thick low-doped epilayers grown by high-temperature CVD [Kordina 95a]. The thickness of the epilayer was 42 μm, and the doping level was $\sim 2 \times 10^{15} \text{ cm}^{-3}$. Figure 31 compares the I-V characteristics of the Schottky diodes fabricated on substrates grown at Cree Research and at Linköping. They utilized the “all-Ni” approach for metallization developed at Cincin-

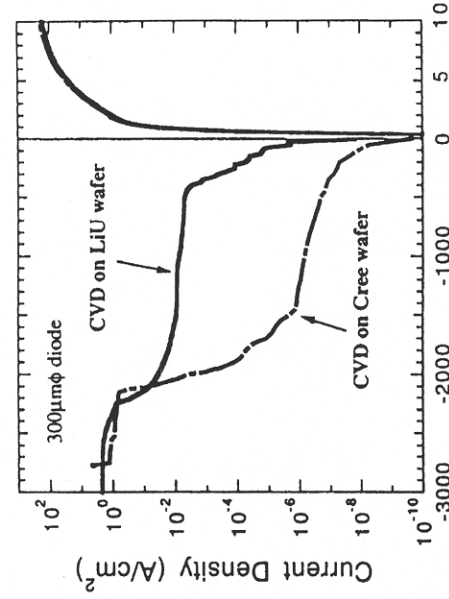


FIG. 31. Comparison of the I-V characteristics of Schottky diodes fabricated on 4H-SiC substrates grown at Cree Research and Linköping [Kimoto 97].

nati [Steckl 93, 94; Su 95, 96; Saxena 96, 98], wherein Ni was used for forming both ohmic and Schottky contacts to the diode. The barrier height was estimated to be 1.69 eV, and an on-resistance of $34 \text{ m}\Omega\text{-cm}^2$ was measured, possibly due to the high resistivity of the substrate and the ohmic contacts. A low reverse leakage current of $7 \times 10^{-7} \text{ A/cm}^2$ was achieved at a reverse bias of 1 kV, and the forward voltage drop at 100 A/cm^2 was 7.4 V. Successful operation of these diodes demonstrates that the high-temperature CVD process has great potential to provide thick epitaxial films useful for future high-power devices.

VI. Metal Contacts to 3C-SiC

Among the SiC polytypes investigated for device fabrication, cubic SiC (3C-SiC) has the highest reported electron mobility (see Table 1). However, the lack of monocrystalline 3C-SiC has limited the development of electronic devices on this polytype material and has led researchers to focus their efforts on hexagonal polytypes (4H- and 6H-SiC) for which the substrates are readily available. 3C-SiC has been grown on Si wafers by several research groups world-wide but the quality of the epitaxial layers requires improvement and does not compare with that of epitaxial layers grown on monocrystalline hexagonal polytype substrates. For the sake of completeness, this section briefly reviews metal contacts to the 3C-SiC polytype. A more detailed discussion has been presented by Porter and Davis [Porter 95].

1. OHMIC CONTACTS TO 3C-SiC

Edmond *et al.* [Edmond 88a] studied ohmic contacts to n-type 3C-SiC using Ni, Au-Ta, Cr, TaSi₂, and Al, and to p-type 3C-SiC using Al-TaSi₂ and Al. TaSi₂ contacts annealed for 5 min at 850°C had the lowest contact resistivity ($2 \times 10^{-2} \Omega\text{-cm}^2$) for n-type, and Al contacts annealed for 3 min at 875°C had the lowest contact resistivity ($3.1 \times 10^{-2} \Omega\text{-cm}^2$) for p-type. These contacts were reported to be stable during electrical operation for 8 h in air at temperatures up to 400°C. At 400°C, the contact resistivity of TaSi₂ and Al on 3C-SiC decreased by a factor of 2 and 10, respectively.

Geib *et al.* [Geib 89] applied Auger electron spectroscopy to study the metal-semiconductor interface of contacts formed by W deposition on 3C-SiC. They reported that although some W-Si and W-C bonding did occur at the interface as a result of the deposition process, the extent of this bonding did not change as the contacts were annealed at higher temperatures, up to 850°C. This was consistent with results on the measured contact resistance, which also did not change considerably with high-temperature

annealing. ρ_c was found to be $0.24 \Omega\text{-cm}^2$ at 23°C and dropped to $8 \times 10^{-2} \Omega\text{-cm}^2$ at 900°C. Baud *et al.* [Baud 95] also investigated the effect of anneal temperature (in the range from 600°C to 1100°C) on the resulting W/3C-SiC interface. They found the contact resistivity to be about $10^{-3} \Omega\text{-cm}^2$.

Chaudhry *et al.* reported Ni, NiCr, W, and Ti, WSi₂ and TiSi₂ ohmic contacts on 3C-SiC [Chaudhry 90, 91]. The minimum contact resistance for Ti and W contacts was 7.6×10^{-3} and $6.1 \times 10^{-3} \Omega\text{-cm}^2$, respectively. The silicides of these metals yielded a lower contact resistance of 1.1×10^{-4} and $3 \times 10^{-4} \Omega\text{-cm}^2$ for TiSi₂ and WSi₂, respectively.

Shor and co-workers [Shor 92, 94] examined the high-temperature operation of W/Pt/Au and Ti/TiN/Pt/Au ohmic contacts on n-type 3C-SiC up to 700°C. Figure 32 shows the variation of the specific contact resistance for these W and Ti contacts, as a function of anneal time. In Fig. 32a, the anneal temperature is 650°C, while in Fig. 32b, each curve represents a different Ti contact annealed at 650°C and 750°C. For W contacts, little change in contact resistivity was observed even after 8 h of annealing. For Ti contacts, annealing at 650°C reduces ρ_c for up to 2 h of anneal time, beyond which time ρ_c increases slowly with anneal time, eventually becoming rectifying after 31 h of annealing.

Low specific resistance ($< 6 \times 10^{-6} \Omega\text{-cm}^2$) TiC ohmic contacts to n-type 3C-SiC (doping concentration of $2 \times 10^{19} \text{ cm}^{-3}$) were reported by Parsons and co-workers [Parsons 94]. The 1500 Å TiC layer was epitaxially grown by CVD using gas precursors at 1260°C.

The effect of post-deposition anneal temperature on the electrical characteristics of Ni-Mo and Ni-Au ohmic contacts to 3C-SiC was studied by Arugu and co-workers [Arugu 95]. The temperature range investigated was from 400 to 1200°C. Lowest contact resistance of 1.41×10^{-4} and $3.05 \times 10^{-4} \Omega\text{-cm}^2$ was observed for Ni-Mo and Ni-Au, respectively, corresponding to anneal temperatures of 1000°C and 700°C.

Moki *et al.* [Moki 95] studied the effect of increasing the surface doping concentration achieved by ion implantation on the contact resistivity of Al and Ti ohmic contacts to 3C-SiC. Figure 33 shows the decrease in ρ_c for Al and Ti contacts as a function of the surface doping concentration. The minimum contact resistivity of 1.4×10^{-5} and $1.5 \times 10^{-5} \Omega\text{-cm}^2$ were measured for Al and Ti contacts, respectively, at the highest surface doping concentration of $3 \times 10^{20} \text{ cm}^{-3}$.

2. SCHOTTKY CONTACTS AND DIODES ON 3C-SiC

The first Schottky diodes on 3C-SiC were reported by Yoshida *et al.* [Yoshida 85] on epitaxially grown n-type layers. Au was used for forming

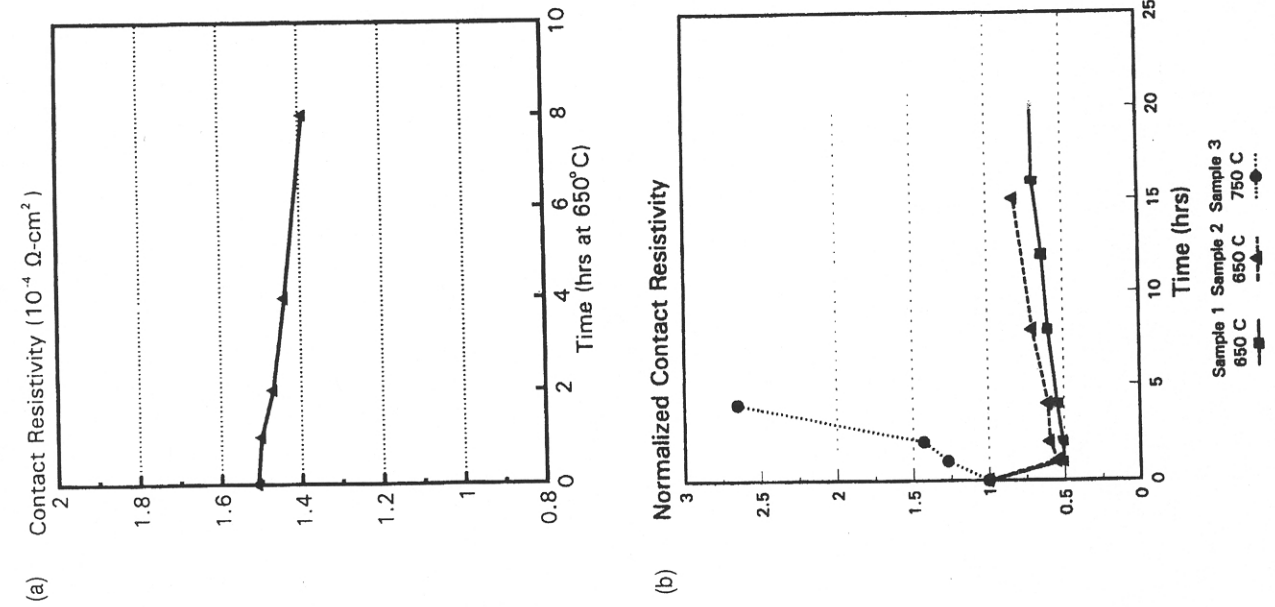


FIG. 32. Specific contact resistivity to 3C-SiC as a function of anneal time for: (a) W contacts; (b) Ti contacts [Shor 94].

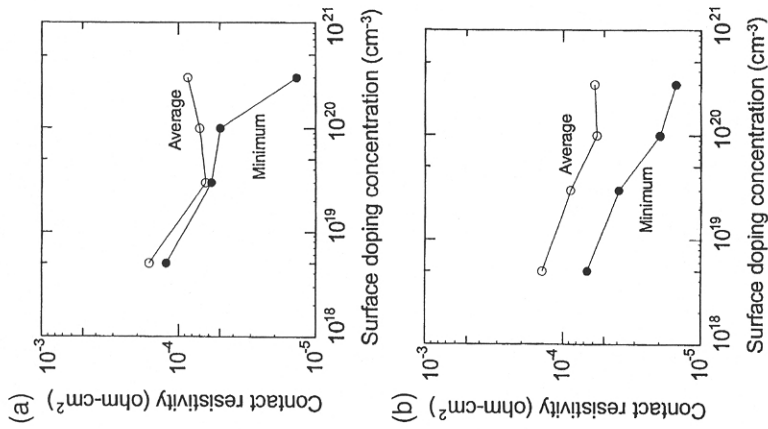


FIG. 33. Specific contact resistivity to 3C-SiC as a function of doping concentration for: (a) Al; (b) Ti [Moki 95].

the Schottky contact and the barrier height was determined to be in the range from 1.11–1.15 eV by C-V and photoresponse measurements.

Daimon *et al.* [Daimon 86] investigated Al and Al-Si metals contacts on n- and p-type 3C-SiC. They observed that as-deposited Al and Al-Si contacts were ohmic on n-type SiC, and their nature changed to rectifying upon annealing at 900°C . On the contrary, Al contacts on p-type Al showed good ohmic behavior only when annealed at 900°C .

Ioannou *et al.* [Ioannou 87] reported Au/3C-SiC Schottky diodes with an ideality factor of 1.5 ± 0.2 , and an SBH of 1.2 eV. The diodes had a turn-on voltage of 0.6 to 1.0 V and breakdown voltages in the range of 8 to 10 V. The contacts remained stable during a 1-hr anneal at 300°C in Ar.

Bermudez [Bermudez 88] reported a barrier height of 1.4 eV for as-deposited Al contacts on 3C-SiC grown on (001) Si. He also studied the physical and electronic structures of the Al-SiC interface using XPS, LEED, and ELS.

Fujii *et al.* [Fujii 88] reported on the dependence of the electrical characteristics of 3C-SiC Schottky diodes on the crystal orientation of the Si substrate [$n(11)$, $n = 6, 5, 4, 3, 1$ and (100)], upon which the SiC films were grown by CVD. The I-V characteristics of diodes that were fabricated on SiC films on Si(611), Si(411), and Si(111) were found to be excellent compared to the conventional diodes on Si(100). They had a lower reverse leakage current and ideality factors closer to unity. The barrier height of the Pt-Schottky diodes was found to be 1.3 to 1.8 eV and that of Au-Schottky diodes was 1.0 to 1.6 eV, depending on the substrate orientation. ϕ_{Bn} for SiC films on Si(111) and Si(611) were found to be larger than for the other orientations.

Papanicolaou *et al.* [Papanicolaou 89] examined the electrical properties of Pt-Schottky contacts on 3C-SiC as a function of annealing temperature. They used Auger analysis to study the metallurgical reactions at the Pt/SiC surface and found that short annealing cycles in the 350 to 800°C temperature range led to the formation of a mixed structure of PtSi_x and PtC at the interface. The interfacial reaction is dominated by the diffusion of Pt into the SiC layer. Figure 34 shows the variation of the Pt/3C-SiC structure SBH ϕ_B , the ideality factor η , and the reverse saturation current I_R as a function of anneal temperature. Annealing at each temperature is performed for 20 min. The barrier height was found to increase steadily as the anneal temperature was increased, from 0.95 eV for the as-deposited contacts to 1.35 eV for contacts annealed at 800°C. Minimum leakage current is obtained after the 450°C anneal. This anneal temperature also corresponds to the operation of these diodes, with an ideality factor close to unity.

Waldrop and Grant [Waldrop 90] investigated the Schottky barriers for several metals, including Pd, Au, Co, Ti, Ag, Tb, and Al, on 3C-SiC. The interfacial chemistry and the SBH were studied using XPS, and the electrical behavior was studied by measuring the current-voltage and capacitance-voltage characteristics. I-V characteristics showed that Pd, Au, and Co formed rectifying contacts, whereas Ti, Ag, Tb, and Al contacts showed ohmic behavior. Figure 35 shows the SBH obtained for various metals from the XPS studies plotted as a function of the work function of the respective metals. Similar to 6H and 4H polytypes, we see a strong correlation between ϕ_B and ϕ_M , once again ruling out the possibility of Fermi-level pinning on the surface. A wide range of ϕ_B (0.95–0.16 eV) is observed for different metals.

Wahab *et al.* [Wahab 91] reported Au Schottky diodes on sputtered 3C-SiC films deposited on Si substrates. The ideality factor of the diodes was 1.27 and a barrier height of 1.04 eV was determined from both I-V and C-V characteristics.

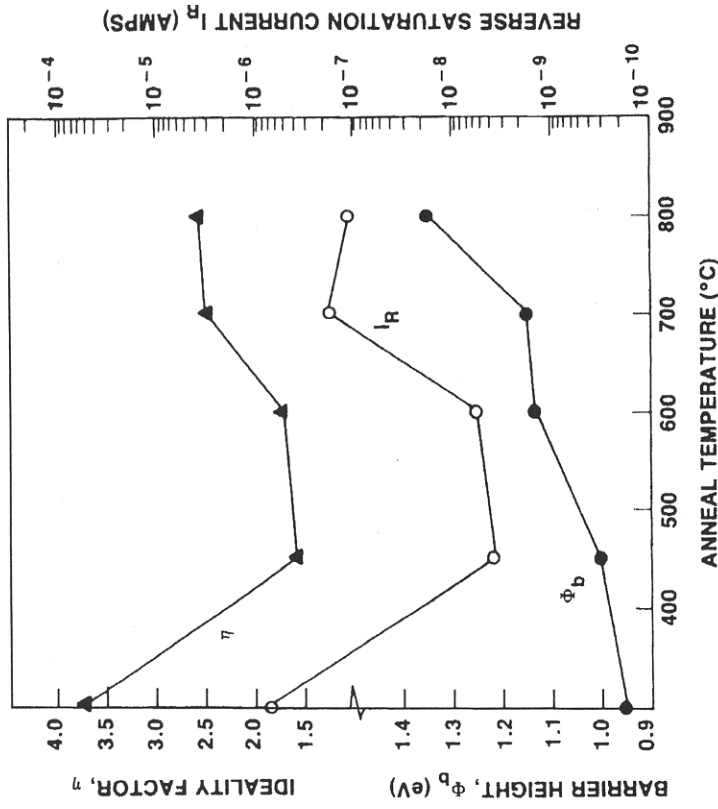


FIG. 34. SBH, ideality factor, and reverse saturation current for Pt/3C-SiC contacts as a function of anneal temperature [Papanicolaou 89].

Steckl and Su [Steckl 93, 94] reported the "all-Ni technology" for the first time in 1993 utilizing Ni for forming both the ohmic and Schottky contacts. The resulting Schottky diodes exhibited high breakdown voltages in excess on 150 V.

Shenoy and co-workers [Shenoy 94] reported Pt-Schottky barrier diodes on n^-/n^+ 3C-SiC grown on n^+ -Si substrates. These diodes had a low specific on-resistance of $\sim 6.1 \times 10^{-4} \Omega\text{-cm}^2$ and a relatively large breakdown voltage of ~ 85 V for a 4- μm -thick drift layer. Figure 36 shows the forward and reverse I-V characteristics for these diodes as a function of postmetallization anneal temperature. The $\log(I)$ versus V plot for the forward characteristics showed linearity over four decades with an ideality factor of 1.25. The SBH for these contacts was found to be ~ 0.85 V.

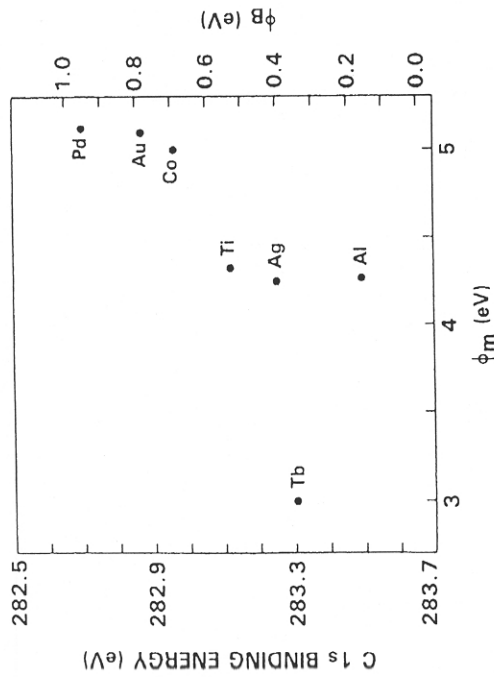


FIG. 35. SBH as a function of metal work function for 3C-SiC [Waldrop 90].

VII. SiC p-n Junctions Diode Rectifiers

Early techniques for fabricating *grown* p-n junctions in SiC used the traveling solvent (TS) method and the solution growth (SG) technique. Both of these techniques require very high temperatures, and the junctions obtained are often contaminated. In the TS technique [Campbell 71, 81], SiC crystals were grown together, and p-n junctions were formed by maintaining a heat zone across two SiC crystals of opposite conductivity type separated by a solvent metal (Pt, Cr). The temperature gradient across the thin solvent zone causes dissolution at both solvent-solid interfaces. However, the solubility of SiC in the solvent at the hotter interface is higher than that at the cooler interface. Thus, SiC diffuses through the solute and precipitates on the cooler crystal. In the SG technique [Campbell 71, 81], a small amount of SiC is dissolved in a molten metal (Fe, Cr, or Si). As the melt is cooled slowly, SiC crystals nucleate and grow in crucibles fabricated on graphite substrates.

More recently, p-n junction fabrication techniques have relied on the incorporation of impurities during either growth of the p- or n-type layers (so-called *in situ* doping) or incorporation after growth by impurity diffusion or by ion implantation. Commonly used techniques to grow epitaxial layers include sublimation epitaxy (SE), container-free liquid-phase epitaxy

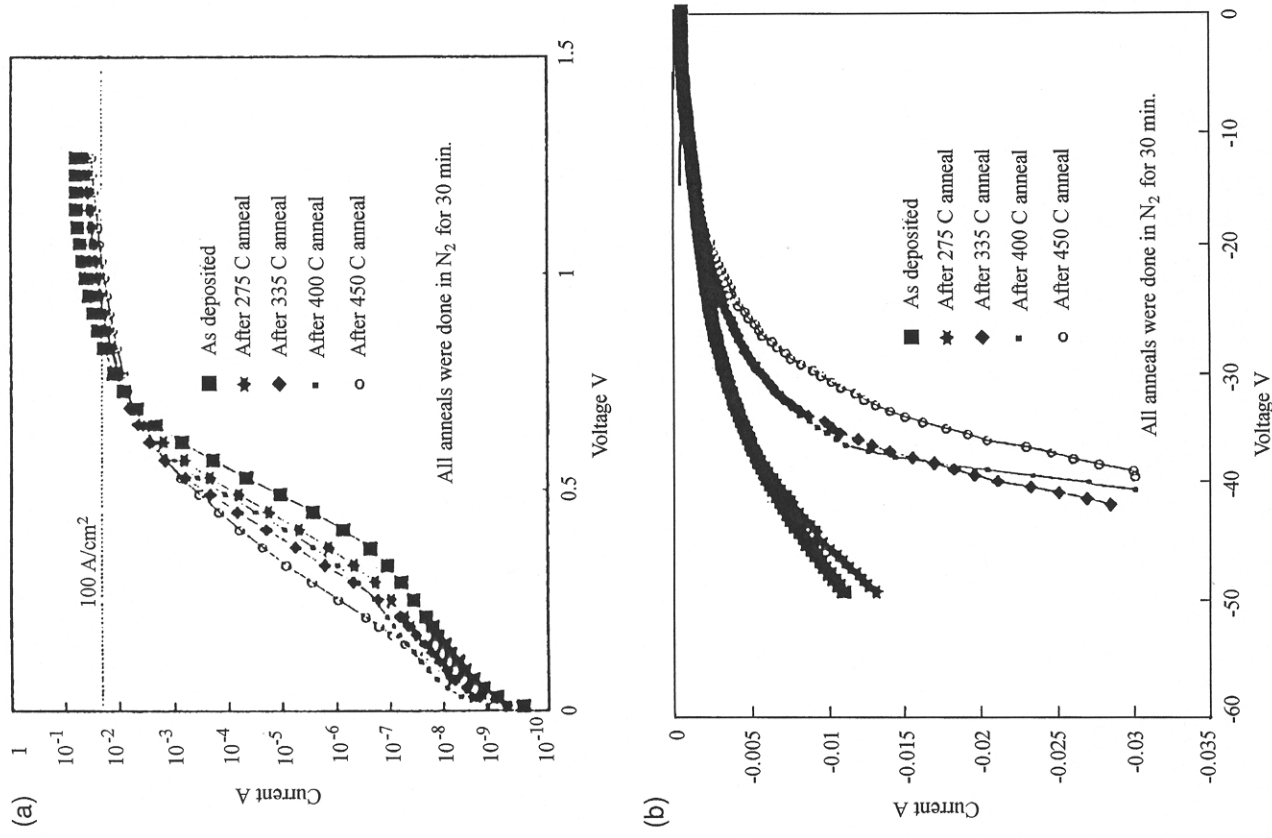


FIG. 36. Variation of current-voltage characteristics of Pt/3C-SiC SBDs with post metalization annealing: (a) forward bias; (b) reverse bias [Shenoy 94].

(CFLPE), and CVD [Lebedev 96]. *In situ* doping is performed by adding proper dopants to the ambient during the growth of these epitaxial layers. This technique, however, does not lend itself to the fabrication of planar structures. Therefore, etching of a mesa structure is required to produce individual p-n junction diodes. Postgrowth diffusion processes require high temperatures (in excess of 2000°C) and relatively long diffusion times to accomplish the mass transport required for device fabrication [Davis 91]. Prolonged exposure to such high temperatures results in the decomposition of SiC. Furthermore, oxide masks cannot be used for selective doping, as they vaporize at these temperatures. Thus, diffused junctions are very difficult to form in SiC.

The majority of the SiC planar p-n junctions are fabricated using the ion implantation technique. Implantation can be performed using a thin film mask and therefore eliminates the need for subsequent mesa formation. For p-type impurities, group IIIA elements (B, Al, Ga, In, Tl) have been implanted in 6H-SiC, while group VA elements (N, P, Sb, Bi) have been implanted for n-type doping [Davis 91]. A quantitative discussion on ion implantation for SiC doping is presented in Chapter 2.

The following discussion summarizes the electrical properties and characteristics of the p-n junctions on different polytypes of SiC fabricated using the aforementioned techniques. Properties of selected high-voltage (>100 V) SiC p-n junction diodes are summarized in Table VIII.

1. 3C-SiC p-n JUNCTIONS

Suzuki *et al* [Suzuki 86] fabricated mesa structure p-n junction diodes on 3C-SiC and studied their high-temperature operation up to 500°C. At room temperature, the diode has a forward turn-on voltage of 1.2 V and a reverse current of 5 μ A at 5 V. The diodes showed different current behaviors in three distinct voltage regimes under forward bias operation. At voltages lower than about 0.6 V, the diodes showed excess current. The current increased exponentially in the voltage range of 0.6 to 1.1 V. Beyond 1.1 V, there was a gradual increase in the current.

Furukawa *et al.* [Furukawa 86] studied the I-V and C-V characteristics of mesa structure diodes obtained by reactive ion etching (RIE) of CVD grown 3C-SiC on Si substrates. These diodes had a cut-in voltage of \sim 1.4 V, an ideality factor of 3.3, and a reverse leakage current smaller than 10 μ A at -5 V.

Avila and co-workers [Avila 87] reported p-n junction diodes formed by ion implantation of B or Al in 3C-SiC/Si and annealing at 1365°C. The Al-implanted diodes did not show good rectification. The B-implanted

TABLE VIII

HIGH VOLTAGE (>100 V) p-n JUNCTION DIODES ON 3C, 4H, AND 6H-SiC

Polytype/Structure	Growth Technique	Background Doping Concentration (cm ⁻³)	Junction Depth or Epilayer Thickness (μ m)
6H epitaxially grown layers	Growth using "double charge" method	n layer: 10^{17} – 10^{19} p layer: 5×10^{19}	0.6
6H p-n mesas on grown layers on n-6H substrates; oxide passivation	Epilayers: CVD; substrates: Acheson	n-epi: 2×10^{16}	n-epi: 2 p-epi: 2
6H p-n mesas on grown layers on n-6H substrate; oxide passivation	Epilayers: CVD; substrates: Acheson and Lely	7×10^{16} 1.5×10^{17}	n-epi: 3 p-epi: 1.5
6H p-n mesas on grown layers on n-6H substrate; oxide passivation	Epilayers: CVD—site competition epitaxy; substrates: Cree Res.	n-epi: 2×10^{16}	n-epi: 4 p-epi: 0.75
6H p-n mesas, B ⁺ into epitaxial n/n ⁺ 6H wafers; oxide passivation	B ion-implantation; substrates: Cree Res.	n-epi: 3.5×10^{15}	n-epi: 3.5
6H p-n mesas on grown layers on n-6H substrate; oxide passivation	Epilayers: CVD; substrates: Cree Res.	n-epi: 2×10^{16}	NR
3C p ⁺ -n-n ⁺ mesas grown on 6H n/n ⁺ epitaxial wafer:	Epilayers: CVD—site competition epitaxy; substrates: Cree Res.	(i) n-epi: 5– 20×10^{15} (ii) n-epi: 3– 5×10^{15}	n-epi: 5 n-epi: 24
(i) with oxide passivation (ii) with no oxide	Epilayers: site competition epitaxy; substrates: Cree Res.	n-epi: 2 – 5×10^{15}	p ⁺ -epi: 1 n-epi: 24 n ⁺ -epi: 8 n-epi: 1.2
6H p ⁺ -n-n ⁺ mesas grown on 6H n ⁺ wafer	Epilayers: site competition epitaxy; substrates: Cree Res.	n-epi: 2 – 5×10^{15}	p ⁺ -epi: 1 n-epi: 24 n ⁺ -epi: 8 n-epi: 1.2
3C heterojunction (SiC/Si) mesa diodes; with oxide passivation	n-type 3C-SiC layer grown by RTCVD on p-Si substrate.	NR (unintentional)	n-epi: 10 junction depth: 0.62
6H planar, B ⁺ into epitaxial 6H n/n ⁺ wafers; oxide passivation	Conversion of n-layer to p-type by B ⁺ ; substrates: Cree Res.	n-epi: 6 – 7×10^{15}	n-epi: 10 junction depth: 0.62
6H p ⁺ -n-n ⁺ mesa on 6H substrates	Hot-wall CVD	p ⁺ -epi: 1×10^{18} n-epi: 1×10^{15}	p ⁺ -epi: 2 n-epi: 45

diodes showed rectification with ideality factors of 2.2, which increased with temperature up to 270°C. The diodes had breakdown voltages between 5 and 10 V and series resistance of the order of 20kΩ.

Edmond and co-workers [Edmond 88b] prepared mesa structure junction diodes by ion implantation of Al in n-type and N in p-type 3C-SiC films. Rectification was observed in both types of diodes in the temperature range studied (300–673 K), with ideality factors in excess of 2. The forward characteristics also showed that the space-charge limited current in the presence of traps was the dominating mechanism for current transport. The temperature dependence of the forward and reverse bias characteristics for N- and Al-implanted diodes are shown in Figs. 37 and 38, respectively.

Diode Ideality Factor	Saturation Current Density (A/cm ²)	Forward Current Density at X Volts (A/cm ²)	Breakdown Voltage and Nature of Breakdown	Reverse Leakage Current Density (A/cm ²) at X Volts	Ref.
NR	NR	NR	167, NR	NR	[van Opdorp 1969]
NR	NR	NR	100, soft	NR	[Shibahara 87, Nishino 87]
2.5	1.2×10^{-32}	0.158 at 3.4 V	200, soft	3×10^{-4} at -100 V	[Wang 91]
NR	NR	~0.8 at 3	1000, hard	Leakage current: 0.4mA at -300 V	[Matus 91]
1.77	NR	$\sim 1 \times 10^{-2}$ at 1.6	650, hard	10^{-10} at -10	[Ghezzi 93]
1.5–2	NR	$\sim 5 \times 10^{-6}$	710, soft	$< 5 \times 10^{-4}$ at -710, $\sim 10^{-9}$ at -200	[Edmond 93]
3.07	3.8×10^{-11}	$\sim 4.5 \times 10^{-2}$ at 2	200 V, soft	~0.3 at -200	[Neudeck 93, 94a]
NR	NR	~0.15 at 2	300 V, soft	~0.15 at -300	
2.05	5×10^{-22}	$\sim 1 \times 10^{-5}$ at 2	2000	0.1 at -2000	[Neudeck 94a, 94c]
1.05	NR	0.16 at 0.4	150	3×10^{-4} at -10	[Yih 94]
3.2–3.5	NR	100 at 7–8	800	$\sim 5 \times 10^{-5}$ at -800	[Shenoy 95]
—	—	100 at ~6		$< 5 \times 10^{-3}$ at -1100 ~ 10 at 4500	[Kordina 95b]

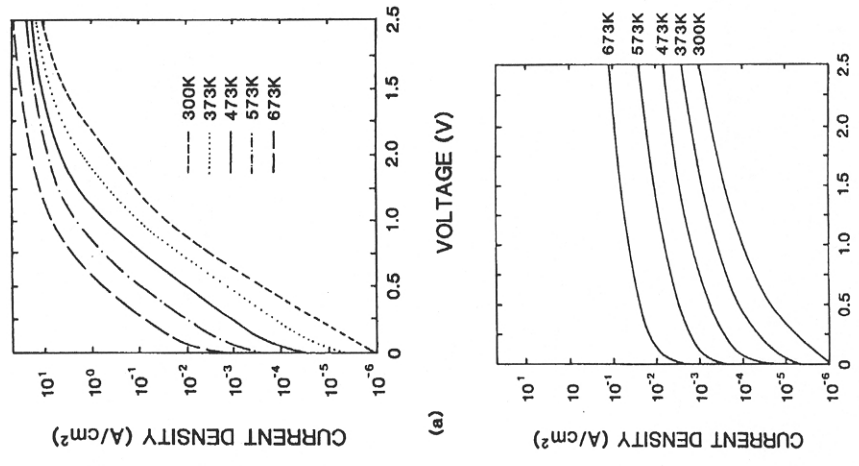


Fig. 37. Temperature dependence of current density versus voltage for N-implanted 3C-SiC p-n diode: (a) forward-bias; (b) reverse-bias [Edmond 88a].

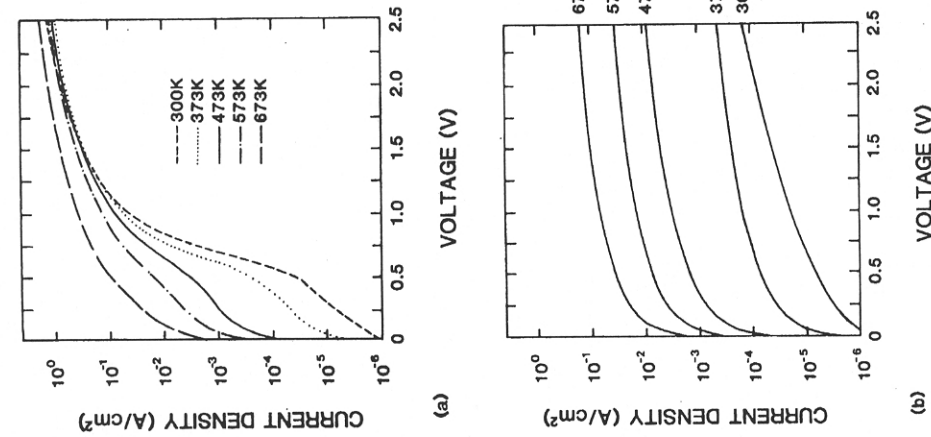


FIG. 38. Temperature dependence of current density versus voltage for Al-implanted 3C-SiC p-n diode: (a) forward-bias; (b) reverse-bias [Edmond 88a].

Neudeck and co-workers at NASA Lewis [Neudeck 93, 94a] reported improved electrical characteristics of p-n junctions with mesa structures on 3C-SiC layer grown by CVD on commercially available 6H-SiC substrates. The resulting 3C-SiC layers had increased crystal purity, no double positioning boundary (DPB) defects, and greatly reduced stacking fault densities. Best results were observed from diodes on 3C material with low doping densities ($3\text{--}5 \times 10^{15} \text{ cm}^{-3}$) grown by utilizing the dopant control process developed by Larkin *et al.*: "site competition epitaxy" [Larkin 94]. These diodes showed a breakdown at $\sim 300 \text{ V}$. The soft breakdown

characteristics was attributed to current leakage along the mesa perimeter. Diodes with higher doping densities ($> 8.5 \times 10^{16} \text{ cm}^{-3}$) showed avalanche characteristics indicating bulk junction breakdown. The diodes on 3C-SiC layers with doping in the range of 0.5 to $2 \times 10^{16} \text{ cm}^{-3}$ were tested at temperatures up to 300°C . The forward characteristics of these diodes (ideality factor, current density at a given voltage drop) improved at higher temperatures, but the blocking voltage decreased slightly (from -200 V at 24°C to -170 V at 300°C). The saturation current density was $3.8 \times 10^{-11} \text{ A/cm}^2$ at room temperature and increased to $1.1 \times 10^{-6} \text{ A/cm}^2$ at 300°C .

The SiC group at Cincinnati [Yih 94] reported SiC/Si heterojunction p-n diodes fabricated by two different techniques. The first technique utilized self-selective growth of n-type SiC on p-type Si wafers patterned with an oxide layer to produce planar diodes. The second technique utilized mesa etching after a blanket deposition of an n-type SiC layer on p-type Si. The SiC layers were deposited using the rapid thermal chemical vapor deposition (RTCVD) process developed by Steckl and Li [Steckl 92]. The planar diodes had a breakdown voltage of 50 V , an ideality factor of 1.36 , and a diode rectification ratio (defined at $\pm 1 \text{ V}$ bias) of 1.6×10^4 at room temperature. The corresponding numbers for the mesa structure diode were 150 V , 1.05 , and 1.6×10^4 .

2. 6H-SiC p-n JUNCTIONS

Early p-n junctions on SiC were grown on the 6H polytype at high temperatures, such as 1740°C (traveling solvent method) and 1650°C (epitaxial growth from saturated silicon melts) [Campbell 71, 81]. The first p-n junctions fabricated by room-temperature implantation of 6H-SiC were reported by Dunlop and Marsh [Dunlop 69]. These junctions were obtained by the formation of n-type layers with ion-implanted N or Sb into p-type 6H-SiC. With this technique, SiC p-n junctions were produced without having to maintain high temperatures for hours for the impurity diffusion to take place during growth. Instead, only a few minutes of postimplant annealing was needed at 1400 to 1600°C for the activation of impurities. The resulting p-n junction diodes obtained from N and Sb implants had similar electrical characteristics. In the temperature range from 23 to 400°C , the diodes showed an ideality factor of 1.45 . The dominating current mechanism at lower forward bias was suspected to be recombination in the depletion region. At higher forward bias, the diffusion current component dominated. The reverse characteristics showed avalanche breakdown at $\sim 46 \text{ V}$.

van Opdorp and Vrakking fabricated $1 \times 1 \text{ mm}^2$ p-n junctions on 6H-SiC by epitaxial growth procedure using the "double charge" method [van Opdorp 1969]. They used grinding and sawing to produce diodes with junction planes perpendicular to the c-axis. Alloyed ohmic contacts were used to make electrical connections to the n and p type layers. Breakdown voltage up to 167 V were obtained and the maximum breakdown electric field was found to be in the range 2.8–5 MV/cm.

Muench and Pfaffeneder [Muench 77] studied the electrical breakdown of p-n junctions in 6H-SiC obtained by vapor growth and mesa etching. Breakdown fields in the range of 2.0 to $3.7 \times 10^6 \text{ V/cm}$ were observed for these p-n junctions. The diodes exhibited a linear dependence between breakdown voltage and background p-type doping concentration in the range of 6×10^{17} to $2 \times 10^{18} \text{ cm}^{-3}$. At lower doping levels, the breakdown voltage did not increase as expected. This could be attributed to the leakage around the mesa periphery and to local crystal imperfections [Edmond 93].

6H-SiC p-n junctions and devices based on them were reported by Dmitriev *et al.* [Dmitriev 85a, 85b, 87] and Anikin *et al.* [Anikin 84, 88, 89]. These devices were mostly fabricated on bulk crystals or on epitaxial films. The earlier reports were for devices on n^- -p $^+$ and n^+ -n-p-p $^+$ structures on n^+ substrates [Dmitriev 85]. Cr and Al were utilized in these structures for ohmic contacts to n- and p-type SiC, respectively. The effective doping concentration of the n-type region was $N_d - N_a = 5 \times 10^{17}$ to 10^{18} cm^{-3} , and that of the p-type region was $N_a - N_d = 2 \times 10^{18}$ to 10^{19} cm^{-3} . The diode cut-in voltage was 2.7 V, and the saturation current density varied between 10^{-14} and 10^{-19} A/cm^2 . The critical avalanche breakdown field was determined to be approximately $1.5 \times 10^6 \text{ V/cm}$. Later investigations [Dmitriev 87] resulted in better quality diodes, with ideality factors somewhat closer to unity and with higher breakdown fields (2 – $3 \times 10^6 \text{ V/cm}$) [Davis 91].

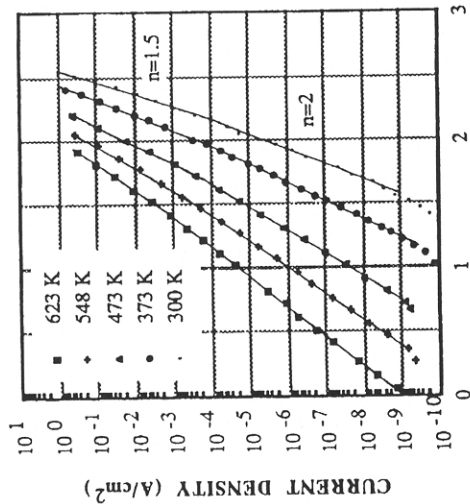
Anikin *et al.* reported p $^+$ -n mesa structures grown on 6H-SiC by the sublimation sandwich method on the Si (0001) face of single-crystal 6H-SiC wafers. The n-n $^+$ structures were fabricated [Anikin 84, 88] by implantation of Al ions followed by annealing. Final mesa structures were obtained by reactive ion etching. In the initial study [Anikin 84], the doping density for the n-type base region in the two samples studied was $6 \times 10^{16} \text{ cm}^{-3}$ and $2 \times 10^{17} \text{ cm}^{-3}$. A study of the I-V characteristics at high temperatures (293–780 K) indicated a positive temperature coefficient of $5 \times 10^{-3} \text{ V/degree}$ for the current-voltage dependence under forward bias. Two distinct linear regimes were observed: one for voltages up to 2 V, and the other for voltages from 2 to 2.3 V. The ideality factors for different temperatures for these regimes were found to be 1.7 to 1.98 and 1.15 to 1.4, respectively. The I-V characteristics at voltages higher than 2.3 V were limited by the series

resistance of the diodes. Later studies [Anikin 88] indicated similar behavior in the I-V characteristics with two distinct linear regimes. The ideality factor for the regime corresponding to lower voltages was found to be in the range of 1.65 to 2.00 for the temperature range from 370 to 720 K. The ideality factor for higher voltages was independent of temperature and was found to be ~ 1.5 . The reverse leakage currents in these diodes were attributed to leakage along the periphery of the mesa structures.

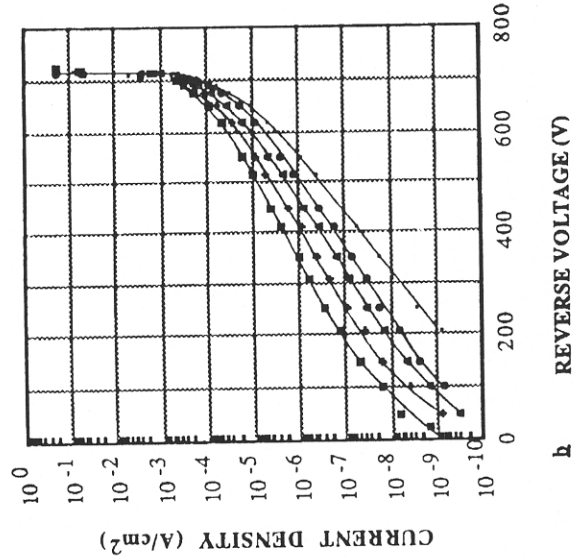
Mesa-type 6H-SiC diodes fabricated by *in situ* doping and capable of high blocking voltages have been reported by Edmond and co-workers [Edmond 92, 93; Davis 91]. Rectifiers with breakdown voltages as high as 1400 V were reported in their studies. Low-current forward and reverse bias testing was performed on these diodes for the temperature range from 300 to 623 K. Figure 39 shows the I-V characteristics of a 710-V SiC diode as a function of temperature. As seen in Fig. 39a, the forward I-V characteristics show two distinct linear regimes: the generation-recombination current regime with ideality factor close to 2.0, followed by the regime with both diffusion and generation-recombination currents, with somewhat lower ideality factors. This behavior is similar to that observed by Anikin *et al.* [Anikin 84] in diodes fabricated by implantation. At 300 K, these regimes occur in the voltage range of 1.5 to 2.2 V and 2.2 to 2.55 V, respectively. As shown in Fig. 39a, the respective ideality factors are 2.0 and 1.5. At 623 K, the ideality factors corresponding to these two regimes were found to be 1.9 and 1.6. As expected, the reverse leakage current density (Fig. 39b) increases with temperature. However, the leakage at 623 K and 710 V (prior to the onset of avalanche) was still very low ($\sim 5 \times 10^{-4} \text{ A/cm}^2$). The diodes reported by this group also displayed a fast switching speed. As shown in Fig. 40, the reverse recovery time (t_{rr}) for a typical high-voltage (1200 V) diode was found to be less than 14 ns at room temperature, and increased by only 20% at 625 K.

Kaneda *et al.* [Kaneda 87] reported p-n junctions formed by growing p-type 3C-SiC by Molecular Beam Epitaxy (MBE) on n-type 6H-SiC substrates. A high breakdown electric field $6.7 \times 10^5 \text{ V/cm}$ was determined from the avalanche breakdown characteristics of the diodes.

High-voltage mesa-style p-n diodes were fabricated on CVD-grown n- and p-type 6H-SiC layers by Matus and co-workers [Matus 91]. These diodes showed excellent rectification up to the highest temperature tested, 600°C, and high breakdown voltage of 1000 V. The maximum electric field at breakdown was found to be $2.7 \times 10^6 \text{ V/cm}$, and the reverse bias leakage current measured at 300 V increased from $0.4 \mu\text{A}$ at room temperature to $5 \mu\text{A}$ at 600°C. The built-in potential obtained from C-V characteristics was -2.7 V .



a FORWARD VOLTAGE (V)



b REVERSE VOLTAGE (V)

FIG. 39. Current-voltage characteristic of 6H-SiC p-n junction diode as a function of temperature [Edmond 93].

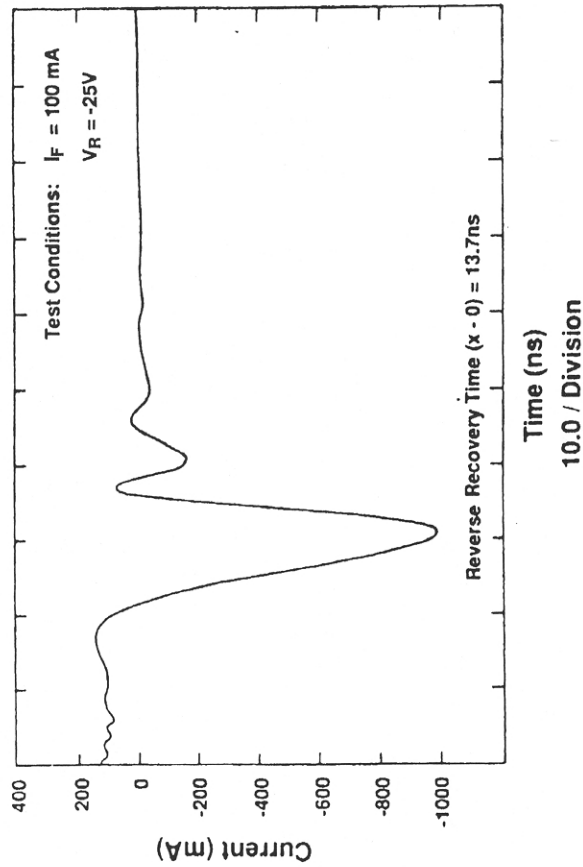


FIG. 40. Switching speed of high-voltage (1200 V) 6H-SiC p-n diode at 293 K [Davis 91].

Ghezzi *et al.* [Ghezzi 93] applied N implantation at high temperatures (up to 1000°C) to fabricate low leakage current diodes on 6H-SiC. These diodes also had a mesa structure and were patterned using reactive ion etching. The diodes had an ideality factor of 1.95 and a leakage current of $5 \times 10^{-11} \text{ A/cm}^2$ at a reverse bias of 10 V. In a later study, Ghezzi and co-workers [93] reported p-n junction diodes on 6H-SiC fabricated by boron implantation at room temperature and at 1000°C, followed by postimplant anneal at 1300°C. As shown in Fig. 41, diodes fabricated by high-temperature implantation had better forward and reverse characteristics. Figure 41a shows the forward characteristics of these diodes at room and elevated temperatures (170 or 181°C), for both room-temperature implantation (left-hand side) and 1000°C implantation (right-hand side). The diode obtained by high-temperature implantation clearly has lower forward drops for any given current density. Figure 41b shows a histogram of reverse diode current densities measured at 21°C and -10 V for 6H-SiC diodes with the same implantation conditions. Once again, the diodes with high-temperature implant often had superior characteristics: a tighter distribution and a much smaller median value for the reverse current density. The best diodes had an ideality factor of 1.77, a reverse bias leakage of 10^{-10} A/cm^2 at -10 V , and a breakdown voltage of -650 V .

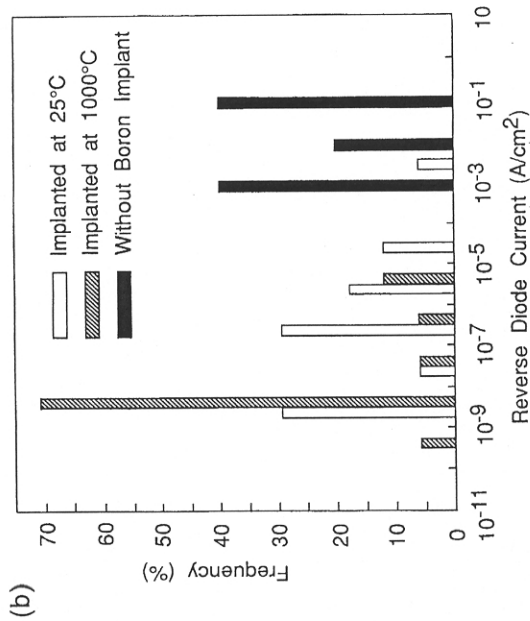
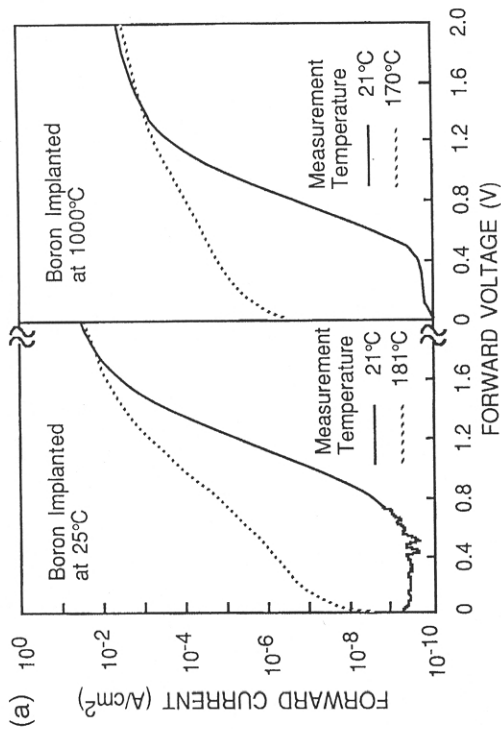


FIG. 41. Electrical characteristics of boron-implanted 6H-SiC diodes: (a) forward bias characteristics as a function of implantation and measurement temperature; (b) histogram of room-temperature reverse bias current density at -10V as a function of implantation conditions [Ghezzi 93].

Vassilevski *et al.* [Vassilevski 93, 94] reported the pulsed power characteristics of 6H-SiC p-n diodes grown by liquid-phase epitaxy (LPE). These diodes operated at a high current density of 60 kA/cm^2 (input power density of 9 MW/cm^2) for a current pulse duration of 60 ns, prior to experiencing avalanche breakdown at $\sim 80\text{ V}$. The temperature coefficient of avalanche breakdown ($\beta = V^{-1} dV/dT$) was found to first decrease with temperature over a broad range (300–750 K) and then increase with temperature from 750 to 900 K.

Neudeck and co-workers at NASA Lewis Research Center [Neudeck 94a, 94b, 94c] first reported high-voltage rectification exceeding 2000 V using SiC p-n junction diodes. The mesa structure 6H-SiC p⁺-n junction diodes were fabricated on 6H-SiC epilayers grown by atmospheric CVD utilizing site competition epitaxy [Larkin 94] on commercially available 6H-SiC wafers. Figure 42 shows the current-voltage characteristics for these diodes. The forward characteristics of the diodes are very well behaved, exhibiting saturation current densities below 10^{-20} A/cm^2 , and ideality factors close to 2. The peak junction electric field was calculated to be in the range of 1.4 to 1.8 MV/cm .

High-voltage p-n diodes fabricated on 6H-SiC grown by CVD in a hot-wall reactor [Kordina 95a] were reported by Kordina *et al.* [Kordina 95b, Janzen 96]. The mesa structure p-n junction was fabricated by growing a 2- μm -thick p-type layer over a 45- μm -thick n-type epitaxial layer on an n⁺ substrate. As shown in Fig. 43, these diodes [Kordina 95b] had a

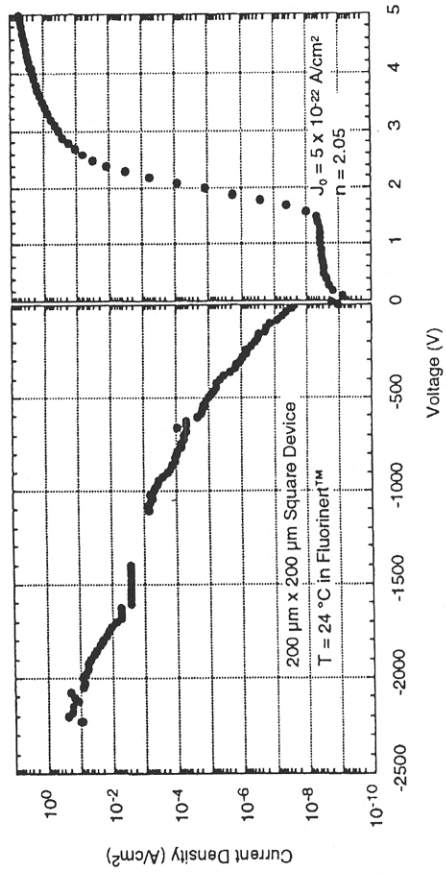


FIG. 42. 6H-SiC p-n junction current-voltage characteristics at room temperature. Note different voltage scales for forward and reverse bias [Neudeck 94c].

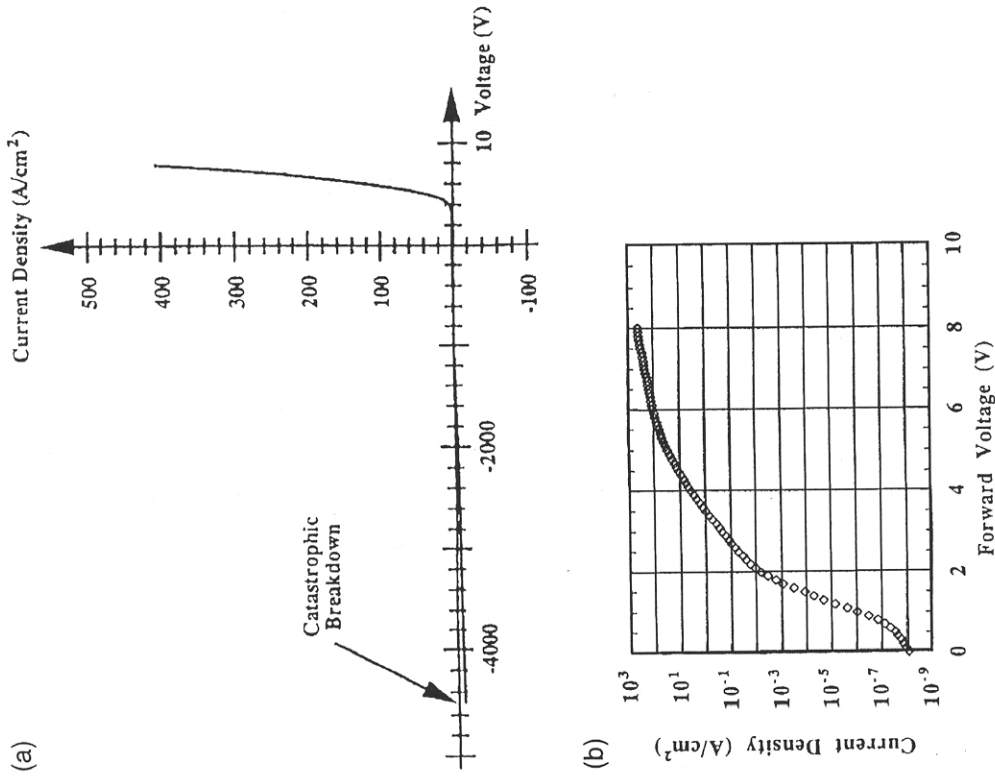


FIG. 43. Characteristics of a 4.5-kV Si rectifier: (a) I-V characteristics; (b) measured forward voltage drop versus current density [Kordina 95b].

breakdown voltage of 4.5 V before a catastrophic failure occurred. The forward voltage drop at a current density of $100 A/cm^2$ was $\sim 6 V$.

The first planar p-n junction diodes on 6H-SiC were fabricated by Shenoy and Baliga [Shenoy 95, 96] by room-temperature boron implantation through a pad oxide. These diodes had a breakdown voltage of 800 V and had a low leakage current of less than $5 \times 10^{-5} A/cm^2$ until breakdown

occurred. Figure 44 shows the current-voltage characteristics of these diodes for two junction depths (x_j), 0.2 and $0.62 \mu m$. The diodes exhibit forward bias linearity over three decades of the log (I) versus V plots, with an ideality factor of 3.2 to 3.5. Series resistance effects were observed at current densities above $1 A/cm^2$. This resulted in a high forward voltage drop of 7 to 8 V at $100 A/cm^2$. In reverse bias, the breakdown voltage increases significantly with the increase in junction depth. For $x_j = 0.2 \mu m$, the highest breakdown was 480 V, whereas for $x_j = 0.62 \mu m$, it was up to 810 V.

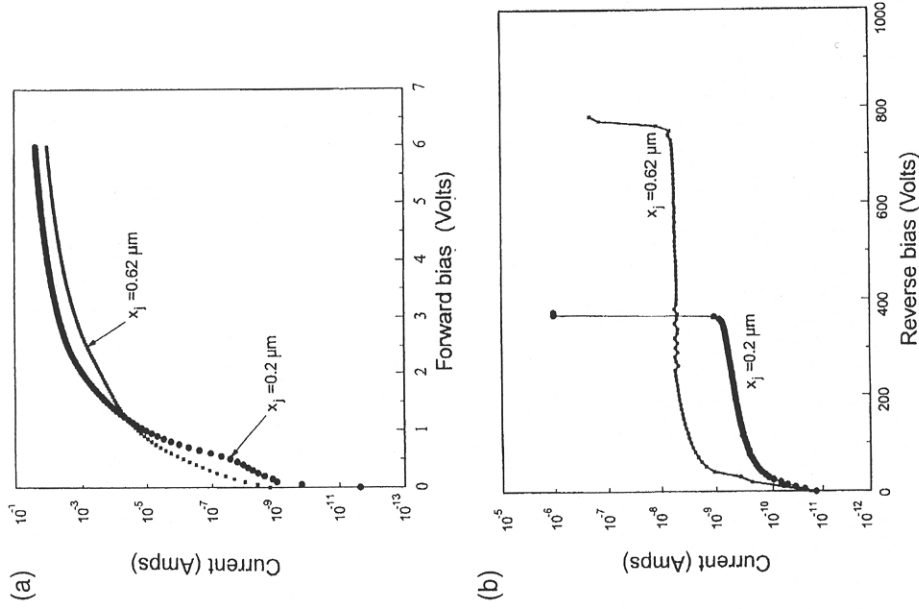


FIG. 44. Current-voltage characteristics of planar 6H-SiC p-n diodes for junction depths of 0.2 and $0.62 \mu m$: (a) forward characteristics; (b) reverse characteristics [Shenoy 95].

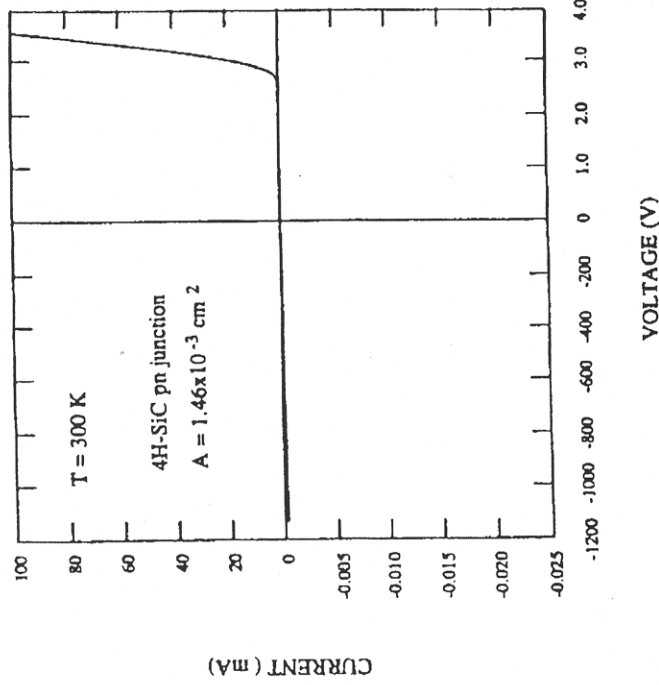


FIG. 46. I-V characteristics of a 4H-SiC mesa p^+-n diode [Palmour 94].

coefficient behavior, thus leading to the conclusion that the latter is related to the defects (dislocations, micropipes, and deep levels) that negatively impact the breakdown properties of the SiC $p-n$ junctions.

4H-SiC $p-n$ junctions grown by LPE on 30- and 35-mm wafers have also been reported [Rendakova 97]. The breakdown across the bulk region occurred at fields in the range of 2 to 4 MV/cm. No degradation in device characteristics occurred upon passing current densities as high as 100 A/cm^2 during reverse bias.

Recent results from the Cree Research group [Irvine 98] indicate the enhanced blocking voltage obtainable with thick, high quality epi-layers on 4H-SiC. Irvine et al. [Irvine 98] report a blocking voltage of 5.5 kV for a p^+ emitter layer of $83 \mu\text{m}$.

Kuznetsov and Dmitriev [Kuznetsov 96] reported linearly graded $p-n$ junctions on 4H-SiC substrates. The diodes had a p^+-p-n^+ mesa structure patterned by reactive ion etching. The three epitaxial layers were grown sequentially on 4H-SiC wafers. The n^+ layer grown first was $1 \mu\text{m}$ thick and had a net concentration of $\sim 2 \times 10^{18} \text{ cm}^{-3}$. Next a $3\text{-}\mu\text{m}$ -thick p -layer was grown, followed by a 0.5-mm -thick p^+ contact layer. The N_a-N_d profile in

3. 4H-SiC $p-n$ JUNCTIONS

Palmour and co-workers first reported $p-n$ junction diodes on 4H-SiC [Palmour 94]. These diodes had a mesa structure and were fabricated on n -type 4H substrates with doping concentration in the range of $(4 \text{ to } 10) \times 10^{18} \text{ cm}^{-3}$. The epitaxial layers were doped in the range of 8×10^{15} to $2.2 \times 10^{18} \text{ cm}^{-3}$. Both p^+-n and n^+-p diode structures were studied on Si- and C-face SiC wafers. The thickness of the low-doped epitaxial layer was in the range of 0.5 to $15.0 \mu\text{m}$. Figure 45 shows the breakdown voltage and the corresponding electric field as a function of background doping. All diodes shown in the illustration, except for the lowest doped sample, showed avalanche breakdown characteristics. The I-V characteristics of the diode showing highest breakdown are shown in Fig. 46. The breakdown voltage of the diode was 1130 V , and a forward current density of 68 A/cm^2 was obtained at 3.6 V .

Mesa structure p^+-n diodes on 4H-SiC were reported by Neudeck and Fazi [Neudeck 97]. The homoepitaxial 4H-SiC layers were grown on commercially available 4H-SiC substrates. The n -type doping was found to be in the range of 0.25 to $1.5 \times 10^{18} \text{ cm}^{-3}$. The majority of smaller size diodes tested were reported to have a stable positive temperature coefficient behavior indicating stable breakdown characteristics. However, the larger size diodes ($> 1 \times 10^{-4} \text{ cm}^2$) exhibited negative temperature breakdown

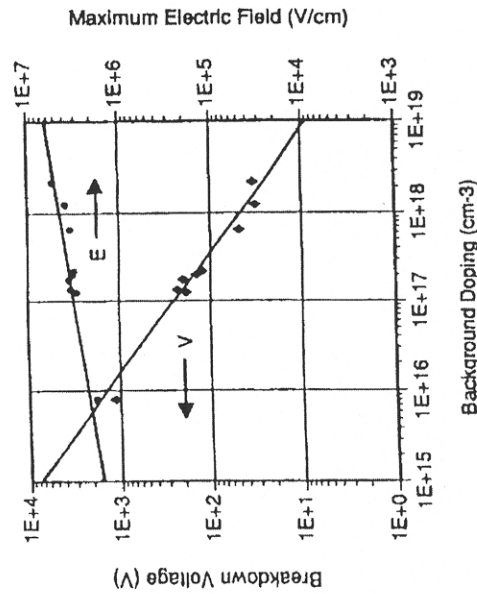


FIG. 45. Breakdown voltage and electric breakdown field as a function of background doping for 4H-SiC $p-n$ diodes [Palmour 94].

the p-layer determined by C-V measurements was found to increase linearly with distance from the junction. The impurity gradient was determined to be $\sim 5 \times 10^{21} \text{ cm}^{-4}$. The I-V characteristics of these diodes were studied as a function of temperature in the range from 200 to 600 K. The ideality factor was found to be independent of temperature, with a measured value of 1.9. The current conduction in the temperature range investigated was attributed to the recombination of carriers in the space-charge region, through a deep level located near the middle of the bandgap. The saturation current density was determined to be 10 to 25 A/cm² at 300 K. The diodes showed an abrupt breakdown at 300 V at all temperatures, and the breakdown electric field was calculated as $3 \times 10^6 \text{ V/cm}$.

Neudeck and Fazi [Neudeck 96a, 96b] reported that p-n diodes fabricated on both 6H- and 4H-SiC failed catastrophically when subjected to single-shot reverse bias pulses. This failure occurred at pulse voltages much lower (60–80%) than the DC reverse bias voltages which these diodes were capable of blocking. Microscopic examination of the diodes subjected to these pulses showed highly localized damage to the device mesa and contact. It is believed that a current-filamentation type of failure occurs in the bulk of the device. When such a filament occurs, the current density in a localized spot drastically increases, greatly stressing the junction material, often to the point of failure.

VIII. Summary and Conclusions

SiC SBDs and p-n junctions have been shown to exceed the performance of Si-based counterparts for applications requiring high-power and high-temperature operation. SiC SBDs could rapidly become commercially viable as an attractive alternative to the slower Si-based p-i-n diodes currently being used in several power electronics applications. A useful figure of merit for rectifiers is the on:off current ratio, which combines the current-carrying capability in forward bias with the leakage current in reverse bias. A summary of published ON:OFF ratios of 4H- and 6H-SiC SBDs is shown in Fig. 47 as a function of reported breakdown voltage. This summary was only able to include results where all the necessary characteristics (forward current, leakage current, and breakdown voltage) were available in the published literature. As can be seen, ON:OFF ratios of one million or more have been obtained by several groups for diodes with breakdown voltages of ~ 1000 to 1100 V. SiC SBDs are also likely to allow operation beyond 300°C, which is the upper limit of Si SOI-based devices. SiC p-n junctions also have the potential to serve as rectifiers with very low off-state leakage

- Arnodo, C., Tye, S., Wyzisk, F., and Brylinski, C. (1996). "Nickel and molybdenum ohmic contacts on silicon carbide," in: *Silicon Carbide and Related Materials VI—Kyoto 1995*, *Inst. Phys. Conf. Ser.* **142**, pp. 577–580.
- Arugu, D. O., Harris, G. L., and Taylor, C. (1995). "Effect of anneal temperature on the electrical characteristics of nickel-based ohmic contacts to β -SiC," *Electronics Lett.* **31** (Apr.), pp. 678–680.
- Avila, R. E., Kopanski, J. J., and Fung, C. D. (1987). "Behavior of ion-implanted junction diodes in 3C-SiC," *J. Appl. Phys.* **62** (October), pp. 3469–3471.
- Bardeen, J. (1947). "Surface states and rectification at a metal semiconductor contact," *Phys. Rev.* **71**, 717–727.
- Baud, L., Jaussaud, C., Madar, R., Bernard, C., Chen, J. S., and Nicolet, M. A. (1995). "Interfacial reactions of W thin film on single-crystal (001) β -SiC," *Mater. Sci. Eng.* **29**, pp. 126–130.
- Baud, L., Billon, T., Lassagne, P., Jaussaud, C., and Madar, R. (1996). "Low contact resistivity W ohmic contacts to n-type 6H-SiC," in: *Silicon Carbide and Related Materials VI—Kyoto 1995*, *Inst. Phys. Conf. Ser.* **142**, pp. 597–600.
- Berger, H. H. (1972). "Contact resistance and contact resistivity," *J. Electrochem. Soc.* **119** (Apr.), pp. 507–514.
- Bermudez, V. M. (1988). "Growth and structure of aluminum films on (001) silicon carbide," *J. Appl. Phys.* **63** (May), pp. 4951–4959.
- Bhatnagar, M., McLarty, P. K., and Baliga, B. J. (1992). "Silicon carbide high-voltage (400 V) Schottky barrier diodes," *IEEE Electron Dev. Lett.* **13** (Oct), pp. 501–503.
- Bhatnagar, M., Nakanishi, H., Bothra, S., McLarty, P. K., and Baliga, B. J. (1993a). "Edge Terminations for SiC High Voltage Schottky Rectifiers," in: *International Symposium on Power Semiconductor Devices & ICs*, *IEEE Cat. No. 93CH33142*, pp. 89–94.
- Bhatnagar, M. and Baliga, B. J. (1993b). "Comparison of 6H-SiC, 3C-SiC, and Si for Power Devices," *IEEE Trans. Electr. Dev.* **40** (3), pp. 645–655.
- Bhatnagar, M., Baliga, B. J., Kirk, H. R., and Rozgonyi, G. A. (1996). "Effect of surface inhomogeneities on the electrical characteristics of SiC Schottky contacts," *IEEE Trans. on Electron Dev.* **43** (Jan), pp. 150–156.
- Campbell, R. B. (1971). "Silicon Carbide Junction Devices," in *Semiconductors and Semimetals, Part B*, P. K. Willardson and A. C. Beer. Academic Press: NY, **7**, pp. 625–683.
- Campbell, R. B. (1981). "What happened to silicon carbide?" in: *Conference on High Temperature Electronics—Tucson 1981*, The Institute of Electrical and Electronics Engineers, Piscataway, NJ (IEEE Catalog No. 81CH1658-4), pp. 71–74.
- Chaddha, A. K., Parsons, J. D., and Kruaval, G. B. (1995). "Thermally stable, low specific resistance ($1.30 \times 10^{-5} \Omega \text{ cm}^2$) TiC ohmic contacts to n-type 6H-SiC," *Appl. Phys. Lett.* **66**, pp. 760–762.
- Chaudhry, M. I., Berry, W. B., and Zeller, M. V. (1990). "Ohmic contacts on β -SiC," *Mat. Res. Soc. Symp. Proc.* **162**, pp. 507–512.
- Chaudhry, M. I., Berry, W. B., and Zeller, M. V. (1991). "A study of ohmic contacts on β -SiC," *Int. J. Electronics* **71**, pp. 439–444.
- Chen, J. S., Bachli, A., Nicholet, M.-A., Baud, L., Jaussaud, C., and Madar, R. (1995). "Contact resistivity of Re, Pt and Ta films on n-type β -SiC: preliminary results," *Mater. Sci. Eng.* **29**, pp. 185–189.
- Cheung, S. K. and Cheung, N. W. (1986). "Extraction of Schottky diode parameters from forward current-voltage characteristics," *Appl. Phys. Lett.* **49** (Jul), pp. 85–87.
- Choyke, W. J., Patrick, L., and Hamilton, D. R. (1964). In *Int. Conf. Semicond.*—Paris 1964, p. 751.
- Cooper, J. A., "Recent advances in SiC Power devices" in *Silicon Carbide, III-Nitrides and Related Materials—VII Stockholm 1997*, edited by G. Pensl, H. Morkoc, B. Monemar and E. Janzen, Materials Science Forum **264–268**, pp. 895–900 (1998).

- Cox, R. H. and Strack, H. (1967). "Ohmic contacts for GaAs devices," *Solid-State Electron.* **10** (Dec), pp. 1213-1218.
- Crofton, J., Ferrero, J. M., Barnes, P. A., Williams, J. R., Bozack, M. J., Tin, C. C., Ellis, C. D., Spitznagel, J. A., and McMullin, P. G. (1992). "Metallization studies on epitaxial 6H-SiC," in: *Amorphous and Crystalline Silicon Carbide IV—Santa Clara 1991*, Springer, *Proc. Phys.* **71**, pp. 176-182.
- Crofton, J., Barnes, P. A., and Williams, J. R. (1993). "Contact resistance measurements on p-type 6H-SiC," *Appl. Phys. Lett.* **62** (Jan), pp. 384-386.
- Crofton, J., McMullin, P. G., Williams, J. R., and Bozack, M. J. (1995). "High-temperature ohmic contact to n-type 6H-SiC using nickel," *J. Appl. Phys.* **77** (Feb), pp. 1317-1319.
- Crofton, J., Luckowski, E. D., Williams, J. R., Isaacs-Smith, T., Bozack, M. J., and Siergiej, R. (1996a). "Specific contact resistance as a function of doping for n-type 4H and 6H-SiC," in: *Silicon Carbide and Related Materials VI—Kyoto 1995*, *Inst. Phys. Conf. Ser.* **142**, pp. 569-572.
- Crofton, J. and Sriram, S. (1996b). "Reverse leakage current calculations for SiC Schottky contacts," *IEEE Trans. on Electron. Dev.* **43** (Dec), pp. 2305-2307.
- Daimon, H., Yamana, M., Sakuma, E., Misawa, S., and Yoshida, S. (1986). "Annealing effects on Al and Al-Si contacts with 3C-SiC," *Jpn. J. Appl. Phys.* **25** (Jul), pp. 592-594.
- Davis, R. F., Kelner, G., Shur, M., Palmour, J. W., and Edmond, J. A. (1991). "Thin film deposition and microelectric and optoelectric device fabrication and characterization in monocrytalline alpha beta silicon carbide," *Proc. of IEEE* **79** (May), pp. 677-701.
- Dmitriev, V. A., Ivanov, P. A., Strelchuk, A. M., Syrkin, A. L., Popov, I. V., and Chelnokov, V. E. (1985a). "SiC tunnel diodes," *Sov. Tech. Phys. Lett.* **11** (Aug), pp. 403-404.
- Dmitriev, V. A., Ivanov, P. A., Korin, I. V., Monozenko, Y. V., Popov, I. V., Sidorva, T. A., Strelchuk, A. M., and Chelnokov, V. E. (1985b). "Silicon carbide p-n structures synthesized by liquid-phase epitaxy," *Sov. Tech. Phys. Lett.* **11** (Feb), pp. 98-99.
- Dmitriev, V. A., Ivanov, P. A., Levin, V. I., Popov, I. V., Strelchuk, A. M., Tanisov, Y. M., Tsvetkov, V. F., and Chelnokov, V. E. (1987). "Fabrication of epitaxial silicon carbide structures obtained from bulk SiC crystals," *Sov. Tech. Phys. Lett.* **13** (Nov), pp. 489-490.
- Dmitriev, V. A., Fekade, K., and Spencer, M. G. (1992). "Dependence of the Au-SiC(6H) Schottky barriers height on the SiC surface treatment," in *Amorphous and Crystalline Silicon Carbide IV—Santa Clara 1991*, Springer *Proc. Phys.* **71**, pp. 352-355.
- Dmitriev, V. A., Irvine, K., and Spencer, M. (1994). "Low resistivity ($\sim 10^{-5} \Omega \text{cm}^2$) ohmic contacts to 6H silicon carbide fabricated using cubic silicon carbide contact layer," *Appl. Phys. Lett.* **64** (Jan), pp. 318-320.
- Dunlop, H. L. and Marsh, O. J. (1969). "Diodes in silicon carbide by ion implantation," *Appl. Phys. Lett.* **15** (Nov), pp. 311-313.
- Edmond, J. A., Ryu, J., Glass, J. T., and Davis, R. F. (1988a). "Electrical contacts to beta silicon carbide thin films," *J. Electrochem. Soc.* **135** (Feb), pp. 359-362.
- Edmond, J. A., Das, K., and Davis, R. F. (1988b). "Electrical properties of ion-implanted p-n junction diodes in β -SiC," *J. Appl. Phys.* **63** (Feb), pp. 922-929.
- Edmond, J. A., Kong, H.-S., and Carter, Jr., C. H. (1992). "High-temperature rectifiers, UV photodiodes, and blue LEDs in 6H-SiC," in: *Amorphous and Crystalline Silicon Carbide IV—Santa Clara 1991*, Springer *Proc. Phys.* **71**, pp. 344-351.
- Edmond, J. A., Kong, H.-S., and Carter, Jr., C. H. (1993). "Blue LEDs, UV photodiodes and high-temperature rectifiers in 6H-SiC," *Physica B* **185**, pp. 453-460.
- Ferry, D. K. (1975). "High-field transport in wide-band-gap semiconductors," *Phys. Rev. B* **12**, p. 2361-2369.
- Fröjd, C., and Patterson, C. S. (1996). "Comment on Temperature dependence of the barrier height of metal-semiconductor contacts on 6H-SiC," *J. Appl. Phys.* **80**, pp. 6570-6571.
- Fujii, Y., Shigeta, M., Furukawa, K., and Suzuki, A. (1988). "Dependence on the Schottky metal and crystal orientation of the Schottky diode characteristics of β -SiC single crystals grown by chemical vapor deposition," *J. Appl. Phys.* **64** (Nov), pp. 5020-5025.
- Furukawa, K., Uemoto, A., Shigeta, M., Suzuki, A., and Nakajima, S. "3C-SiC p-n junction diodes," *Appl. Phys. Lett.* **48**, pp. 1536-1537.
- Geib, K. M., Mahan, J. E., and Wilmsen, C. W. (1989). "W/SiC contact resistance at elevated temperatures," in: *Amorphous and Crystalline Silicon Carbide and Related Materials II—Santa Clara 1989*, **43**, pp. 224-229.
- Ghezzi, M., Brown, D. M., Downey, E., Kretschmer, J., Hennessy, W., Polla, D. L., and Bakhr, H. (1992). "Nitrogen-Implanted SiC Diodes Using High-Temperature Implantation," *IEEE Electron Device Letters*, **13**, pp. 639-641.
- Ghezzi, M., Brown, D. M., Downey, E., and Kretschmer, J. (1993). "Boron-implanted 6H-SiC diodes," *Appl. Phys. Lett.* **63** (Aug), pp. 1206-1208.
- Glass, R. C., Spellman, L. M., and Davis, R. F. (1991). "Low energy ion-assisted deposition of titanium nitride ohmic contacts on alpha (6H)-silicon carbide," *Appl. Phys. Lett.* **59** (22), pp. 2868-2870.
- Glass, R. C., Spellman, L. M., Tanaka, S., and Davis, R. F. (1992). "Chemical and structural analyses of the titanium nitride/alpha (6H)-silicon carbide interface," *J. Vac. Sci. Technol. A* **10** (4), pp. 1625-1631.
- Glass, R. C., Palmour, J. W., Davis, R. F., and Porter, L. M. (1994). "Method of forming ohmic contacts to p-type wide bandgap semiconductors and resulting ohmic contact structure." US Patent No. 5323022.
- Goesmann, F. and Schmid-Fetzer, R. (1995). "Temperature-dependent interface reactions and electrical contact properties of titanium on 6H-SiC," *Semiconductor Sci. & Tech.* **10** (Dec), pp. 1652-1658.
- Goodman, A. M. (1963). "Metal-semiconductor barrier height measurement by the differential capacitance method—one carrier system," *J. Appl. Phys.* **34** (Feb), pp. 329-338.
- Gorin, S. N. and Pletyushkin, A. A. (1965). *Growth Crystal* **6** (USSR), p. 210.
- Hagen, S. H. (1968). "Surface-barrier diodes on silicon carbide," *J. Appl. Phys.* **39** (3), pp. 1458-1461.
- Hall, R. N. (1958). "Electrical contacts to silicon carbide," *J. Appl. Phys.* **29** (6), pp. 914-917.
- Hallin, C., Yakimova, R., Krastev, V., Marinova, T. S., and Janzén, E. (1996). "Interface chemistry and electrical properties of annealed Ni and Ni/Al-6H SiC structures," in *Silicon Carbide and Related Materials VI—Kyoto 1995*, *Inst. Phys. Conf. Ser.* **142**, pp. 601-604.
- Hallin, C., Yakimova, R., Péc, B., Georgieva, A., Marinova, T. S., Kasamakova, L., Kakanaokov, R., and Janzén, E. (1997). "Improved Ni Ohmic contact on n-type 4H-SiC," *J. Electron. Mat.* **26** (3), pp. 119-122.
- Ioannou, D. E., Papanicolaou, N. A., and Nordquist, P. E. (1987). "The effect of heat treatments on Au Schottky contacts on β -SiC," *IEEE Trans. Electron. Dev.* **34** (Aug), pp. 1694-1699.
- Itoh, A., Kimoto, T., and Matsunami, H. (1995a). "High performance of high-voltage 4H-SiC Schottky barrier diodes," *IEEE Electron Dev. Lett.* **16** (Jun), pp. 280-282.
- Itoh, A., Takemura, O., Kimoto, T., and Matsunami, H. (1995b). "Barrier height analysis of metal/4H-SiC Schottky contacts," in *Silicon Carbide and Related Materials VI—Kyoto 1995*, *Inst. Phys. Conf. Ser.* **142**, pp. 685-688.
- Itoh, A., Kimoto, T., and Matsunami, H. (1995c). "Low power-loss 4H-SiC Schottky rectifiers with high blocking voltage," in *Silicon Carbide and Related Materials VI—Kyoto 1995*, *Inst. Phys. Conf. Ser.* **142**, pp. 689-692.
- Itoh, A., Kimoto, T., and Matsunami, H. (1996). "Excellent reverse blocking characteristics of high-voltage 4H-SiC Schottky rectifiers with boron-implanted edge termination," *IEEE Electron Dev. Lett.* **17** (3), pp. 139-141.
- Janzén, E. and Kordina, O. (1996). "Recent progress in epitaxial growth of SiC for power device applications," in: *Silicon Carbide and Related Materials VI—Kyoto 1995*, *Inst. Phys. Conf. Ser.* **142**, pp. 653-658.

- Kaneda, S., Sakamoto, Y., Mihara, T., and Tanaka, T. (1987). "MBE growth of 3C SiC/6H SiC and the electric properties of its p-n junction," *J. Crystal Growth* **81**, pp. 536–542.
- Kelner, G., Shur, M. S., Binari, S., Slegler, K. J. and Kong, H. S. (1989). "High-transconductance β -SiC Buried-Gate JFETs," *IEEE Trans. Electron. Dev.* **36**, pp. 1045–1048.
- Kelner, G., Binari, S., Shur, M. and Palmour, J. W. (1991). "High temperature operation of α -silicon carbide buried-gate junction field-effect transistors," *Electron. Lett.* **27**, pp. 1038–1040.
- Kimoto, T., Urushidani, T., Kobayashi, S., and Matsunami, H. (1993). "High-voltage (>1 kV) SiC Schottky barrier diodes with low on-resistances," *IEEE Electron Dev. Lett.* **14** (Dec), pp. 548–550.
- Kimoto, T., Wahab, Q., Ellison, A., Forsberg, U., Tuominen, M., Yakimova, R., Henry, A., and Janzén, E. (1998). "High-voltage (>2.5 kV) 4H-SiC Schottky rectifiers processed on hot-wall CVD and high-temperature CVD layers," in: *Silicon Carbide, III-Nitrides and Related Materials VII—Stockholm 1997*, edited by G. Pensl, H. Morkoc, B. Monemar and E. Janzén, *Materials Science Forum*, **264**–268, pp. 921–924.
- Kneifel, M., Silber, D., and Held, R. (1996). "Predictive modeling of SiC power Schottky diode for investigations in power electronics," in: *Proc. IEEE Appl. Power Elec. Conf. and Expo., IEEE Cat. No. 95CH35748*, pp. 239–245.
- Kordina, O., Henry, A., Bergman, J. P., Son, N. T., Chen, W. M., Hallin, C., and Janzén, E. (1995a). "High quality 4H-SiC epitaxial layers grown by chemical vapor deposition," *Appl. Phys. Lett.* **66** (Mar), pp. 1373–1375.
- Kordina, O., Bergman, J. P., Henry, A., and Janzén, E. (1995b). "A 4.5 kV 6H silicon carbide rectifier," *Appl. Phys. Lett.* **67** (Sept), pp. 1561–1563.
- Kuznetsov, N. I. and Dmitriev, V. A. (1996). "Electrical characteristics of 4H-SiC pn structures," in: *Third International High Temperature Electronic Conference—Albuquerque 1996*, **2**, pp. P/77–P/82.
- Lang, M., Isaac-Smith, T., Tin, C. C., and Williams, J. R. (1996). "Ni, Al, and Ti Schottky diodes and their electrical characterization on 6H-SiC," in: *Silicon Carbide and Related Materials VI—Kyoto 1995*, *Inst. Phys. Conf. Ser.* **142**, pp. 681–684.
- Larkin, D. J., Neudeck, P. G., Powell, J. A., and Matus, L. G. (1994). "Site-competition epitaxy for controlled doping of CVD silicon carbide," in: *Silicon Carbide and Related Materials V—Washington 1993*, *Inst. Phys. Conf. Ser.* **137**, pp. 51–54.
- Lebedev, A. A., Strelchuk, A. M., Ortolland, S., Raynaud, C., Locatelli, M. L., Planson, D., and Chante, J. P. (1996a). "The negative temperature coefficient of the breakdown voltage of SiC p-n structures and deep centers in SiC," in: *Silicon Carbide and Related Materials VI—Kyoto 1995*, *Inst. Phys. Conf. Ser.* **142**, pp. 701–704.
- Lebedev, A. A., Rastegaeva, M. G., Savkina, N. S., Tregubova, A. S., Chelnokov, V. E., and Scheglov, M. P. (1996b). "New results and prospects in the development of high power and high temperature SiC based diodes," in: *Third International High Temperature Electronic Conference—Albuquerque 1996*, **2**, pp. P/161–166.
- Liu, S., Reinhardt, K., Severt, C., and Scofield, J. (1996). "Thermally stable ohmic contacts on n-type 6H- and 4H-SiC based on silicide and carbide," in: *Silicon Carbide and Related Materials VI—Kyoto 1995*, *Inst. Phys. Conf. Ser.* **142**, pp. 589–592.
- Lundberg, N., Zetterling, C. M., and Östling, M. (1993). "Temperature stability of cobalt Schottky contacts on n- and p-type 6H silicon carbide," *Applied Surface Science* **73** (Nov), pp. 316–321.
- Lundberg, N. and Östling, M. (1994). "Cobalt disilicide (CoSi₂) Schottky contacts to 6H-SiC," *Physica Scripta* **134**, pp. 273–277.
- Lundberg, N. (1995). "CoSi₂ ohmic contacts to n-type 6H-SiC," *Solid-State Electronics* **38** (Dec), pp. 2023–2028.
- Lundberg, N., Tägstöm, P., Jansson, U., and Östling, M. (1996a). "CVD of tungsten Schottky diodes to 6H-SiC," in: *Silicon Carbide and Related Materials VI—Kyoto 1995*, *Inst. Phys. Conf. Ser.* **142**, pp. 677–680.
- Lundberg, N. and Östling, M. (1996b). "Chemical vapor deposition of tungsten Schottky diodes to 6H-SiC," *J. Electrochem. Soc.* **143** (May), pp. 1662–1667.
- Lundberg, N. and Östling, M. (1996c). "Thermally stable low ohmic contacts to p-type 6H-SiC using cobalt silicides," *Solid-State Electronics* **39** (Nov), pp. 1559–1565.
- Marlow, G. S. and Das, M. B. (1982). "The effects of contact size and non-zero metal resistance on the determination of specific contact resistance," *Solid-State Electronics* **25** (2), pp. 91–94.
- Mead, C. A. and Spitzer, W. G. (1964). "Fermi level position at metal-semiconductor interfaces," *Physical Review* **134** (3A), pp. A713–A716.
- Mead, C. A. (1966). "Metal-semiconductor surface barriers," *Solid-State Electronics* **9**, pp. 1023–1033.
- Moki, A., Shenoy, P., Alok, D., Baliga, B. J., Wongchotigul, K., and Spencer, M. G. (1995). "Low resistivity as-deposited ohmic contacts to 3C-SiC," *J. Electron. Mat.* **24** (Apr), pp. 315–318.
- Mott, N. F. (1938). "Note on the contact between a metal and an insulator or a semiconductor," *Proc. Camb. Phil. Soc.* **34**, p. 568.
- Muench, W. v. and Pfaffeneder, I. (1977). "Breakdown field in vapor-grown silicon carbide p-n junctions," *J. Appl. Phys.* **48** (Nov), pp. 4831–4833.
- Nelson, W. E., Halden, F. A., and Rosengreen, A. (1966). "Growth and properties of β -SiC single crystals," *J. Appl. Phys.* **37** (Jan), pp. 333–336.
- Neudeck, P. G., Larkin, D. J., Starr, J. E., Powell, J. A., Salupo, C. S., and Matus, L. G. (1993). "Greatly improved 3C-SiC p-n junction diodes grown by chemical vapor deposition," *IEEE Electron Dev. Lett.* **14** (Mar), pp. 136–139.
- Neudeck, P. G., Larkin, D. J., Salupo, C. S., Powell, J. A., and Matus, L. G. (1994a). "2000 V 6H-SiC on junction diodes," in: *Silicon Carbide and Related Materials V—Washington 1993*, *Inst. Phys. Conf. Ser.* **137**, pp. 475–479.
- Neudeck, P. G., Larkin, D. J., Powell, J. A., and Matus, L. G. (1994b). "2000 V 6H-SiC p-n junction diodes grown by chemical vapor deposition," *Appl. Phys. Lett.* **64** (Mar), pp. 1386–1388.
- Neudeck, P. G., Larkin, D. J., Starr, J. E., Powell, J. A., Salupo, C. S., and Matus, L. G. (1994c). "Electrical properties of epitaxial 3C- and 6H-SiC p-n junction diodes produced side-by-side on 6H-SiC substrates," *IEEE Trans. Electron. Dev.* **41** (May), pp. 826–835.
- Neudeck, P. G., Fazi, C., and Parsons, J. D. (1996). "Fast risetime reverse bias pulse failures in SiC PN junction diodes," in: *Third International High Temperature Electronic Conference—Albuquerque 1996*, **2**, pp. XXVI/15–20.
- Neudeck, P. G. and Fazi, C. (1997). "Positive temperature coefficient of breakdown voltage in 4H-SiC pn junction rectifiers," *IEEE Electron Dev. Lett.* **18** (Mar), pp. 96–98.
- Norde, H. (1979). "A modified forward I-V plot for Schottky diodes with high series resistance," *J. Appl. Phys.* **50** (Jul), pp. 5052–5053.
- Nordell, N., Savage, S., and Schöner, A. (1996). "Aluminum doped 6H-SiC: CVD growth and formation of ohmic contacts," in: *Silicon Carbide and Related Materials VI—Kyoto 1995*, *Inst. Phys. Conf. Ser.* **142**, pp. 573–576.
- Palmour, J. W., Kong, H. S., Waltz, E. D., Edmond, J. A., and Carter, C. H. (1991). In: *First International High Temperature Electronics Conference, Albuquerque, NM*, edited by D. B. King and F. V. Thome.
- Palmour, J. W., Edmond, J. A., Kong, H. S., and Carter, C. H. (1994). "Vertical power devices in silicon carbide," in: *Silicon Carbide and Related Materials V—Washington 1993*, *Inst. Phys. Conf. Ser.* **137**, pp. 499–502.

- Papanicolaou, N. A., Christou, A., and Gipe, M. L. (1989). "Pt and PtSi_x Schottky contacts on n-type β -SiC," *J. Appl. Phys.* **65** (May), pp. 3526–3530.
- Parsons, J. D., Kruval, G. B., and Chaddha, A. K. (1994). "Low specific resistance ($<6 \times 10^{-6} \Omega \text{cm}^2$) TiC ohmic contacts to n-type β -SiC," *Appl. Phys. Lett.* **65** (Oct), pp. 2075–2077.
- Petit, J. B. and Zeller, M. V. (1992). "Electrical and chemical characterization of contacts to silicon carbide," *Mat. Res. Soc. Symp. Proc.* **242**, pp. 567–572.
- Petit, J. B., Neudeck, P. G., Salupo, C. S., Larkin, D. J., and Powell, J. A. (1994). "Metal contacts to n- and p-type 6H-SiC: electrical characteristics and high-temperature stability," in: *Silicon Carbide and Related Materials V—Washington 1993*, *Inst. Phys. Conf. Ser.* **137**, pp. 679–682.
- Philip, H. R. and Taft, E. A. (1960). "Intrinsic optical absorption in single crystal silicon carbide," in: *Silicon Carbide: A High Temperature Semiconductor*, Eds. J. R. O'Connor and J. Smitens. Pergamon Press: Oxford, pp. 366–370.
- Porter, L. M., Glass, R. C., Davis, R. F., Bow, J. S., Kim, M. J., and Carpenter, R. W. (1993). "Chemical and electrical mechanism in titanium, platinum, and hafnium contacts to alpha (6H) silicon carbide," *Mat. Res. Soc. Symp. Proc.* **282**, pp. 471–477.
- Porter, L. M., Davis, R. F., Bow, J. S., Kim, M. J., and Carpenter, R. W. (1994). "Deposition and characterization of Schottky and Ohmic contacts on n-type alpha (6H)-SiC (0001)," in: *Silicon Carbide and Related Materials V—Washington 1993*, *Inst. Phys. Conf. Ser.* **137**, pp. 581–584.
- Porter, L. M. and Davis, R. F. (1995a). "A critical review of ohmic and rectifying contacts for silicon carbide," *Materials Science and Engineering B* **34**, pp. 83–105.
- Porter, L. M. and Davis, R. F. (1995b). "Chemistry, microstructure, and electrical properties at interfaces between thin films of cobalt and alpha (6H) silicon carbide (0001)," *J. Mat. Res.* **10** (Jan), pp. 26–33.
- Porter, L. M. and Davis, R. F. (1995c). "Chemistry, microstructure, and electrical properties at interfaces between thin films of titanium and alpha (6H) silicon carbide (0001)," *J. Mat. Res.* **10** (Mar), pp. 668–679.
- Porter, L. M. and Davis, R. F. (1995d). "Chemistry, microstructure, and electrical properties at interfaces between thin films of platinum and alpha (6H) silicon carbide (0001)," *J. Mat. Res.* **10** (Sep), pp. 2336–2342.
- Porter, L. M. and Davis, R. F. (1996). "Issues and status of ohmic contacts for p-type silicon carbide," in: *Third International High Temperature Electronic Conference—Albuquerque 1996*, **1**, pp. VII/3–8.
- Proctor, S. J. and Linholm, L. W. (1982). "A direct measurement of interfacial contact resistance," *IEEE Electron Dev. Lett.* **EDL-3** (Oct), pp. 294–296.
- Proctor, S. J. and Linholm, L. W. (1983). "Direct measurements of interfacial contact resistance, end resistance, and interfacial contact layer uniformity," *IEEE Electron Dev.* **ED-30** (Nov), pp. 1535–1542.
- Ragunathan, R., Alok, D., and Baliga, B. J. (1995). "High voltage 4H-SiC Schottky barrier diodes," *IEEE Electron Dev. Lett.* **16** (Jun), pp. 226–227.
- Ramungul, N., Khemka, V., Tyagi, R., Chow, T. P., Ghezzi, M., Nuedeck, P. G., Kretschmer, J., Henessy, W., and Brown, D. M. (1996). "Comparison of aluminum- and boron-implanted vertical 6H-SiC p⁺n junction diodes," in: *Silicon Carbide and Related Materials VI—Kyoto 1995*, *Inst. Phys. Conf. Ser.* **142**, pp. 713–717.
- Rastegaev, M. G., Andreev, A. N., Zelenin, V. V., Babanin, A. I., Nikitina, I. P., Chelnokov, V. E., and Rastegaev, V. P. (1996a). "Nickel-based metallization in processes of the 6H-SiC device fabrication: ohmic contacts, masking and packaging," in: *Silicon Carbide and Related Materials VI—Kyoto 1995*, *Inst. Phys. Conf. Ser.* **142**, pp. 581–584.
- Raynaud, C., Ducroquet, F., Brounkow, P. N., Gullot, G., Porter, L. M., Davis, R. F., Jaussaud, C., and Billon, T. (1996). "Electrical characterization of epitaxial 6H-SiC admittance spectroscopy," *Materials Sci. and Tech.* **12** (Jan), pp. 94–97.
- Reddy, C. V., Fung, S., Belling, C. D., and Brauer, G. (1996). "Current transport at low temperature in Al/6H-SiC Schottky barriers," in: *Silicon Carbide and Related Materials VI—Kyoto 1995*, *Inst. Phys. Conf. Ser.* **142**, pp. 669–673.
- Rendakova, S., Ivanisov, V., and Dmitriev, V. (1998). "High quality 6H and 4H-SiC pn structures with stable electric breakdown grown by liquid phase epitaxy," in: *Silicon Carbides, III—Nirides and Related Materials VII—Stockholm 1997*, edited by G. Pensl, H. Morkoc, B. Monemar and E. Janzén, *Materials Science Forum*, pp. 163–166.
- Rhoderick, E. H. and Williams, R. H. (1988). "Metal-Semiconductor Contacts," Clarendon Press: Oxford.
- Saxena, V., Steckl, A. J., Vichare, M., Ramalingam, M. L., and Reinhardt, K. (1996). "Temperature effects in the operation of high voltage Ni/6H-SiC Schottky rectifiers," in: *Third International High Temperature Electronic Conference—Albuquerque 1996*, **1**, pp. VII/15–20.
- Saxena, V. and Steckl, A. J. (1997). "High Temperature Operation of High Breakdown Voltage Schottky Diodes on 4H and 6H-SiC" in International Semiconductor Device Research Symposium—1997, pp. 539–542.
- Saxena, V. and Steckl, A. J. (1998). "High voltage Pt and Ni Schottky barrier diodes on 4H-SiC," in: *Silicon Carbide, III—Nirides and Related Materials—VII Stockholm 1997*, edited by G. Pensl, H. Morkoc, B. Monemar and E. Janzén, *Materials Science Forum*, pp. 264–268, pp. 937–940.
- Schadt, M., Pensl, G., Devaty, R. P., Choyke, W. J., Stein, R., and Stephani, D. (1994). "Anisotropy of the electron Hall mobility in 4H, 6H and 15R silicon carbide," *Appl. Phys. Lett.* **65** (Dec), pp. 3120–3122.
- Schaffer, W. J., Negley, G. H., Irvine, K. G., and Palmour, J. W. (1994). "Conductivity anisotropy in epitaxial 6H and 4H SiC," *Mat. Res. Soc. Symp. Proc.* **337**, pp. 595–600.
- Schroder, D. K. (1990). "Semiconductor Material and Device Characterization," John Wiley & Sons, Inc.: New York.
- Schroder, C., Heiland, W., Held, R., and Loose, W. (1996). "Analysis of reverse current-voltage characteristics of Ti/6H-SiC Schottky diodes," *Appl. Phys. Lett.* **68** (Apr), pp. 1957–1959.
- Shalish, I., Gasser, S., Kolawa, E., and Nicolet, M.-A. (1996). "Stability of Schottky contacts with Ta-Si-N amorphous diffusion barriers and Au overlayers on 6H-SiC," in: *Third International High Temperature Electronic Conference—Albuquerque 1996*, **1**, pp. VII/21–26.
- Shenoy, P., Moki, A., Baliga, B. J., Alok, D., Wongchotigul, K., and Spencer, M. (1994). "Vertical Schottky barrier diodes on 3C-SiC grown on Si," in: *Tech. Digest Intl. Electron Dev. Meeting, IEEE Cat. No. 94CH35706*, pp. 411–414.
- Shenoy, P. M., and Baliga, B. J. (1995). "Planar, ion implanted, high voltage 6H-SiC p-n junction diodes," *IEEE Electron Dev. Lett.* **16** (Oct), pp. 454–456.
- Shenoy, P. M. and Baliga, B. J. (1996). "Planar, high voltage, boron implanted 6H-SiC p-n junction diodes," in: *Silicon Carbide and Related Materials VI—Kyoto 1995*, *Inst. Phys. Conf. Ser.* **142**, pp. 717–721.
- Shibahara, K., Kuroda, N., Nishino, S., and Matsunami, H. (1987). "Fabrication of p-n junction diodes using homoepitaxially grown 6H-SiC at low temperature by chemical vapor deposition," *Jpn. J. Appl. Phys.* **26** (Nov), pp. 1815–1817.
- Shier, J. S. (1970). "Ohmic contacts to silicon carbide," *J. Appl. Phys.* **41**, pp. 771–773.
- Schockley, W., Goetzberger, A., and Scarlett, R. M. (1964). "Research and investigation of inverse epitaxial UHF power transistors." U.S. Air Force Avionics Lab., Wright Patterson Air Force Base (Report No. AFAL-TDR-64-207): Dayton, OH.

- Shor, J. S., Weber, R. A., Provost, L. G., Goldstein, D., and Kurtz, A. D. (1992). "High temperature ohmic contacts for n-type β -SiC sensors," *Mat. Res. Symp. Proc.* **242**, pp. 573-581.
- Shor, J. S., Weber, R. A., Provost, L. G., Goldstein, D., and Kurtz, A. D. (1994). "High temperature ohmic contact metallizations for n-type 3C-SiC," *J. Electrochem. Soc.* **141** (Feb), pp. 579-581.
- Smith, S. R., Ewarye, A. O., and Mitchell, W. C. (1995). "Temperature dependence of the barrier height of metal-semiconductor contacts on 6H-SiC," *J. Appl. Phys.* **79** (Jan), pp. 301-304.
- Smith, S. R., Ewarye, A. O., and Mitchell, W. C. (1996). "Reply to 'Comment on 'Temperature dependence of the barrier height of metal-semiconductor contacts on 6H-SiC,'" *J. Appl. Phys.* **80**, pp. 6572-6573.
- Spellman, L. M., Glass, R. C., Davis, R. F., Humphreys, T. P., Jeon, H., Nemanich, R. J., Chevacharoenkul, S., and Parikh, N. R. (1991). "Heteroepitaxial growth and characterization of titanium films on alpha 6H silicon carbide," *Mat. Res. Soc. Symp. Proc.* **221**, pp. 99-104.
- Spellman, L. M., Glass, R. F., Davis, R. F., Humphreys, T. P., Nemanich, R. J., Das, K., and Chevacharoenkul, S. (1992). "Electrical characteristics of epitaxial titanium contacts to alpha (6H) silicon carbide," in: *Amorphous and Crystalline Silicon Carbide IV—Santa Clara 1991*, Springer Proc. Phys. **71**, pp. 417-422.
- Spies, L., Nennwitz, O., and Pezoldt, J. (1996). "Improved ohmic contacts to p-type 6H-SiC," in: *Silicon Carbide and Related Materials VI—Kyoto 1995*, *Inst. Phys. Conf. Ser.* **142**, pp. 585-588.
- Steckl, A. J. and Li, J. P. (1992). "Epitaxial growth of β -SiC on Si by RTCVD with C_3H_8 and SiH_4 ," *IEEE Trans. Electron Dev.* **39** (Jan), pp. 64-74.
- Steckl, A. J. and Su, J. N. (1993). "High voltage, temperature-hard 3C-SiC Schottky diodes using all-Ni metallization," *Tech. Digest Intl. Electron Dev. Meeting, IEEE Cat. No. 93CH3361-3*, pp. 695-698.
- Steckl, A. J., Su, J. N., Yih, P. H., Yuan, C., and Li, J. P. (1994). "Ohmic and rectifying contacts to 3C-SiC using all-Ni technology," in: *Silicon Carbide and Related Materials V—Washington 1993*, *Inst. Phys. Conf. Ser.* **137**, pp. 653-656.
- Steckl, A. J., Devraj, J., Tlali, S., Jackson, H. E., Tran, C., Gorin, S. N., and Ivanova, L. M. (1996). "Characterization of 3C-SiC grown by thermal decomposition of methyltrichlorosilane," *Appl. Phys. Lett.* **69** (Dec), pp. 3824-3826.
- Su, J. N. and Steckl, A. J. (1995). "300°C operation of high voltage SiC Schottky rectifier," in: *Workshop on High Temperature Power Electronics—Ft. Monmouth, NJ*, pp. 50-53.
- Su, J. N. and Steckl, A. J. (1996). "Fabrication of high voltage SiC Schottky barrier diodes by Ni metallization," in: *Silicon Carbide and Related Materials VI—Kyoto 1995*, *Inst. Phys. Conf. Ser.* **142**, pp. 697-700.
- Suzuki, A., Uemoto, A., Shigota, M., Furukawa, K., and Makajima, S. (1986). "p-n junction diodes in beta-SiC," *Extended Abstracts, 18th Int. Conf. Solid State Devices and Materials*, p. 101.
- Teraji, T., Hara, S., Okushi, H., and Kajimura, K. (1996). "Ti ohmic contact without post-annealing process to n-type 6H-SiC," in: *Silicon Carbide and Related Materials VI—Kyoto 1995*, *Inst. Phys. Conf. Ser.* **142**, pp. 593-596.
- Teraji, T., Hara, S., Okuslei, H., and Kajimura, K. (1997). "Ideal ohmic contact to n-type 6H-SiC by reduction of Schottky barrier height," *Appl. Phys. Lett.* **71** (Aug), p. 689.
- Uemoto, T. (1995). "Reduction of ohmic contact resistance on n-type 6H-SiC by heavy doping," *Jpn. J. Appl. Phys.* **34** (Jan), pp. 7-9.
- Ueno, K., Urushidani, T., Hashimoto, K., and Seki, Y. (1995). "The guard-ring termination for the high-voltage SiC Schottky barrier diodes," *IEEE Electron Dev. Lett.* **16** (Jul), pp. 331-332.
- Ueno, K., Urushidani, T., Hashimoto, K., and Seki, Y. (1996). "The guard-ring termination for 6H-SiC Schottky barrier diodes," in: *Silicon Carbide and Related Materials VI—Kyoto 1995*, *Inst. Phys. Conf. Ser.* **142**, pp. 693-696.
- Urushidani, T., Kobayashi, S., Kimoto, T., and Matsunami, H. (1994). "High-voltage Au/6H-SiC Schottky barrier diodes," in: *Silicon Carbide and Related Materials VI—Washington*, *Inst. Phys. Conf. Ser.* **137**, pp. 471-474.
- van der Ziel, A. (1968). "Solid State Physical Electronics," Prentice Hall: Englewood Cliffs, NJ.
- van Elsbergen, V., Kampen, T. U., and Monch, W. (1996). "Electronic properties of cesium on 6H-SiC surfaces," *J. Appl. Phys.* **79** (Jan), pp. 316-321.
- van Opdorp, C. and Vrakking, J. (1969). "Avalanche breakdown in epitaxial SiC p-n junctions," *J. Appl. Phys.* **40**, pp. 2320-2322.
- Vassilevski, K. V., Dmitriev, V. A., and Zorenko, A. V. (1993). "Silicon carbide diode operating at avalanche breakdown current density of 60 kA/cm²," *J. Appl. Phys.* **74** (12), pp. 7612-7614.
- Vassilevski, K. V., Zorenko, A. V., and Novozhilov, V. V. (1994). "Temperature dependence of avalanche breakdown voltage of pn-junctions in 6H-SiC at high current density," in: *Silicon Carbide and Related Materials V—Washington 1993*, *Inst. Phys. Conf. Ser.* **137**, pp. 659-661.
- Wahab, Q., Karlsteen, M., Willander, M., and Sundgren, J. E. (1991). "Au Schottky barrier diodes on β -SiC thin films deposited on silicon substrates by reactive magnetron sputtering technique," *J. Electron. Mat.* **20** (Nov), pp. 899-901.
- Wahab, Q., Kimoto, T., Ellison, A., Hallin, C., Tuominen, M., Yakimova, R., Henry, A., Bergman, J. P., and Janzén, E. (1998). "A 3 kV Schottky barrier diode in 4H-SiC," *Appl. Phys. Lett.* **72** (Jan. 25), pp. 445-447.
- WalDROP, J. R. and Grant, R. W. (1990). "Formation and Schottky barrier height of metal contacts to β -SiC," *Appl. Phys. Lett.* **56** (Feb), pp. 557-559.
- WalDROP, J. R., Grant, R. W., Wang, Y. C., and Davis, R. F. (1992). "Metal Schottky barrier contacts to alpha 6H-SiC," *J. Appl. Phys.* **72** (Nov), pp. 4757-4760.
- WalDROP, J. R. and Grant, R. W. (1993). "Schottky barrier height and interface chemistry of annealed metal contacts to alpha 6H-SiC: Crystal face dependence," *Appl. Phys. Lett.* **62** (21), pp. 2685-2687.
- WalDROP, J. R. (1994). "Schottky barrier height of metal contacts to p-type alpha 6H-SiC," *J. Appl. Phys.* **75** (May), pp. 4548-4550.
- Wang, Y. C. and Davis, R. F. (1991). "In-situ incorporation of Al and N and p-n junction diode fabrication in alpha (6H)-SiC thin films," *J. Electron. Mat.* **20**, pp. 289-294.
- Weitzel, C. E., Palmour, J. W., Carter, C. H., Moore, K., Nordquist, K. J., Allen, S., Thero, S., and Bhatnagar, M. (1996). "Silicon carbide high-power devices," *IEEE Trans Electron Dev.* **43** (Oct), pp. 1732-1741.
- Wu, S. Y. and Campbell, R. B. (1974). "Au-SiC Schottky barrier diodes," *Solid-State Electronics* **17**, pp. 683-687.
- Yasuda, K., Hayakawa, T., and Saji, M. (1987). "Annealing effects of Al/n-type 6H-SiC rectifying contacts," *IEEE Trans. Electron Dev.* **34** (9), pp. 2002-2008.
- Yih, P. H., Li, J. P., and Steckl, A. J. (1994). "SiC/Si heterojunction diodes fabricated by self-selective and by blanket rapid thermal chemical vapor deposition," *IEEE Trans. Electron Dev.* **41** (Mar), pp. 281-287.
- Yoshida, S., Sasaki, K., Sakuma, E., Misawa, S., and Gonda, S. (1985). "Schottky barrier diodes on 3C-SiC," *Appl. Phys. Lett.* **46** (April), pp. 766-768.
- Zhang, Y. G., Li, X. L., Li, A. Z., and Milnes, A. G. (1996). "Characterization of Schottky contacts on n type 6H-SiC," in: *Silicon Carbide and Related Materials VI—Kyoto 1995*, *Inst. Phys. Conf. Ser.* **142**, pp. 665-668.